UNIVERSITY OF BIRMINGHAM

Project 1: Elucidating the role of *carbon storage regulator A*, *csrA*, in regulating the AcrAB-TolC efflux system in *Salmonella enterica* serovar Typhimurium

Project 2: Exploring the dynamics of *Pseudomonas aeruginosa* attachment to host cells during anti-adhesion therapy

by

Victoria Attah

A combined research thesis submitted to the University of Birmingham as part of the requirements for the degree of MRes in Molecular and Cellular Biology

Institute of Microbiology and Infection

School of Biosciences

University of Birmingham

August 2014

UNIVERSITY OF BIRMINGHAM

Project 1: Elucidating the role of *carbon storage regulator A*, *csrA*, in regulating the AcrAB-TolC efflux system in *Salmonella enterica* serovar Typhimurium

by

Victoria Attah

Supervisors: Professor Laura Piddock and Dr Vito Ricci

A research thesis submitted to the University of Birmingham as part of the requirements for the degree of MRes in Molecular and Cellular Biology

Antimicrobials Research Group

Institute of Microbiology and Infection

School of Biosciences

University of Birmingham

Abstract

In MDR isolates of Enterobacteriaceae, except *Escherichia coli* and *Shigella* spp., RamA, locally regulated by RamR, activates the transcription of the tripartite efflux pump, AcrAB-TolC. The pump is known to efflux a number of structurally distinct antibiotics, dyes, detergents, biocides and host-derived molecules.

TraDIS sequencing of *Salmonella enterica* serovar Typhimurium SL1344 generated gene-deletion mutants, which were interrogated with pMW82-p*ramA,* encoding a green fluorescent protein (GFP) fused to the *ramA* promoter sequence. Disruption of the *csrA* gene in SL1344 resulted in a significant increase in the fluorescence of pMW82-p*ramA*, therefore it was hypothesised that CsrA is involved in the regulation of RamA and the generation of antimicrobial resistance by upregulation of AcrAB-TolC.

The aims of this study were to create and characterise a *csrA*::*aph* mutant in SL1344. The results indicated that the *csrA*::*aph* mutant overexpressed the transcriptional activators *ramA, marA* and *soxS*, but did not overexpress *acrA, acrB* and *tolC,* compared to SL1344. Consistently, the mutant did not display a MDR phenotype, compared to a SL1344 *ramR*::*aph* mutant. However, the mutant displayed an inability to biofilm. *ramR* expression was unaffected in the *csrA*::*aph* mutant, therefore the results suggest CsrA could regulate the expression of *ramA* by a distinct mechanism to that by RamR.

Acknowledgements

I am grateful to my supervisor, Professor Laura Piddock, for giving me the opportunity to undertake my research project with the Antimicrobials research group (ARG). I am also very thankful to Dr Vito Ricci for his help, advice and feedback during my time in the laboratory and during the writing of my thesis.

I would like to thank all other members of ARG for their help and kindness throughout my time with the group.

Contents

3.0 Results

4.0 Discussion

5.0 References

List of figures used in the study

List of tables used in the study

1.0 Introduction

1.1 Multi-drug resistance and bacterial efflux

Multi-drug (MDR) resistance poses a major threat to clinical healthcare, due to the difficulties associated with eradicating infections caused by resistant bacteria. Multi-drug resistant bacteria are those which are capable of surviving in the presence of distinct structural classes of therapeutic drugs, at concentrations high enough to kill susceptible cells in the population (Ramos, Ales et al. 1996), (Glynn, Bopp et al. 1998), (Yamasaki, Nikaido et al. 2013). Fewer treatment options are usually available for these bacteria (Levy 1998).

Salmonella enterica is an enteric gram-negative pathogen responsible for an increasing number of MDR infections in many parts of the world (Su, Chiu et al. 2004). There are six subspecies of *S. enterica* and over 2000 different serotypes, although the subspecies *enterica* is most commonly associated with disease (Fierer and Guiney 2001). *S. enterica* colonises the gastrointestinal tract of animals and humans, by invading the intestinal epithelial cells and macrophages (RichterDahlfors, Buchan et al. 1997), triggering an inflammatory response and leading to the dissemination of the organism into the blood. Once spread, *S. enterica* replicates intracellularly, within Salmonella-containing vacuoles (SCVs) (Finlay, Ruschkowski et al. 1991), in the phagocytic cells of the liver, kidneys and spleen (Steele-Mortimer, Brumell et al. 2002).

S. enterica can cause both gastrointestinal and systemic diseases, and this is dependent on the serovar and the host immune status (Fierer and Guiney 2001). Although the organism does not always infect and cause disease in animals,

transmission of *S. enterica* to humans through animal contact (Fey, Safranek et al. 2000), and contaminated water and food (Zhao, Qaiyumi et al. 2003), can enable the development of serious, life-threatening infections that require immediate treatment. For example, *S. enterica* serovar Typhimurium phage type DT104 was heavily reported in the 1990s as being a highly pathogenic strain that caused a worldwide, MDR epidemic, and was thought to have originated from cattle in the United Kingdom (Threlfall 2000); although other environmental factors, travel and imported food were also likely contributors to the spread of the infection in humans (Mather, Reid et al. 2013).

Therapeutic compounds used to treat bacterial infections, including those caused by *S. enterica*, are classed as either bacteriostatic or bactericidal. Bacteriostatic compounds are designed to interfere with the pathways and proteins that the bacteria require for growth and proliferation, such as the tetracycline antibiotics, which inhibit successful translation of bacterial proteins by binding to bacterial ribosomes and inhibiting their function (Chopra and Roberts 2001). However, when treatment with a bacteriostatic compound is removed, the bacteria can usually begin growing again, therefore the infection may not be fully eradicated. Bactericidal compounds are those which kill the bacteria, including the broad-spectrum glycopeptide antibiotic, vancomycin, which interferes with bacterial cell wall synthesis (Jordan 1961), leading to lysis of the bacterial cell.

Selective pressure generated from inappropriate or mismanaged antibiotic use is an important factor in the development and transmission of resistance, as antibiotic

exposure enables bacteria capable of surviving to proliferate and dominate in a bacterial population. Antibiotic resistance in bacteria is typically mediated by genes coding for proteins that degrade or inactivate antibiotics (Levy 1998). Alternatively, spontaneous mutations in one or more of the genes that are the targets of therapeutic drugs can facilitate resistance, such as mutations in the genes that encode DNA gyrase (*gyrA*, *gyrB*) and topoisomerase IV (*parE*, *parC*) enzymes, which confers a high-level of resistance to broad-spectrum fluoroquinolones (Casin, Breuil et al. 2003).

Intrinsic bacterial resistance in bacteria can also be mediated by decreasing bacterial membrane permeability (Nikaido and Vaara 1985), (Nikaido 2003), or by increasing the expression of efflux pumps, a resistance mechanism which was first described in *Escherichia coli* (Mcmurry, Petrucci et al. 1980). Efflux pumps are protein complexes that span the inner and outer bacterial membranes, and are ubiquitous among both gram-positive and gram-negative bacteria. They are responsible for the transport of various substrates including antibiotics (Li, Livermore et al. 1994), dyes, biocides, detergents and host-derived antimicrobials such as bile salts (Thanassi, Cheng et al. 1997), from the bacterial periplasm and/or cytoplasm to the extracellular space. By reducing the intracellular concentration of toxic substrates to sub-lethal levels, bacteria can inhibit therapeutic compounds from reaching their target active site, therefore escaping eradication by their mechanism of action.

Five classes of bacterial efflux pumps have been characterised to date: Resistance Nodulation Division (RND), Major Facilitator superfamily (MFS), Multi-drug and Toxic

Compound Extrusion (MATE), Staphylococcal Multi-resistance (SMR) and ATP-binding cassette (ABC). Examples of the classes of efflux pumps in both gram-positive and gram-negative bacteria and the types of substrate they export are shown in Figure 1.1. In addition to the types of substrate exported, an efflux pump may be categorised into one of the five above mentioned groups depending on the energy source used for efflux, the number of components involved in the system, and the number of transport protein membrane-spanning regions (Piddock 2006).

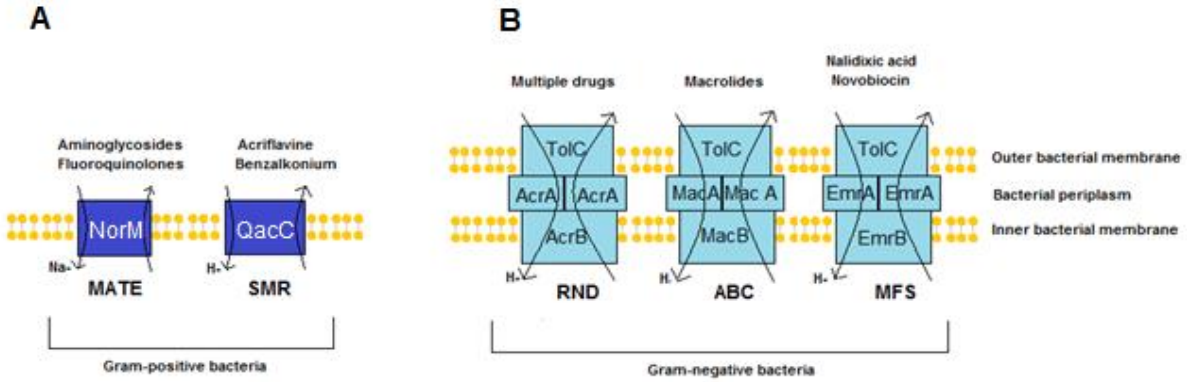

Figure 1.1: Efflux pumps in (A) gram-positive and (B) gram-negative bacteria. Inner and outer bacterial membranes are composed of a lipid bilayer (yellow). Example transport protein complexes that are part of each class are shown (coloured boxes), in addition to the energy source used for efflux and the types of antimicrobial substrates exported (adapted from Piddock 2006).

The genome of *S. enterica* serovar Typhimurium is now known to encode nine efflux pumps: AcrAB, AcrD, AcrEF, MdsABC, MdsAB (RND family), EmrAB, MdfA (MFS family), MdtK (MATE family) and MacAB (ABC family) (Nishino, Latifi et al. 2006). An increase in bacterial efflux activity is proposed to contribute to resistance and treatment failure, by preventing therapeutic compounds from reaching their target active site. Therefore, an improved understanding of bacterial efflux, and the development of antimicrobials that can inhibit efflux may help to alleviate the burden of untreatable infections caused by MDR bacteria.

1.2 The AcrAB-TolC efflux pump in Enterobacteriaceae

AcrAB-TolC is an RND efflux pump that has been well studied in *E. coli* and Salmonella, and is thought to be functionally similar in both species, as shown by amino acid sequence analysis. Three protein components make up AcrAB-TolC: AcrA, AcrB (Ma, Cook et al. 1993) and TolC (Fralick 1996), which together form a tripartite complex (Figure 1.2). The energy that drives the efflux of substrates via AcrAB-TolC is generated by proton motive force, in which the movement of hydrogen ions across an electrochemical gradient drives the substrate from the periplasm and/or cytoplasm to the extracellular space. The outer membrane channel, TolC, is able to export diverse substrates through its interactions with inner membrane protein complexes in addition to AcrAB, such as AcrEF in *S. enterica* serovar Typhimurium (Horiyama, Yamaguchi et al. 2010), MacB and EmrB (Figure 1.1).

The AcrAB-TolC complex must be intact in order to produce antimicrobial resistance. Pradel et al (2002)., reported that in the absence of *acrAB* and *tolC*, *Enterobacter aerogenes* became significantly more susceptible to chloremphenicol, norfloxacin and other antimicrobials, and this was a phenotype that reversed in the presence of complemented, plasmid-encoded efflux proteins in the same mutants (Pradel and Pages 2002). Similar observations were described following disruption to *acrB* and *tolC* genes in *S. enterica* serovar Typhimurium, which led to decreases in minimum inhibitory concentrations (MICs) for quinolones and tetracyclines (Baucheron, Tyler et al. 2004), (Eaves, Ricci et al. 2004). Testing fluoroquinolones against *acrB*-inactivated *S. enterica* serovar Typhimurium in combination with a known efflux inhibitor, Phe-Arg-β-naphthylamide (PAβN) also significantly reduced the MICs

(Baucheron, Imberechts et al. 2002).

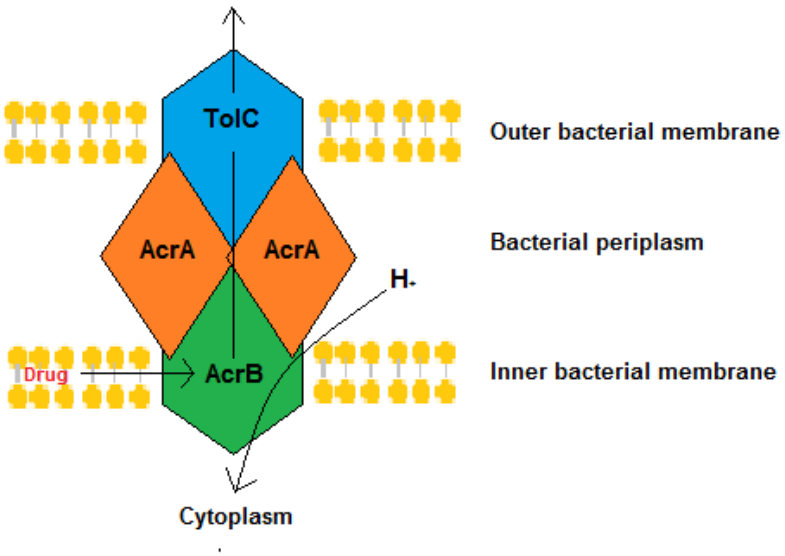

Figure 1.2: The AcrAB-TolC tripartite efflux pump. Inner and outer bacterial membranes are composed of a lipid bilayer (yellow). AcrB (green) is an integral membrane protein located within the cytoplasmic membrane, TolC (blue) is an outer membrane protein, which is anchored to AcrB by the membrane fusion protein AcrA (orange) - a periplasmic adapter protein (PAP), which spans the inner and outer bacterial membranes (Adapted from Pos 2009).

Although other efflux systems are capable of exporting compounds including clinically-relevant antibiotics, AcrAB-TolC is considered the major efflux pump system of clinical relevance in bacteria including *E. coli* and Salmonella. Deletion of homologues of *acrB*, such as *acrD* and *acrF*, which encode AcrD and AcrF, respectively, lead to modest increases in antimicrobial susceptibility, compared with when genes encoding *acrAB-tolC* are disrupted (Eaves, Ricci et al. 2004). This is likely because AcrAB-TolC has much broader substrate specificity than other efflux complexes, and is therefore able to efflux a number of structurally diverse compounds. Studies by Oethinger et al., and Baucheron et al., have also suggested that efflux via AcrAB-TolC confers a higher level of quinolone resistance than double mutations in the DNA gyrase gene *gyrA* in *E. coli* and *S. enterica* serovar

Typhimurium DT104 (Oethinger, Kern et al. 2000), (Baucheron, Tyler et al. 2004).

1.3 The AcrAB-TolC efflux pump and pathogenicity

In addition to the export of various antibiotics, dyes, biocides and detergents, AcrAB-TolC is capable of exporting host-derived molecules, including bile salts (Thanassi, Cheng et al. 1997) and other factors produced by the host immune system, such as α-haemolysin (Vakharia, German et al. 2001). In the presence of high bile concentrations, higher than those likely to be encountered during infection in a host environment, the expression of S. Typhimurium *acrAB* was shown to increase (Prouty, Brodsky et al. 2004). Bacterial efflux of host-derived antimicrobials is likely to enhance bacterial survival during initial infection, enabling bacteria to persist in the harsh environment of host immune defences.

The interplay between bacterial resistance and pathogenicity is further evidenced by experiments in which inactivated *acrB* or *tolC* efflux components conferred a defect in biofilm formation (Baugh, Ekanayaka et al. 2012). A biofilm is formed when bacteria colonise the same space or surface, forming aggregates of cells suspended in an extracellular matrix (Costerton, Stewart et al. 1999) and it is thought that over 90% of bacteria found in nature exist in a biofilm (Costerton, Cheng et al. 1987). Biofilms are complex structures that consist of actively growing bacterial cells and bacteria which are metabolically slow or inactive, also known as persister cells. The complex nature of biofilms poses a clinical burden because they are difficult to eradicate, and therefore considered to be reservoirs of infection. Biofilms enable bacteria to survive antibiotics (Stewart 2002) and host-derived factors of the immune system, therefore

compared to planktonic bacteria, much higher concentrations of drugs are usually needed to remove bacteria within a biofilm. Preventing biofilm formation on surfaces in close contact with humans or animals, including contaminated foods, domestic and healthcare-associated water supplies and medical devices continues to be an important area of research (Donlan 2001).

The composition of biofilm matrix during the formation of competent biofilm is dependent on a number of factors, including temperature and growth conditions, however *S. enterica* serovar Typhimurium biofilm matrix is generally composed of cellulose and curli fibres (Romling, Bian et al. 1998), (Kikuchi, Mizunoe et al. 2005). Curli are proteinaceous amyloid fibres and it has been suggested that curli are important for surface attachment (Pawar, Rossman et al. 2005), successful bacterial colonisation and biofilm formation (White, Gibson et al. 2006), and have been investigated in several Enterobacteriaceae including Salmonella and *E. coli*. Curli production in bacteria can be visualised by plating a bacterial suspension of known concentration onto Congo Red medium, the main constituent of which will bind to curli fibres that have been synthesised by the bacteria, making the colony appear red and rough on the media (Nilsson 2004).

1.4 Regulation of the AcrAB-TolC efflux pump in *S. enterica* serovar Typhimurium

It is likely that AcrAB-TolC plays an important role in enabling bacteria to survive and establish infection, as disruption to *acrA, acrB* or *tolC* genes has been associated with increased antimicrobial susceptibility and reduced biofilm formation (Pradel and

Pages 2002), (Baucheron, Tyler et al. 2004), (Eaves, Ricci et al. 2004), (Baugh, Ekanayaka et al. 2012). Inactivation of *acrA, acrB* or *tolC* also decreases the ability of cells to invade IMT-401 and RAW-264.7 tissue culture cell lines *in vitro* (Buckley, Webber et al. 2006), mirrored by a decrease in the expression of Salmonella pathogenicity island (SPI) genes, involved in bacterial pathogenicity (Webber, Bailey et al. 2009). Consistent with this, deletion mutants are not able to colonise the gut of chickens, to a similar level seen for wild type strains (Buckley, Webber et al. 2006). Inactivation of *acrA*, *acrB* and *tolC* also decreases the expression of genes involved in colonisation, such as flagella, chemotaxis and anaerobic respiration genes (Webber, Bailey et al. 2009).

The regulation of AcrAB-TolC has been best characterised in *E. coli*, and involves local genetic elements, located in the same gene clusters, and global regulatory elements, located in other areas of the genome, the latter of which may be involved in the regulation of other cellular functions (Figure 1.3). This indicates that there is strict transcriptional control over the expression of the efflux system, influenced by various environmental stimuli. In Enterobacteriaceae, the expression of *acrAB* is mediated by the local repressor, *acrR*. Although mutations in this gene have been shown to modestly increase resistance to structurally distinct antibiotics (Olliver, Valle et al. 2004), mutations in *acrR* in resistant isolates of *S. enterica* serovar Typhimurium are rare (Piddock, White et al. 2000), suggesting multiple levels of regulation are involved in mediating the expression of the efflux system.

The global transcriptional activators of *acrAB* in Salmonella and other

Enterobacteriaceae, are encoded by the genes *ramA, marA, soxS and rob* (Figure 1.3). These proteins mediate antibiotic resistance by initiating the transcription of *acrAB* (Perez, Poza et al. 2012). The initiation of *acrAB* transcription by the efflux activator, indole, is dependent on *ramA*, and not *marA, soxS* or *rob*, and it has been suggested that RamA is central to the regulation of the AcrAB-TolC multidrug efflux system in Salmonella (van der Straaten, Janssen et al. 2004). *ramA,* however, is not present in *E. coli* and *Shigella* spp., although *marA* has been well characterised in *E. coli* and has been suggested to contribute to antimicrobial resistance in *E. coli* clinical isolates (Keeney, Ruzin et al. 2008). It has been suggested that induction of *acrAB-tolC* is different in *E. coli* and Salmonella (Nishino, Nikaido et al. 2009).

RamA is a DNA-binding protein that is a member of the AraC-XylS family of transcriptional activators. AraC-XylS regulators are common positive regulators that share amino acid sequence homology in their DNA binding domains (Gallegos, Schleif et al. 1997). The only negative regulator to date that is part of the AraC-XylS family of regulators is *celD*, renamed *chbR*, which forms part of the *cel* operon, renamed the *chb* operon, involved in the metabolism of a chitin disaccharide in *E. coli* (Parker and Hall 1990), (Keyhani and Roseman 1997). RamA binds upstream of *acrAB* and positively regulates the transcription of these genes (Figure 1.3).

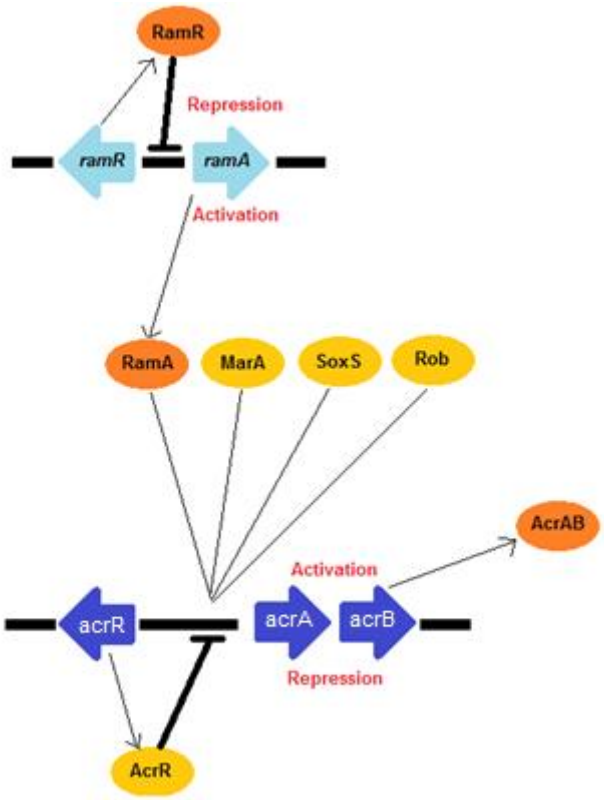

Figure 1.3: Gene and protein interactions. *acrA* and *acrB* are positively regulated by RamA, MarA, SoxS and Rob, and negatively regulated by local repressor, AcrR. RamA is thought to be central to the regulation of the AcrAB-TolC efflux pump in Enterobacteriaceae, except *E. coli* and *Shigella* spp. Genes are represented by arrows, and proteins are represented by circles. Gene activation is shown by a thin black line and gene repression is shown by a thick black line.

Increasing the expression of *ramA* increases the expression of *acrAB*, in both clinical isolates and laboratory mutants of Salmonella (Nikaido, Yamaguchi et al. 2008), (Ricci and Piddock 2009), (O'Regan, Quinn et al. 2009). Overexpression of *marA* and *soxS* was not observed in the same isolates, suggesting that RamA has a central role in the transcriptional regulation of *acrAB*. Consistently, *acrB* and *tolC* inactivation causes a significant increase in *ramA* expression in *S. enterica*, 1,226.41 and 25.41-fold, respectively, compared to wild type strains (Webber, Bailey et al. 2009). This further suggests that RamA is centrally involved in the regulation of the transcription of *acrAB* in Salmonella.

The overexpression of *acrAB*, as a result of *ramA* overexpression, correlates with increased resistance to multiple drugs, including nalidixic acid, chloremphenicol and tetracycline (Ricci and Piddock 2009), where efflux was reported to be increased in MDR isolates. Additionally, the induction of *ramA* through an isopropyl-β-D-thiogalactopyranoside (IPTG)-inducible *ramA* plasmid lead to observed increases in the antibiotic resistance profile of *S. enterica* serovar Typhimurium against structurally distinct antibiotics, investigated by disk diffusion (van der Straaten, Janssen et al. 2004), consistent with *acrAB* overexpression (Bailey, Ivens et al. 2010). Further studies carried out by Van der Straaten et al., also reported that induced *ramA* expression in *marA*-deficient and wild-type *E. coli* strains, lead to a significant increase in observed MDR in both strains, despite the presence of the transcriptional activator, *marA*, again suggesting a more prominent regulatory role for RamA in generating resistance to multiple drugs by the upregulation of the AcrAB-TolC efflux pump (van der Straaten, Janssen et al. 2004).

Additional studies of *ramA* transcriptional activity identified that this gene is also involved in activating the transcription of *micF*, the gene product of which inhibits the synthesis of an outer membrane porin, OmpF (O'Regan, Quinn et al. 2009). This protein is involved in making the bacterial membrane less permeable, thereby not facilitating the entry of compounds, including clinically-relevant substrates. The importance of *ramA* in conferring drug resistance via active efflux is further evidenced by experiments in which the deletion of *ramA* from the transcriptome of Salmonella is not conducive for the selection of spontaneous resistant mutants (Ricci and Piddock 2009). However, despite this, *ramA*-deleted mutants do not display hypersuseptibility

to the same number of compounds as does the deletion of *acrAB* or *tolC*; taken together, these data suggest that other intrinsic or acquired resistance determinants remain intact despite inactivation of *ramA.*

Regulation of *ramA* expression is via its local repressor gene, *ramR*. This gene was first identified by Abouzeed et al., after inactivation and complementation studies, and is located upstream of *ramA* (Abouzeed, Baucheron et al. 2008) (Figure 1.3). Yamasaki et al., recently revealed the crystal structure of the RamR dimer and found that its dissolved molecular weight in solution is 36kDa, whilst the monomer is 21kDa. The RamR dimer and monomer consist of a dimerization domain and a DNA-binding domain, composed of nine α-helices in total (α1-9). The accompanying amino acid sequence subdivides α7 and α8 into α7a and α7b, and α8a and α8b, respectively, due to tortuosity of these α-helices (Yamasaki, Nikaido et al. 2013). RamR binds to a region spanning the *ramA* promoter sequence; this region includes the *ramA* transcriptional start site, a -10 conserved region and two inverted repeats (Baucheron, Coste et al. 2012), (Ricci, Busby et al. 2012), (Yamasaki, Nikaido et al. 2013).

An increase in *ramR* expression confers a decrease in the level of cellular RamA, and one or more mutations in *ramR* or the *ramR-ramA* intergenic region typically characterises significant overexpression of *ramA* (Ricci and Piddock 2009), with accompanying MDR in Salmonella isolates (Abouzeed, Baucheron et al. 2008). It is thought that RamR binds to the same drugs that are substrates of efflux by AcrAB-TolC (Yamasaki, Nikaido et al. 2013), therefore in the presence of high levels of toxic compounds, the active binding of RamR to these substrates sequesters its ability to

repress *ramA*. This has been investigated by the studies of Yamasaki et al., who studied the binding interaction of a putative RamR substrate-recognition site with several drugs, including ethidium bromide, chloramphenicol and tetracycline, which are known substrates of the AcrAB-TolC system. In total the team concluded that five of the compounds studied exhibited binding interactions with the RamR protein. They hypothesised that these compounds increase the expression of *ramA* by binding to RamR, and reported a significant increase in *ramA* expression, as assayed by β-Galactosidase activity (Yamasaki, Nikaido et al. 2013). In this way, RamR appears to act as a bacterial environmental sensor, monitoring the concentrations of multiple cytosolic drugs in the immediate bacterial surroundings. Despite these findings, other studies in which *ramR* is inactivated do not lead to excessive *ramA* expression and despite the likely role of bacterial efflux systems in bacterial pathogenesis, *ramR* inactivation had a modest effect on virulence *in vivo* (Bailey, Ivens et al. 2010). This suggests that *ramA* may be regulated by multiple distinct mechanisms.

1.5 Current knowledge about *carbon storage regulator* A (*csrA*)

In addition to DNA-binding proteins and transcription factors, post-transcriptional regulatory systems play a pivotal role in mediating strictly-controlled bacterial gene expression in response to extracellular stimuli, and the interactions between bacteria and host cells (Romeo 1998).

The *carbon storage regulator A* (*csrA)* gene was initially identified in *E. coli* K-12 by transposon mutagenesis (Romeo, Gong et al. 1993) and is homologous to the *repressor of secondary metabolites A* (*rsmA*) gene, which has been characterised in other bacteria, such as *Pseudomonas fluorescens* (Agaras, Sobrero et al. 2013) and

Pseudomonas aeruginosa. In *P. aeruginosa*, the two-component Rsm/Gac network has been proposed to be involved in environmental sensing and the activation of biofilm formation (Goodman, Kulasekara et al. 2004). In this organism, RsmA is thought to increase the expression of genes which contribute to virulence, including those that encode bacterial lipases and those linked to bacterial motility (Heurlier, Williams et al. 2004). To date, only one *csrA* gene has been identified on the *E. coli* chromosome, whereas two homologues, *rsmA* and *rsmB* have been identified in *P. flourescens*. The reason for this is unclear, however it could reflect the environmental niches that *P. flourescens* colonises and the need for tighter control of bacterial gene expression.

CsrA is a 61-amino acid, dimeric RNA-binding protein that binds competitively to target mRNAs, usually around their ribosomal binding site, and blocks their translation or alters their stability. CsrA competitive binding reduces mRNA access to ribosomes, thereby reducing the translation rate of the protein (Figure 1.4). CsrA mRNA sequestration can result in an increase or decrease in mRNA expression (Romeo, Gong et al. 1993), (Barnard, Loughlin et al. 2004), (Romeo, Vakulskas et al. 2013), (Seyll and Van Melderen 2013).

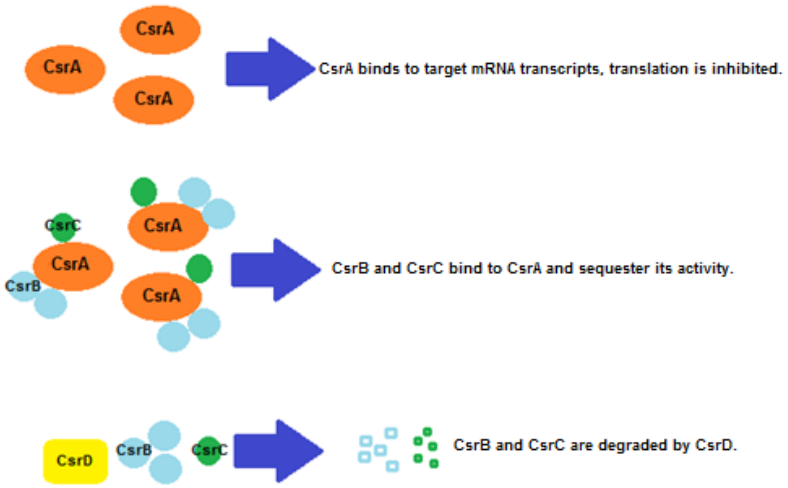

Figure 1.4: CsrA interactions with CsrC, CsrB and CsrD. The CsrA protein (orange) binds to mRNA targets and degrades them or alters their stability. CsrA activity is sequestered by CsrB (blue) and CsrC (green), which mimic CsrA mRNA targets, preventing the binding of CsrA to transcripts. CsrB and CsrC proteins are regulated by CsrD (yellow).

CsrA is involved in the regulation of central carbon metabolism, and is thought to positively regulate glycolysis and negatively regulate glycogen biosynthesis and gluconeogenesis. *csrA* inactivation leads to an observed reduction in the release of ATP energy and glucose consumption, and increased expression of *pckA (*phosphoenolpyruvate carboxylase), which is involved in the gluconeogenesis pathway (Sabnis, Yang et al. 1995).

In *E. coli*, CsrA is thought to be involved in the post-transcriptional regulation of the genes involved in competent biofilm formation and a disruption to this gene results in the increase of poly-beta-1,6-N-acetyl-d-glucosamine (PGA) extracellular matrix (Wang, Dubey et al. 2005). It has been suggested that CsrA both represses and activates biofilm formation in *E. coli* and this is dependent on its role in regulating carbon metabolism (Jackson, Suzuki et al. 2002). Additionally, CsrA is thought to positively regulate motility in *E. coli* by increasing the expression of *flhDC* (FlhD and

FlhC proteins) (Wei, Brun-Zinkernagel et al. 2001), involved in the positive transcriptional activation of flagellar genes, suggesting that the *csrA* gene is important for colonisation and infection in *E. coli.*

In *S.enterica* serovar Typhimurium, CsrA has been suggested to control the expression of genes associated with bacterial invasion, including the expression of fimbrial genes for cellular attachment (Sterzenbach, Nguyen et al. 2013), and both the deletion and overexpression of *csrA* result in a similar phenotype of reduced invasion ability of epithelial cells (Altier, Suyemoto et al. 2000), suggesting that the activity of CsrA must be tightly regulated in Salmonella.

The regulation of *csrA* is via three proteins that modulate CsrA concentration; CsrB, CsrC and CsrD (Figure 1.4). The CsrA dimer binds to two small, non-coding sRNA molecules, CsrB and CsrC, which contain binding sites for CsrA and antagonise the protein by forming ribonucleoprotein complexes with it (Romeo 1998). The binding sites include RNA motifs with conserved GGA amino acid sequences, thought to be the same sequences that CsrA recognises and binds to on target mRNA molecules, blocking access to the Shine-Dalgarno sequence (Dubey, Baker et al. 2003), (Baker, Eory et al. 2007). These molecules mimic the real CsrA targets and are therefore able to outcompete the binding to these mRNA targets by sequestering CsrA activity (Adamson and Lim 2013). CsrB is thought to have greater interaction potential as it can bind 18 subunits (9 dimers) of CsrA (Liu, Gui et al. 1997), whilst CsrC can bind 6-8 subunits (3-4 dimers) (Weilbacher, Suzuki et al. 2003). Increasing the expression of *csrB* and *csrC* blocks CsrA activity, shown by *csrB* overexpression and increased

glycogen accumulation in *E. coli* (Liu, Gui et al. 1997), consistent with the role of CsrA as a negative regulator of glycogen biosynthesis (Sabnis, Yang et al. 1995). Decreasing the expression of the sRNAs enables CsrA to interact with its targets. CsrD is involved in regenerating CsrA, by directing degradation of CsrB and CsrC via RNAse E and PNPase (Suzuki, Babitzke et al. 2006), (Adamson and Lim 2013) (Figure 1.4).

1.6 Research hypothesis and experimental aims

The primary hypothesis investigated in this study was that CsrA is involved in the regulation of RamA in *Salmonella enterica* serovar Typhimurium SL1344 and therefore plays a role in multi-drug resistance by bacterial efflux via AcrAB-TolC, which RamA is a known to be a transcriptional activator of.

This hypothesis arose from Transposon Directed Insertion Site (TraDIS) sequencing, carried out by Ricci & Piddock (unpublished data), in which transposons were inserted into the genome of SL1344. Single gene-deletion mutants were selected, which were interrogated for their effects on the expression of *ramA*. This was carried out by transforming pMW82-p*ramA*, a plasmid containing the cloned *ramA* promoter region fused to a gene encoding a green fluorescent protein (GFP), into the TraDIS library of SL1344 mutants. Screening by flow cytometry revealed populations that expressed *ramA* at a higher level than SL1344. Subsequent experiments and DNA sequencing revealed that transposon disruption of the *csrA* gene resulted in a significant increase in *ramA* promoter activity on two separate occasions. Therefore, it is proposed that CsrA is involved in the regulation of RamA.

The experimental aims of this project were to create and characterise a *csrA*::*aph* mutant in *S. enterica* serovar Typhimurium SL1344, investigating the effects of this gene disruption on growth, expression of *ramA* and other genes involved in the activation of AcrAB-TolC, the effect on the mutant's susceptibility to structurally distinct antimicrobials that are known substrates of the AcrAB-TolC efflux pump (Giraud, Cloeckaert et al. 2000), (Baucheron, Imberechts et al. 2002), (Baucheron, Chaslus-Dancla et al. 2004), and the effect of the *csrA* gene disruption on the strain's ability to produce curli and competent biofilm, both known to be influenced by the expression of *acrAB-tolC* (Baugh, Ekanayaka et al. 2012). The *csrA* gene disruption in SL1344 was constructed using the gene inactivation method described by Datsenko and Wanner (Datsenko and Wanner 2000).

2.0 Materials and Methods

Table 2.1: Bacterial strains used in the study.

Laboratory Reference	Bacteria	Source and Description	Growth
I633	*Escherichia. coli*	BW25141/pkD4 amp^R kan^R Datsenko & Wanner	LB media supplemented with 50 µg/mL ampicillin & 50 µg/mL kanamycin
I114	*Escherichia. coli*	VLA 3992/96 Clone 1	LB media not supplemented
L354	Salmonella typhimurium	SL1344 (VLA)	LB media not supplemented
L642	Salmonella typhimurium	SL1344 pKD46 amp^R Datsenko & Wanner plasmid	LB media supplemented with 50 µg/mL ampicillin
L828	Salmonella typhimurium	ATCC 14028S Nishino lab	LB media not supplemented
L829	Salmonella typhimurium	Δ *tolC* EG16564 Nishino lab	LB media not supplemented
L1007	Salmonella typhimurium	SL1344 *ramR*::*aph* (P22 transduced from L1005)	LB media not supplemented
L1232	Salmonella Typhimurium	SL1344 + pMW82-*ramA* promoter 290bp	LB media supplemented with 50 µg/mL ampicillin
L1361	Salmonella Typhimurium	SL1344 pMW82p*acrAB*	LB media supplemented with 50 µg/mL ampicillin
L1406	Salmonella Typhimurium	SL1344 + pMW82p*tolC*	LB media supplemented with 50 µg/mL ampicillin
L1410	Salmonella Typhimurium	SL1344 + pMW82p*ramA* (261 bp) Amp^R)	LB media supplemented with 50 µg/mL ampicillin
L1412	Salmonella Typhimurium	SL1344 + pMW82p*ramA* (184 bp) (Amp^R)	LB media supplemented with 50 µg/mL ampicillin
L1413	Salmonella Typhimurium	SL1344 + pMW82p*ramA* (95 bp) (Amp^R)	LB media supplemented with 50 µg/mL ampicillin
L1606	Salmonella Typhimurium	SL1344 *csrA*::*aph* (Kan^R)	LB media supplemented with 50 µg/mL kanamycin
L1607	Salmonella Typhimurium	14028S *csrA*::*aph* (Kan^R)	LB media supplemented with 50 µg/mL kanamycin
L1608	Salmonella Typhimurium	SL1344 *csrA*::*aph* + pMW82-*acrAB* promoter in SL1344	LB media supplemented with 50 µg/mL kanamycin & 50 µg/mL ampicillin

Laboratory Reference	Bacteria	Source and Description	Growth
L1609	Salmonella Typhimurium	SL1344 *csrA*::*aph* + pMW82-*tolC* promoter in SL1344	LB media supplemented with 50 µg/mL kanamycin & 50 µg/mL ampicillin
L1610	Salmonella Typhimurium	SL1344 *csrA*::*aph* + pMW82-*ramA* promoter in SL1344 290bp	LB media supplemented with 50 µg/mL kanamycin & 50 µg/mL ampicillin
L1611	Salmonella Typhimurium	SL1344 *csrA*::*aph* + pMW82p*ramA* (261 bp) Amp^R)	LB media supplemented with 50 µg/mL kanamycin & 50 µg/mL ampicillin
L1612	Salmonella Typhimurium	SL1344 *csrA*::*aph* + pMW82p*ramA* (184 bp) (Amp^R)	LB media supplemented with 50 µg/mL kanamycin & 50 µg/mL ampicillin
L1613	Salmonella Typhimurium	SL1344 *csrA*::*aph* + pMW82p*ramA* (95 bp) (Amp^R)	LB media supplemented with 50 µg/mL kanamycin & 50 µg/mL ampicillin

Table 2.2: Primers used in the study.

Primer Name	Description	5' to 3' sequence
Kt	Internal kan^R check primer pKD4 reverse	CGGCCACAGTCGATGAATCC
K2	Internal kan^R check primer pKD4 forward	CGGTGCCCTGAATGAACTGC
ramA-prom-*BamHI*-F	*BamHI-ramA*-F	ATGGATCCGATACCGGATTGCGCTA
gfp mut2 R	*gfp* mut2 from pUA66pacp	GCTAGTTGAACGCTTCCATC
SmaI ramA promo FW	RamA promo primers for pUA66 plasmid	ACGTCCCGGGCACGTTACCCTTATGTCTGG
AcrApromoterGFP F	AcrA promoter for GFP fusion forward	GCGGGATCCGCTCCCAGATCTCACTGAAT
TolCpromoterGFP F	TolC promoter for GFP fusion forward	GCGGGATCCGTTTCCCGTGCAATAATTTC
csrA knock-out forward	*csrA* KO primers forward	ATGCTGATTCTGACTCGTCGAGTTGGTGAGACCCTCATGAGTGTAGGCTGGAGCTGCTTC
csrA knock-out reverse	*csrA* KO primers reverse	CAGCCTGGATACGCTGGTAGATCTCTTCACGATGGACAGAGGGAATTAGCCATGGTCCAT
csrA check forward	*csrA* Kan^R check primer forward	ATGCTGATTCTGACTCGTCG
csrA check reverse	*csrA* Kan^R check primer reverse	AAGTCATGAAGGGACAACGC
acrA Forward RT-PCR primer	SL1344 *acrA* Forward RT-PCR primer	GTAATTTCGTTGAGGGAAGTGA
acrA Reverse RT PCR primer	SL1344 *acrA* Reverse RT-PCR primer	TCGTAAGTCGCCTGGTAG
acrB qRT F	*acrB* qRT-PCR F	GTCCTCAAGTAGCTTCCT
acrB qRT R	*acrB* qRT-PCR R	GTAATCCGAAATATCCTCCTG
tolC RT RT F	*tolC* Salmonella Typhimurium RT F	AGTACGACGATAGCAACA
tolC RT RT R	*tolC* Salmonella Typhimurium RT R	TTAACCATCCCACCTTGA

Primer Name	Description	5' to 3' sequence
*ramA*_RT F	Forward RealTime primer for S. Typhimurium *ramA*	TGAATCAGCCGTTACG
*ramA*_RT R	Reverse RealTime primer for S. Typhimurium *ramA*	AGACTCTCCCCTTTGTA
*marA*_RT F	Foward RealTime primer for S. Typhimurium *marA*	CAACACTGACGCTATTACTA
*marA*_RT R	Reverse RealTime primer for S. Typhimurium *marA*	CAGGTGCCATTTGGAA
*soxS*_RT F	Forward RealTime primer for S. Typhimurium *soxS*	CGCATCAGCAGATAATTCAGAC
*soxS*_RT R	Reverse RealTime primer for S. Typhimurium *soxS*	ACTTGGAGTAGCCCGATTT
rob Forward RT-PCR primer	SL1344 Rob Forward RT-PCR primer	GGTCATTCGCCAACTATT
rob Reverse RT-PCR primer	SL1344 Rob Reverse RT-PCR primer	GGAAGTATTCTATACCACCG
rrsH_RT F	Forward RealTime primer for S. Typhimurium rrsH	TACCTGGTCTTGACAT
rrsH_RT R	Reverse RealTime primer for S. Typhimurium rrsH	GACTTAACCCAACATTTC
ramR RT RT F	*ramR* Salmonella Typhimurium RT F	TTATGTCATCGTTCCGTT
ramR RT RT R	*ramR* Salmonella Typhimurium RT F	ATCCATTGTTGTTTCAGC

2.1 Bacterial strains used in this study

All bacterial strains used in this study are listed in Table 2.1.

Unless otherwise stated, all bacterial strains were recovered from storage at -20°C on Protectant beads. One to two beads were used to streak each strain to purity onto Luria Bertani (LB) agar plates, which were then incubated in a static aerobic incubator for 24 hours at 37°C. Plates were checked by eye to ensure they were free from contamination and stored at 4°C for up to two weeks.

LB agar was prepared by autoclaving 17.5 g of powder (Sigma) dissolved in 500 mL sterile distilled water (SDW), and once cooled, agar plates were poured aseptically and oven dried. Unused plates were stored at 4°C for up to two weeks.

Overnight cultures of the strains used in this study were prepared by aliquoting 10 mL sterile LB into sterile 30 mL universal tubes (Sterilin). A single bacterial colony was picked from a LB agar plate, into each universal tube. The tubes were incubated in a shaking aerobic incubator for 24 hours at 37°C.

LB broth was prepared by autoclaving 10g of powder (Sigma) dissolved in 500 mL SDW.

All bacterial cultures used in this study were grown to an OD_{600} of ~0.6 – 1 (mid-logarithmic phase). The OD_{600} was measured using a spectrophotometer, by aliquoting 1 mL of culture into a plastic cuvette, and measuring the optical density against 1 mL of media only (blank).

2.2 Preparation of plasmids

All bacterial strains with plasmids used in this study are listed in Table 2.1.

Unless otherwise stated, overnight bacterial cultures were supplemented with 50 µg/mL ampicillin (Sigma - powder stored at 4°C), to select for cells carrying the plasmid. Plasmid preparations were carried out according to the protocol from GeneJET Plasmid Mini Prep Kit (Thermo Scientific), and checked by agarose gel electrophoresis. The plasmid preparations were stored at 4°C.

2.3 Polymerase chain reaction (PCR)

All PCR primers used in this study are listed in Table 2.2. For *csrA* knock-out primers; XBASE (Chaudhuri, Loman et al. 2007) was used to search for the *csrA* nucleotide sequence within the SL1344 genome and primers were designed to amplify a kanamycin resistance cassette in *E. coli* (plasmid pKD4) to replace *csrA*, with flanking homology to the target gene. For *csrA* check primers; Primer Fox was used to design primers to confirm disruption of *csrA*. All other primers used in this study were taken from -20°C storage from the Antimicrobials Research Group primer collection. Primers were delivered lyophilised from Invitrogen and were reconstituted with nuclease-free water, to a concentration of 100 µM, and stored at -20°C.

The DNA used for PCR amplification was extracted from bacterial cells by preparing cell lysates; one bacterial colony was inoculated into 50 µL of SDW, in a sterile 0.8 mL microtube, and heated for 5 minutes at 95°C using a thermal controller, to release the cellular DNA. The microtube was then centrifuged for 2 minutes at 13,000 x g and the supernatant containing the DNA was used to prepare the PCR reactions.

Unless otherwise stated, the PCR master mixes were prepared with the following volumes, with reagents stored at -20°C and thawed on ice; 45 µL of MyTaq Red Mix (Bioline - diluted from a 2x stock),1 µL of forward primer (25 µM working stock) and 1 µL of reverse primer (25 µM working stock), per PCR sample. From the master mix, 47 µL was aliquoted into sterile 0.8 mL microtubes. Lysate (3 µL) was added to the tubes, resulting in a total reaction volume of 50 µL.

For plasmid preparations; 3 µL of the preparation stored at 4°C was added to 47 µL of the PCR master mix. Unless otherwise stated, the PCR conditions were: 95°C for 5 minutes (denaturation), 95°C for 30 seconds, 50°C for 30 seconds, 72°C for 2 minutes (annealing), for a total of 35 cycles and 72°C for 10 minutes (extension). A negative contamination control was also included in all PCR reactions, containing 47 µL master mix, 3 µL SDW, and no DNA.

Agarose gel electrophoresis

A 1% agarose gel was prepared by dissolving 1 g of agarose powder (Sigma) in 100 mL of 1x Tris-Borate-EDTA (TBE buffer) (AppliChem - diluted from 10x stock), by heating. Cooled agarose agar was supplemented with Midori green advanced DNA stain (Nippon Genetics, Europe), at a volume of 5 µL per 100 mL agarose agar, and the agar was poured across a gel mould. Once set, the gel was removed from the mould and loaded into an electrophoresis gel tank and 1 x TBE buffer was added to coat the gel completely. Hyperladder 1 KB (5 µL) (Bioline) was loaded into the first well of the gel to quantify the DNA products by size. Each PCR reaction (10 µL) was loaded into the following wells. Electrophoresis was carried out at 100 V for 30-40 minutes, and the gel was analysed using Syngene G:Box (Geneflow).

For plasmid preparations and PCR purifications; 7 µL of plasmid preparation or PCR purification was loaded into sterile 0.8 mL microtubes with 3 µL of 5x DNA loading buffer (Bioline). Gel electrophoresis was carried out as previously described.

PCR product purification

All PCR product purifications were carried out using the QIAquick PCR Purification Kit (Qiagen). Briefly; the PCR sample was transferred to a QIAquick spin column and collection tube and 200 µL of Buffer PB was added. To bind the DNA to the spin column membrane, the tubes were centrifuged at 13,000 x g for ~1 minute. The flow-through was discarded into disinfectant and the membrane was washed by adding 750 µL of Buffer PE, and centrifuged at 13,000 x g for 1 minute. The flow-through was discarded and the tubes were centrifuged once more to remove the residual Buffer PE. DNA was eluted from the membrane by transferring the spin column to a sterile 1.5 mL microtube and aliquoting 50 µL of Buffer EB onto the membrane. The tubes were centrifuged at 13,000 x g for 1 minute. Gel electrophoresis was carried out as previously described.

2.4 Construction of the *csrA*::*aph* mutants

pKD4 plasmid preparation

The *csrA* gene was disrupted in SL1344 using the gene inactivation method described by Datsenko and Wanner (Datsenko and Wanner 2000). An overnight culture of *E. coli* pKD4, conferring kanamycin resistance by an aminoglycoside phosphotransferase, (*aph*), was prepared in LB supplemented with 50 µg/mL ampicillin and 50 µg/mL kanamycin to select for the plasmid and the resistance

cassette, respectively, and plasmid preparations were carried out as previously described, with analysis by gel electrophoresis.

The PCR was carried out using pKD4 plasmid preparations, using primers to amplify the kanamycin cassette with flanking *csrA* homology (*csrA* knock-out forward and reverse primers, Table 2.2). The *csrA*-tagged *aph* cassette PCR product (10 µL) was purified and analysed by gel electrophoresis.

Preparation of SL1344 pKD46 competent Cells

The low copy number plasmid, pKD46, was used as a template to replace the *csrA* gene in SL1344, by inducing recombination in host cells via the phage λ Red recombinase enzyme (Datsenko and Wanner 2000).

An overnight culture of SL1344 pKD46 was prepared in LB supplemented with 50 µg/mL ampicillin and 100 µL of 1 M Arabinose (for a final Arabinose concentration of 10 mM), to induce the recombination genes. After 24 hours, 1 mL of bacterial culture was inoculated into 50 mL sterile LB, supplemented with 50 µg/mL ampicillin and 100 µL of 1 M Arabinose (for a final Arabinose concentration of 10 mM). The culture was incubated aerobically at 30°C (to prevent plasmid loss), with shaking, until the OD_{600} reached mid-log phase (~0.6-1) and the culture was transferred to two sterile 30 mL universal tubes, which were kept on ice for ~10 minutes prior to prevent further growth of the bacteria. The tubes were centrifuged at 3600 RPM for 10 minutes at 1°C. The supernatant from each tube was discarded and the cells were washed in 15% ice cold glycerol 4 times. The pelleted cells were resuspended in 400 µL 15% ice cold glycerol by pipetting. Both universal tubes were pooled into one sterile 1.5

mL microtube and stored on ice, or at -20°C.

Electroporation of *csrA*-tagged *aph* cassette

SL1344 pKD46 competent cells (45 µL) were added to 5 µL of purified *csrA*-tagged *aph* cassette, in a pre-cooled electroporation cuvette. A pulse at 2.5 kV/200 ohm, lasting ~5 milliseconds, was used to disrupt the bacterial membrane in SL1344, using a gene pulser (Bio-Rad). Immediately after the pulse, 950 µL of sterile LB was added to the cuvette and the contents were aseptically transferred to a sterile 30 mL universal tube. A negative control was included, with 50 µL of competent cells only, to ensure that electroporation did not affect the viability of the bacteria. Universal tubes were incubated aerobically at 37°C for 2-4 hours to allow the bacteria to recover. Following recovery, 100 µL of the negative control was inoculated onto LB agar and spread with a disposable L-shaped spreader. Competent cells electroporated with the *csrA*-tagged *aph* cassette (100 µL) were inoculated onto LB agar supplemented with 50 µg/mL kanamycin to select for SL1344 cells where successful recombination had occurred. All of the remaining cells were transferred to two sterile 1.5 mL microtubes and centrifuged at 13,000 x g for 2 minutes to capture all of the remaining bacterial cells in the pellet. Each pellet was resuspended in 150 µL of the corresponding supernatant. Negative control cells (150 µL) were inoculated onto LB agar supplemented with 50 µg/mL ampicillin, to select for SL1344 cells with the pKD46 plasmid only. Competent cells with the *csrA*-tagged *aph* cassette (150 µL) were inoculated onto LB agar supplemented with 50 µg/mL kanamycin, as previously described. The plates were incubated statically in an aerobic incubator, at 37°C for 24-48 hours. Single positive colonies were restreaked onto fresh LB agar

supplemented with 50 µg/mL kanamycin and re-incubated.

Identification of *csrA*::*aph* candidates

SL1344 cells carrying the *csrA*-tagged *aph* cassette were identified by the PCR (using *csrA* check forward and reverse primers, Table 2.2) and the products were analysed by agarose gel electrophoresis. Protectant beads of the strain were prepared, and the strains were stored at -20°C.

Growth kinetics of the *csrA*::*aph* mutant

Initial cultures of the *csrA*::*aph* mutant in LB broth lead to the observation that the strain was slow-growing, compared to the wild-type, SL1344. The observed phenotype prompted the investigation of the growth kinetics of the *csrA*::*aph* mutant in LB broth, minimal media with glucose, and minimal media with pyruvate, which were compared to SL1344.

Overnight cultures of both strains in the three mediums were prepared, with the *csrA*::*aph* mutant cultures supplemented with 50 µg/mL kanamycin. After 24 hours, the cultures were diluted to 4% in fresh media (4 µL into 100 µL), in a 96-well flat-bottomed microtitre tray (MTT), as shown by Figure 2.1. The absorbance (at 600nm) of each well was measured for 620 minutes, using a FluoStar Optima (BMG, UK). The data was analysed in Microsoft Excel.

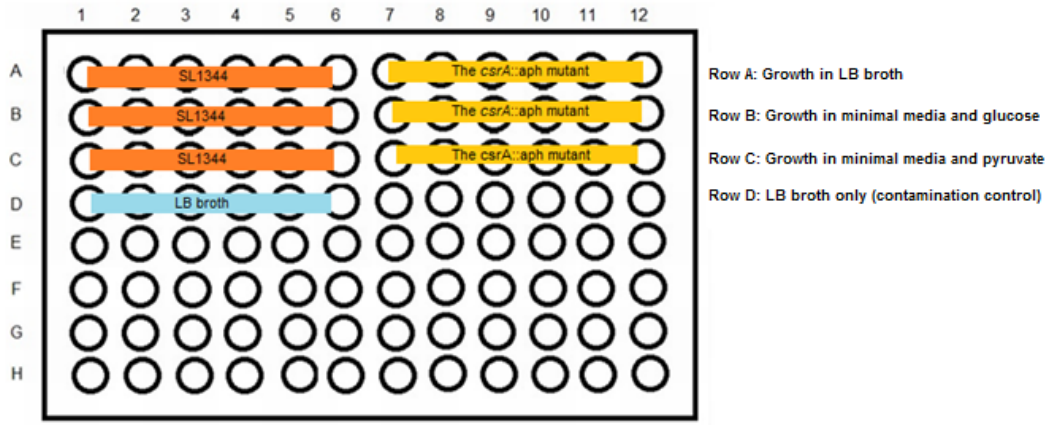

Figure 2.1: MTT layout for investigating the growth kinetics of the *csrA*::*aph* mutant and SL1344 in LB broth, minimal media + glucose, and minimal media + pyruvate.

2.5 Construction of the *csrA*::*aph* mutants with pMW82-p*ramA*, pMW82-p*acrAB* and pMW82-p*tolC* reporters

pMW82-p*ramA*, pMW82-p*acrAB* & pMW82-p*tolC* plasmid preparations

Plasmid pMW82-p*ramA* encodes a GFP fused to a DNA fragment carrying the *ramA* promoter sequence. As a *csrA* deletion had been associated with increased *ramA* expression during previous investigations by Ricci and Piddock (unpublished data), the fluorescence of the pMW82-p*ramA* reporter in the *csrA*::*aph* mutant was investigated and compared to the wild-type strain, SL1344. Additionally, the effect of the *csrA* gene disruption on the fluorescence of *acrAB* and *tolC* reporters (pMW82-p*acrAB* and pMW82-p*tolC*), encoding the components of the AcrAB-TolC efflux pump, was also investigated.

Overnight cultures of each reporter construct were prepared in LB supplemented with 50 µg/mL ampicillin, to select for the plasmids. Plasmid preparations were carried out and analysed by gel electrophoresis.

Preparation of SL1344 *csrA*::*aph* competent cells

Due to the observed slow growth phenotype, *csrA*::*aph* mutant cultures struggled to reach mid-log phase on the day of testing, therefore a 50 mL overnight culture was prepared in LB, supplemented with 50 µg/mL kanamycin, to be used immediately the following day to make competent cells, as previously described, without Arabinose.

Electroporation of pMW82-p*ramA,* pMW82-p*acrAB* & pMW82-p*tolC* reporters

Electroporation was performed using the same conditions as previously described. SL1344 *csrA*::*aph* cells that had taken up the pMW82-p*ramA,* pMW82-p*acrAB* or pMW82-p*tolC* constructs were selected on LB agar supplemented with 50 µg/mL kanamycin and 50 µg/mL ampicillin (to select for the *csrA* disruption and the reporter construct, respectively). The plates were incubated statically in an aerobic incubator, at 37°C for 24-48 hours. Single colonies were restreaked onto fresh LB agar supplemented with 50 µg/mL kanamycin and 50 µg/mL ampicillin and re-incubated.

Identification of *csrA*::*aph* candidates with pMW82-p*ramA,* pMW82-p*acrAB* & pMW82-p*tolC* reporters

Lysate preparations were prepared of candidate *csrA*::*aph* mutants that had successfully taken up each reporter construct, and SL1344 (negative control) as previously described. The PCR reactions were prepared using a set of primers to identify the *csrA* deletion (*csrA* check forward and reverse primers, Table 2.2), and a set of primers to identify if each reporter construct was encoded by the strain (Table 2.2). The PCR conditions were: 95°C for 5 minutes (denaturation), 95°C for 30 seconds, 50°C for 30 seconds, 68°C for 2 minutes (annealing), for a total of 35 cycles

and 68°C for 10 minutes (extension).

The effect of *csrA*::*aph* on the transcription of *acrAB*, *tolC* & *ramA*

The effect of the *csrA* disruption to the transcription of *acrAB*, *tolC* and *ramA* was investigated and compared with the wild-type strain, SL1344, using fluorescence as an empirical measure of promoter activity.

Overnight cultures of SL1344 and the SL1344 *csrA*::*aph* mutant harbouring pMW82-p*ramA*, pMW82-p*acrAB* and pMW82-p*tolC*, were prepared in LB supplemented with 50 µg/mL kanamycin and 50 µg/mL ampicillin. After 24 hours, the cultures were diluted 4% into fresh LB (4 µL into 100 µL LB), in a 96-well flat-bottomed MTT, as shown by Figure 2.2. The absorbance (at 600 nm) and fluorescence (excitation at 492 nm, emission at 520 nm) of each well was measured, using a FluoStar Optima (BMG, UK). The data was analysed in Microsoft Excel.

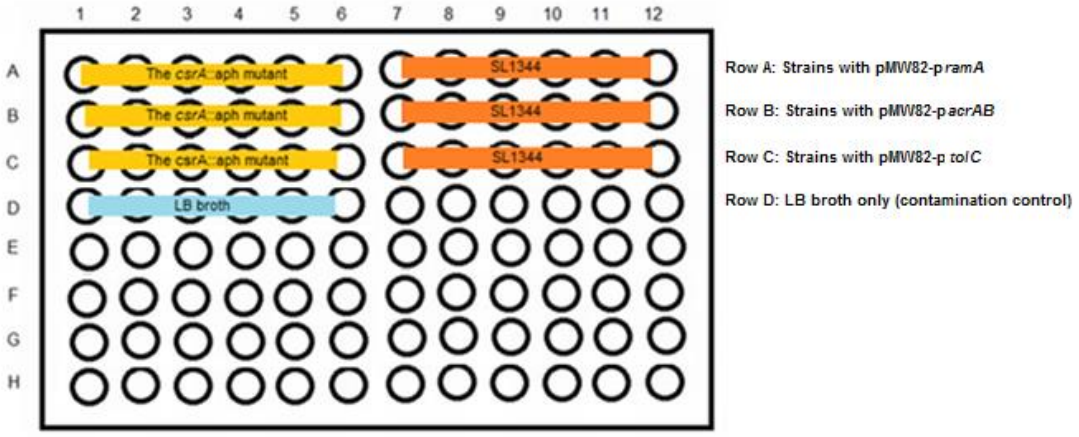

Figure 2.2: MTT layout for investigating the effect of *csrA*::*aph* on the transcription of *ramA, acrAB* and *tolC.*

2.6 The effect of *csrA*::*aph* on the expression of *acrA, acrB, tolC, ramA, marA, soxS*, *rob* & *ramR*

RNA preparation

The global transcriptional activators of *acrAB* in Enterobacteriaceae are encoded by *ramA, marA, soxS and rob* (Perez, Poza et al. 2012), therefore Real-Time (RT) PCR was used to investigate the expression of *acrA, acrB, tolC*, *ramA, marA, soxS, rob and ramR* - the transcriptional repressor of RamA, in the *csrA*::*aph* mutant and compared to the wild-type, SL1344.

The *csrA*::*aph* mutant displayed poor growth in minimal media, the standard media used to make RNA preparations, therefore triplicate overnight cultures of the *csrA*::*aph* mutant and wild-type, SL1344, were set up in LB broth. The *csrA*::*aph* mutant culture was supplemented with 50 µg/mL kanamycin. Triplicate working cultures of SL1344 were prepared on the day of testing by inoculating 200 µL of each overnight culture into 10 mL sterile LB. The tubes were incubated aerobically at 37°C, with shaking, until the cells reached mid-log phase (OD_{600} ~0.6-1). Triplicate overnight cultures of the *csrA*::*aph* mutant were used immediately, due to poor growth of the strain.

Each culture (1 mL) was aseptically transferred to a sterile 1.5 mL microtube and the tubes were centrifuged at 14,000 x g for 2 minutes. The supernatants were removed, and a further 1 mL of culture was added, to increase the concentration of pelleted bacteria and RNA yield. The tubes were centrifuged at 14,000 x g for 2 minutes and the remaining pellet was resuspended in 100 mL of 3 mg/mL Lysozyme (Sigma) in TE buffer, which was prepared from powder stored at -20°C, on the day of testing.

The resuspended pellets were incubated at room temperature for ~5 minutes, before

adding 75 µL of RNA Lysis Buffer and 350 µL of RNA Dilution Buffer (Promega), to break down the cellular material and release the bacterial RNA. The tubes were inverted to mix the contents and 200 µL of 95% ethanol was added to each tube. After pipetting to mix, the contents of each tube were transferred to a spin column and collection tube, and centrifuged at 13,000 x g for 1 minute, to elute the RNA onto the membrane. The solutions were discarded from the collection tubes and 600 µL of RNA wash solution was added to the spin columns. The tubes were centrifuged at 13,000 x g for 1 minute and the solutions were discarded from the collection tubes.

A DNase incubation mixture was prepared using the following reagents (stored at -20°C and thawed on ice), at the following volumes per sample: 40 µL Yellow Core Buffer, 5 µL 0.09M $mnCl_2$ and 5 µL DNase I enzyme. DNase incubation mix (50 µL) was added to the membrane of each spin column, and was incubated for 15 minutes at room temperature to digest contaminating genomic DNA. DNase Stop Solution (200 µL) was added to the spin columns and centrifuged at 13,000 x g for 1 minute. The solutions were discarded from each collection tube, 600 µL of RNA Wash Solution was added and the tubes were centrifuged at 13,000 x g for 1 minute. The solutions were discarded from each collection tube, 250 µL of RNA Wash Solution was added, and the tubes were centrifuged at 13,000 x g for 2 minutes. The spin columns were transferred to sterile RNase-free 1.5 mL microtubes and 100 µL of nuclease-free water was added to each membrane. The tubes were centrifuged at 13,000 x g for 1 minute, to elute the RNA. The RNA preparations were kept on ice and stored at -80°C.

DNA and RNA quantification

The DNA and RNA in each RNA preparation was quantified using a Qubit 2.0 Fluorometer (Invitrogen) and Molecular Probes DNA Labelling and Detection Qubit ds DNA and RNA HS Assay Kits (Invitrogen). The kits contained double-stranded (ds) DNA or double-stranded (ds) RNA HS buffers and dsDNA or dsRNA HS reagents (200x concentrate in Dimethyl Sulfoxide). A master mix was prepared, containing 199 µL of dsDNA or dsRNA HS buffer and 1 µL of dsDNA or dsRNA HS reagent, per sample. Each RNA preparation (1 µL) was added to 199 µL of the master mixture in sterile 0.8 mL RNase-free microtubes. In order to calibrate the Qubit 2.0 Fluorometer before quantification, 2 DNA standards and 2 RNA standards were also prepared by adding 190 µL of the master mix to 10 µL of either dsDNA HS Standard 1 and dsDNA HS Standard 2, or dsRNA HS Standard 1 and dsRNA HS Standard 2 (stored at 4°C), in sterile 0.8 mL RNase-free microtubes.

DNase Treatment

Quantified DNA and RNA in ng/mL per sample was used to calculate the volume of RNA, TURBO DNase, buffer and nuclease-free water to use for an additional DNase treatment (final reaction volume of 50 µL), to maximise the RNA yield from the samples. All reagents were stored at -20°C and thawed on ice. RNA and the above reagents were inoculated into sterile RNase-free 0.8 mL microtubes and incubated for ~20 minutes in a microtube hotplate set to 37°C. DNase Inactivation Reagent (5 µL) was added and mixed by pipetting. The tubes were incubated for 5 minutes at room temperature and centrifuged for 2 minutes at 10,000 x g. The supernatants containing the RNA were transferred to new sterile RNase-free microtubes, and the

DNA and RNA in each RNA preparation was re-quantified as previously described. It was acceptable to proceed to cDNA synthesis if the DNA was < 5% of each RNA preparation.

cDNA synthesis

Re-quantified DNA and RNA in ng/mL per sample was used to calculate the volume of RNA required for cDNA synthesis to proceed with the RT PCR. Random primers, deoxyribonucleotide triphosphate (dNTP), 1st Strand Buffer, DTT, RNase Out and Super-script (reverse transcriptase) were stored at -20°C and thawed on ice. RNA, 2 µL random primers, 1 µL dNTP and nuclease-free water were aliquoted into sterile 1.5 mL RNase-free microtubes, in duplicate, with a total volume of 13 µL per sample. The tubes were heated to 65 °C for 5 minutes on a microtube hotplate, then incubated on ice for a further 5 minutes. 1st Strand Buffer (4 µL), 1 µL 0.1M DTT, 1 µL RNase Out, and 1 µL Super-script were added to one of each duplicate tubes. The second set of tubes were non-reverse transcriptase controls, therefore 1 µL nuclease-free water was used in place of the Super-script. All tubes were incubated at room temperature for 5 minutes, then heated to 50°C for 60 minutes on a microtube hotplate. To inactivate the reaction, the tubes were heated to 70°C for 10 minutes. cDNA preparations were stored on ice or at -20°C.

Real Time PCR (RT-PCR)

acrA, acrB, tolC, ramA, marA, soxS, rob and *ramR* gene expression was investigated in the *csrA*::*aph* mutant and wild-type, SL1344, using RT PCR.

Master mixes were prepared by adding the following reagents, which were stored at -

20°C and thawed on ice: 12.5 µL IQ^{tm} SYBR Green Supermix (Bio-Rad), 1 µL Forward Primer (12 mM working stock) and 1 µL Reverse Primer (12 mM working stock), per sample. To make up the reaction volume to 24 µL, 9.5 µL nuclease-free water was added, per sample. Master mix (24 µL) and 1 µL of cDNA sample were aliquoted into the wells of a RT PCR plate, as shown by Figure 2.3.

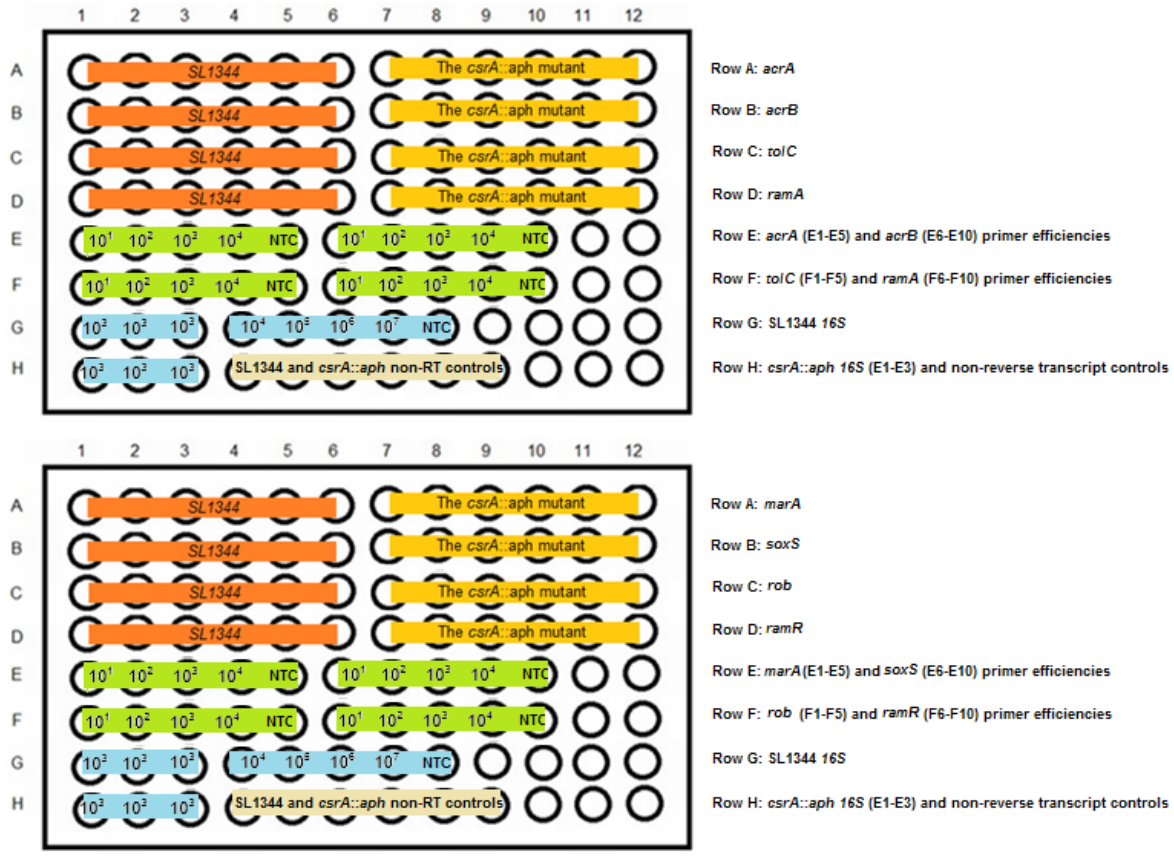

Figure 2.3: RT-PCR plate layout for investigating the effect of *csrA* disruption on the expression of *acrA, acrB, tolC, ramA, marA, soxS*, rob & *ramR.* (NTC: non-transcribed control).

The plate was pulse-centrifuged and loaded into a RT PCR machine (Bio Rad). The PCR conditions were: 95°C for 3 seconds (denaturation), 95°C for 10 seconds, 57.3°C for 20 seconds, 72°C for 20 seconds (annealing), with a total of 29 cycles.

A fluorophore generated fluorescence following each amplification cycle in real-time, so it was possible to compare the initial copy number of the genes in the *csrA*::*aph* mutant and the wild-type, SL1344. The bacterial *16S* "house-keeping" gene was used to normalise gene expression, as it is consistently expressed in bacteria. A melt curve was also included (50°C for 5 seconds and 95°C for 5 seconds). The data was analysed in Microsoft Excel.

2.7 Biofilm formation and curli synthesis in the *csrA*::*aph* mutant (SL1344)

Inactivated *acrB* or *tolC* efflux components have been associated with a defect in biofilm formation (Baugh, Ekanayaka et al. 2012), in addition to an increase in *ramA* expression (Baugh, Phillips et al. 2013). Therefore, a biofilm assay was carried out to determine the effect of the *csrA* disruption on the formation of competent biofilm.

Overnight cultures were set up of the *csrA*::*aph* mutant, wild-type SL1344, 14028S (positive biofilm control) and 14028S Δ*tolC* (negative biofilm control) in sterile LB broth. The *csrA*::*aph* mutant was supplemented with 50 µg/mL kanamycin. After 24 hours, the cultures were diluted to an OD_{600} of ~0.1 in 10 mL sterile LB broth without salt, prepared by dissolving 10 g Tryptone, 5 g Yeast Extract and 15 g Biological Agar (Oxoid), in 1 L of SDW. Each diluted culture (200 µL) was inoculated into the wells of a sterile 96-well MTT, as shown by Figure 2.4. The plate was loosely covered with cling film to prevent evaporation, and incubated at 30°C for 48 hours with gentle shaking, to allow the formation of biofilm. Following incubation, the liquid culture was removed from the wells into a discard pot containing disinfectant solution and the wells were rinsed with SDW. A 1% Crystal Violet solution (200 µL) was used to stain the biofilm in each well for 15 minutes at room temperature, which was then rinsed

away using SDW. A 70% Ethanol solution (200 µL) was added to each well to solubilise the dye and the absorbance (at 600nm) of each well was measured using a FluoStar Optima (BMG UK). The data was analysed in Excel.

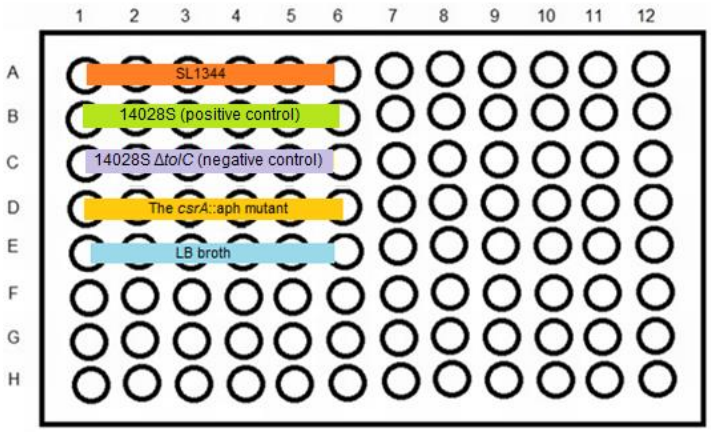

Figure 2.4: MTT layout for investigating biofilm formation in the *csrA*::aph mutant, SL1344 and 14028S positive and negative biofilm controls.

Curli are involved in competent biofilm formation, therefore the production of curli in the *csrA*::*aph* mutant was investigated alongside biofilm formation. Congo Red agar was prepared by autoclaving LB agar without salt, and when cooled, Congo Red was added to a final concentration of 40 µg/mL.

Overnight cultures were set up of the *csrA*::*aph* mutant, wild-type SL1344, 14028S (positive curli control) and 14028S Δ*tolC* (negative curli control). The overnight cultures were diluted 1:100 in sterile Phosphate Buffered Saline (PBS) (Sigma), and four 5 µL aliquots were spotted onto quarterly-divided Congo Red plates, as shown by Figure 2.5. A negative contamination control was prepared by spotting four 5 µL aliquots of sterile PBS. All plates were incubated aerobically in a static incubator, at 30°C for 24-48 hours, and analysed for curli morphology using a light microscope.

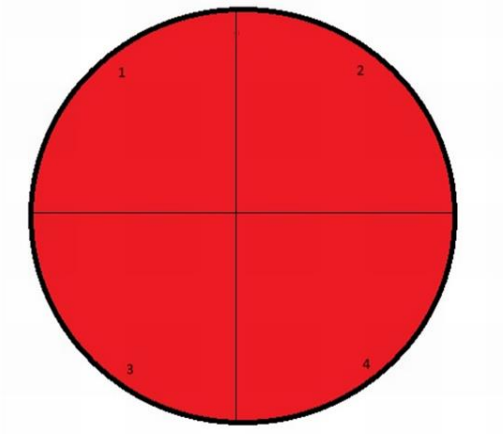

Figure 2.5: Division of Congo Red agar plates for investigating curli synthesis in the *csrA*::*aph* mutant.

P22 transduction of the *csrA*::*aph* mutant into 14028S

The positive biofilm control strain used in this study, 14028S, was able to form competent biofilm to a high level, therefore P22 transduction was carried out to transduce *csrA*::*aph* into the 14028S background, with an aim to repeat the biofilm and curli assays, and confirm the phenotype caused by *csrA* disruption.

A *csrA*::*aph* phage stock was prepared as follows; an overnight culture of the *csrA*::*aph* mutant was prepared in LB broth and after 24 hours, the culture was diluted 1:100 in sterile LB broth containing 10mM $MgSO_4$ and 5 mM $CaCl_2$. The culture was incubated aerobically at 37°C, shaking, for 30 minutes. SL1344 P22 phage stock (5 µL) was added and the culture was incubated aerobically for 24 hours at 37°C, shaking. The following day, the culture was transferred to a 50 mL sterile Falcon tube, and 1 mL chloroform was added. The tube was vortexed and centrifuged at 4000 RPM for 10 minutes at 4°C. The supernatant was transferred to a sterile glass universal tube to prevent chloroform damage, and 200 µL chloroform was added. The *csrA*::*aph* P22 phage stock was stored at 4°C.

An overnight culture of 14028S was prepared in LB broth and after 24 hours, the

culture was centrifuged at 4000 RPM for 5 minutes at room temperature. The supernatant was discarded and the pellet was resuspended in 10mM $MgSO_4$ and 5mM $CaCl_2$. Transductions were prepared with different volumes of phage stock, with an aim of avoiding bacterial cell lysis, as shown by Table 2.3.

Microtube	**Volume of 14028S cells added (µL)**	**Volume of *csrA*::*aph* P22 phage stock added (µL)**
1	100	0
2	100	5
3	100	10
4	100	50
5	100	100
6	100	500

Table 2.3: Volumes of *csrA*::*aph* phage used for *csrA*::*aph* transduction into 14028S.

The transductions were incubated aerobically at 37°C for 15 minutes and were then transferred to sterile 30 mL universal tubes. Sodium Citrate (1 M) and 1 mL sterile LB broth were added to recover the cells. The tubes were incubated aerobically for 45 minutes at 37°C, with shaking. Each transduction (100 µL) was plated in duplicate on LB agar (negative control) and LB agar supplemented with 50 µg/mL kanamycin (to select for the *csrA* deletion in 14028S). Plates were incubated aerobically at 37°C for 24-48 hours. Single positive colonies were restreaked onto fresh LB agar supplemented with 50 µg/mL kanamycin and re-incubated. To confirm *csrA*::*aph* in 14028S, a PCR was carried out using primers to identify the *csrA* deletion, as previously described. Biofilm and curli assays were repeated as previously described.

2.8 Antimicrobial susceptibility of the *csrA*::*aph* mutant

AcrAB-TolC is known to efflux a number of structurally distinct antimicrobial substrates (Giraud, Cloeckaert et al. 2000), (Piddock, White et al. 2000) (Baucheron, Imberechts et al. 2002), (Baucheron, Chaslus-Dancla et al. 2004), (Eaves, Ricci et al. 2004), (Bailey, Ivens et al. 2010), therefore the susceptibility of the *csrA*::*aph* mutant to substrates of the efflux pump was investigated, and compared to the susceptibilities of SL1344, SL1344 *ramR*::*aph* and *E. coli* (Table 2.4).

Antibiotic	**Potency**	**Storage**	**Solubility**	**Concentrations used for testing in µg/mL**
Ciprofloxacin	>98	4°C	Dissolve in 100 µL acetic acid, then SDW	1-0.0075
Nalidixic Acid	≥ 98	-20°C	Dissolve in SDW	64-0.5
Chloremphenicol	>98	4°C (poisons box)	Dissolve in 70% Methanol	32-0.5
Tetracycline	95	-20°C	Dissolve in SDW	32-0.5
Ethidium Bromide	95	Room temperature (poisons box)	Dissolve in SDW	2048-32

Table 2.4: Antimicrobial compounds investigated, their potency, storage, solubility and concentrations tested.

Overnight cultures of each strain were prepared in LB broth. The *csrA*::*aph* mutant was supplemented with 50 µg/mL kanamycin. After 24 hours, three inoculation dilutions were prepared by serial dilution in SDW: 1 x 10^9 cfu/mL (overnight stock), 1 x 10^7 cfu/mL and 1 x 10^5 cfu/mL. Iso-Sensitest agar (1 L) (Oxoid) was prepared and autoclaved on the day of testing. Sterile 30 mL universals and sterile plastic, vented petri dishes were labelled for each antibiotic dilution investigated. “Start” and “Finish” universal tubes and petri dishes were also labelled; these were absent of antibiotic (negative controls), to ensure there was no external contamination during the

duration of the study. The volume of antibiotic dilutions added to each sterile 30 mL universal to achieve the correct concentration in 20mL Iso agar, is summarised by Table 2.5.

Antibiotic concentrations used for testing in µg/mL	**Volume of antibiotic stock added per agar plate**
0.075	15 µL of 10 µg/mL stock
0.015	30 µL of 10 µg/mL stock
0.03	60 µL of 10 µg/mL stock
0.06	13 µL of 100 µg/mL stock
0.12	25 µL of 100 µg/mL stock
0.25	50 µL of 100 µg/mL stock
0.50	100 µL of 100 µg/mL stock
1	20 µL of 1000 µg/mL stock
2	40 µL of 1000 µg/mL stock
4	80 µL of 1000 µg/mL stock
8	160 µL of 1000 µg/mL stock
16	320 µL of 1000 µg/mL stock
32	64 µL of 10,000 µg/mL stock
64	128 µL of 10,000 µg/mL stock
128	256 µL of 10,000 µg/mL stock
256	512 µL of 10,000 µg/mL stock
512	1024 µL of 10,000 µg/mL stock
1024	2048 µL of 10,000 µg/mL stock
2048	4096 µL of 10,000 µg/mL stock

Table 2.5: Volumes of antimicrobial compounds used to obtain the appropriate concentrations for testing. Stocks were prepared by serial 1:10 dilutions from an initial stock of 10,000 µg/mL, which were prepared on the day of testing.

Iso agar (20 mL) was automatically dispensed into each universal tube, and these were immediately poured into the appropriately-labelled petri dishes and oven dried.

An MIC template was prepared as shown in Figure 2.6.

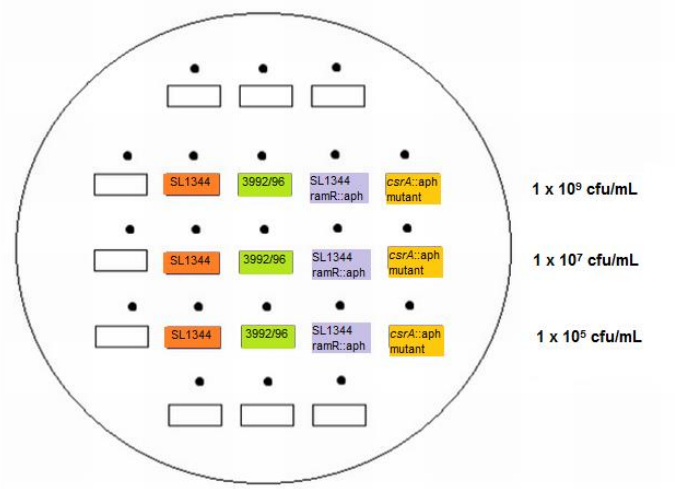

Figure 2.6: MIC template layout for investigating the antimicrobial susceptibility of the *csrA*::*aph* mutant.

A multipoint inoculator was used to dispense 1 µL from the MIC template, onto each agar plate. The final concentration of each spot was 1 x 10^6 cfu/mL, 1 x 10^4 cfu/mL and 1x 10^2 cfu/mL, respectively (Figure 10). All plates were incubated aerobically at 37°C for 24 hours, and analysed by eye. The MIC of each antibiotic was defined as an 80% or greater reduction in the growth of the bacteria.

3.0 Results

3.1 Construction of the *csrA*::*aph* mutants

E. coli plasmid pKD4, conferring kanamycin resistance by an *aph* gene, was used to replace the *csrA* gene in SL1344 with a kanamycin resistance cassette, following the gene activation protocol originally described by Datsenko and Wanner (Datsenko and Wanner 2000). One set of *csrA* knock-out primers was designed to amplify the kanamycin resistance cassette with flanking regions of homology to the *csrA* gene (*csrA*-tagged *aph* cassette), and recombination was stimulated in SL1344 via the low copy number plasmid, pKD46, encoding the phage λ Red recombinase enzyme, where arabinose was used to induce the enzyme promoter.

Duplicate pKD4 plasmid preparations were analysed by gel electrophoresis, producing bands at ~6000 bp (Figure 3.1 A). The DNA in each plasmid preparation was quantified using a Qubit 2.0 Fluorometer (Invitrogen); values were 1.22 µg DNA/mL (pKD4 preparation 1) and 1.51 µg DNA/mL (pKD4 preparation 2). The PCR was used to amplify the *csrA*-tagged *aph* cassette in pKD4, and the PCR amplimer was confirmed by agarose gel electrophoresis both before and after PCR purification, to ensure DNA was not lost during the process. The resulting amplimers were ~1500 bp in size (Figure 3.1 B).

The *csrA*-tagged *aph* cassette was introduced into SL1344 carrying plasmid pKD46 by electroporation, and confirmed by PCR (Figure 3.1 C). The *csrA*-tagged *aph* cassette band size was ~1500 bp, as expected.

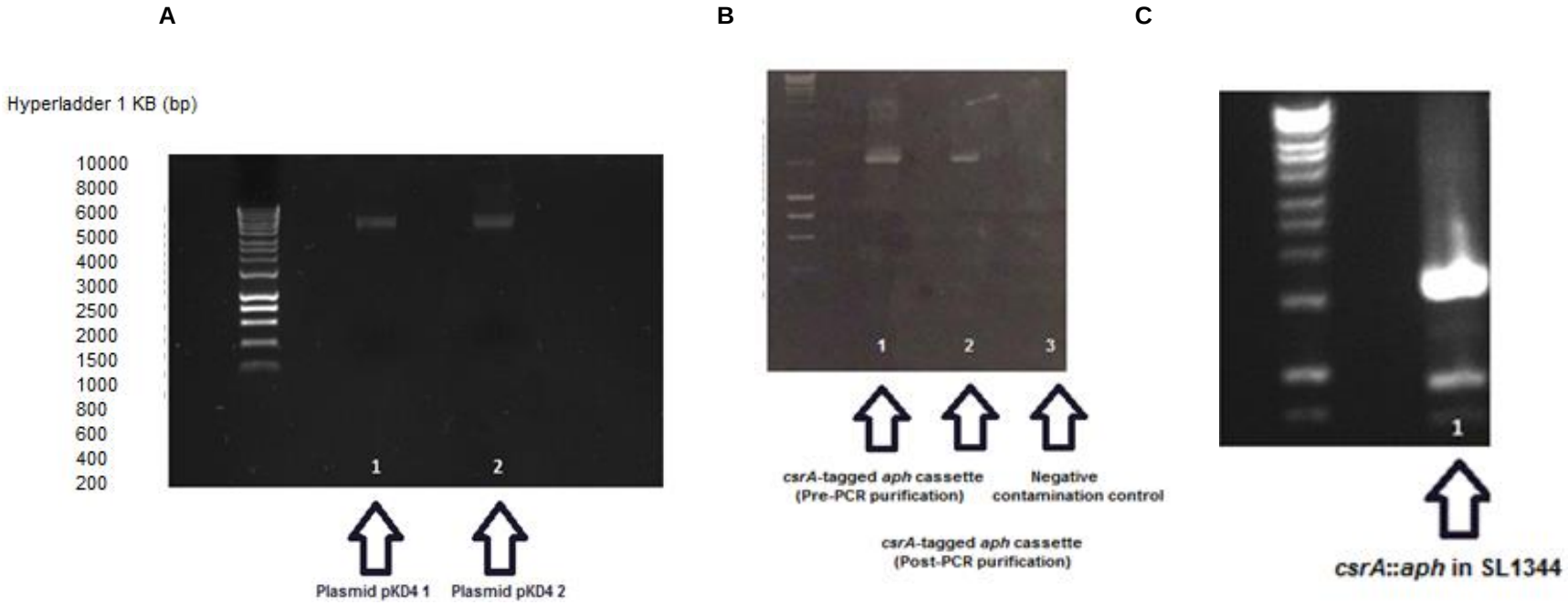

Figure 3.1 A (left): Gel confirmation of pKD4 plasmid preparations (lane 1 and 2). HyperLadder 1KB is annotated to the left of the figure, B (middle): PCR confirmation of *csrA*-tagged *aph* cassette amplification in pKD4 (lane 1 and 2), C (right): PCR confirmation of SL1344 *csrA*::*aph* mutants (lane 1).

3.2 Growth kinetics of the *csrA*::*aph* mutant

Following the selection of the *csrA*::*aph* mutant on LB agar supplemented with kanamycin, it was observed that the mutant displayed a slow-growth phenotype in LB broth supplemented with kanamycin. Therefore, the growth kinetics of the *csrA*::*aph* mutant in LB broth, minimal media with glucose and minimal media with pyruvate were investigated and compared to the wild-type strain, SL1344 (Figures 3.2 A, B, C).

In LB broth, the *csrA*::*aph* mutant had a longer lag-phase compared to SL1344 and struggled to reach mid-log phase (OD_{600} of ~0.6-1) for the duration of the experiment (Figure 3.2 A). Extrapolation of the data suggests that where it took ~90 minutes for the OD_{600} of SL1344 to double (OD_{600} 0.2 to 0.4), the *csrA::aph* mutant had a much longer generation time of ~140 minutes (Table 3.1). A similar trend between the strains was observed when they were grown in minimal media with glucose and minimal media with pyruvate (Figures 3.2 B and C, Table 3.1), although both strains struggled to reach mid-log phase in these media. In minimal media with pyruvate, the *csrA*::*aph* mutant reached a maximum OD_{600} of 0.12, after which, cell division ceased and cell death began to occur (Figure 3.2 C). Of the three media tested, the *csrA*::*aph* mutant grew best in LB broth, therefore all further studies involving this mutant were carried out in LB media.

Media Tested	SL1344 Generation Time	csrA::*aph* mutant Generation Time
LB Broth	OD_{600} 0.2 – 0.4: ~90 minutes	OD_{600} 0.2 – 0.4: ~140 minutes
Minimal media with glucose	OD_{600} 0.05 – 0.1: ~50 minutes	OD_{600} 0.05 – 0.1: ~350 minutes
Minimal media with pyruvate	OD_{600} 0.05 – 0.1: ~70 minutes	OD_{600} 0.05 – 0.1: ~150 minutes

Table 3.1: Generation times of the *csrA*::*aph* mutant and wild-type, SL1344, in LB broth, minimal media and glucose and minimal media and pyruvate. Extrapolated from Figure 3.2.

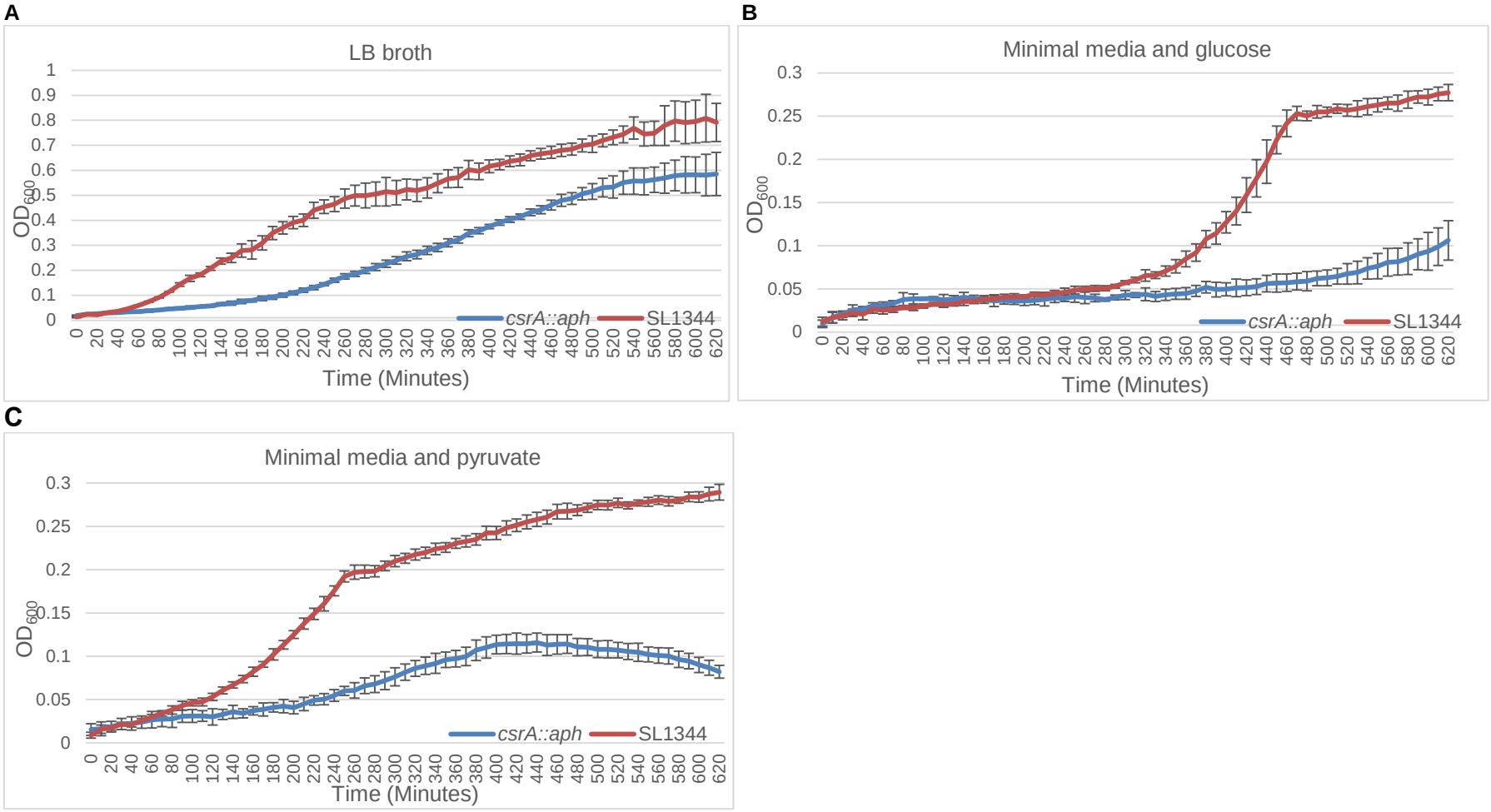

Figure 3.2 A: Growth of the *csrA*::*aph* mutant and SL1344 in LB broth over 620 minutes (n=6, +/- SD), B: Growth of the *csrA*::*aph* mutant and SL1344 in minimal media with glucose over 620 minutes (n=6, +/- SD), C: Growth of the *csrA*::*aph* mutant and SL1344 in minimal media with pyruvate over 620 minutes (n=6, +/- SD).

3.3 Identification of *csrA*::*aph* candidates with pMW82-p*ramA,* pMW82-p*acrAB* & pMW82-p*tolC* reporters

TraDIS sequencing of SL1344 associated a *csrA* deletion with increased *ramA* expression (Ricci and Piddock, unpublished data), therefore plasmid pMW82-p*ramA* encoding a GFP fused to a DNA fragment carrying the *ramA* promoter was prepared to investigate *ramA* transcription activity in the *csrA*::*aph* mutant, compared to the wild-type, SL1344. Additionally, strains containing the *acrAB* and *tolC* GFP reporter plasmids were prepared, to investigate the effect of *csrA* disruption on the expression of genes encoding the AcrAB-TolC efflux pump, of which RamA is a transcriptional activator.

The pMW82-p*ramA* plasmid preparation was analysed by gel electrophoresis, producing an amplimer at ~5000-6000 bp (Figure 3.3 A). The plasmid was introduced into the *csrA*::*aph* mutant by electroporation and confirmed by PCR (Figure 3.3 B). As expected, the strain had both the *csrA* deletion (Figure 3.3 B, lane 1) and the insertion of pMW82-p*ramA* (Figure 3.3, lane 4). The pMW82-p*ramA* amplimer size was ~800-1000 bp, which was not present in the wild-type strain, SL1344 (Figure 3.3 B, lane 5). The wild-type *csrA* amplimer size in SL1344 was ~240 bp, reflecting the size of the gene (Figure 3.3 B, lane 2). Similarly, pMW82-p*acrAB* and pMW82-*ptolC* plasmid preparations were analysed by gel electrophoresis (Figure 3.3 C) and introduced into the *csrA*::*aph* mutant by electroporation, confirmed by PCR. Each plasmid was ~800-1000 bp in size (Figure 3.3 D lanes 1 and 4), and not present in the wild-type strain, SL1344 (Figure 3.3 D, lanes 2 and 5).

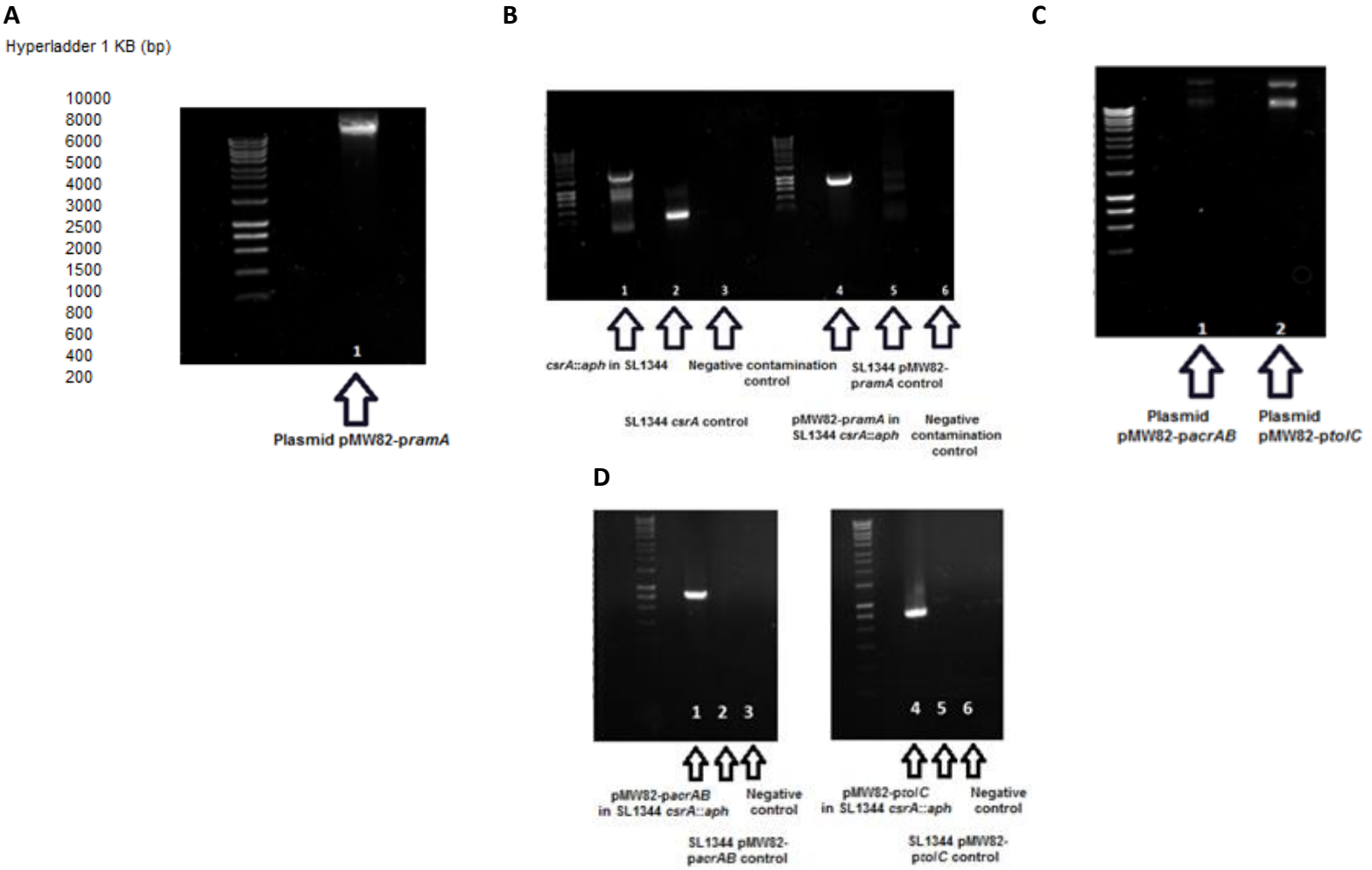

Figure 3.3 A: Gel confirmation of pMW82-p*ramA* plasmid preparations (lane 1). HyperLadder 1KB is annotated to the left of the figure, B: PCR confirmation of *csrA*::*aph* mutants with pMW82-p*ramA* reporter (lane 4), C: Gel confirmation of pMW82-p*acrAB* & -p*tolC* plasmid preparations (lane 1 and 2), D: PCR confirmation of *csrA*::*aph* with pMW82-p*acrAB* & -p*tolC* reporters (lane 1 and lane 4).

The effect of *csrA*::*aph* on the transcription of *acrAB*, *tolC* & *ramA*

Following the construction of SL1344 *csrA*::*aph* mutants encoding a GFP fused to the promoter regions of *acrAB*, *tolC* and *ramA*, GFP expression and therefore promoter activity for each gene, was measured in the *csrA*::*aph* mutant and compared to that in SL1344 containing the reporter constructs.

The student T-Test was used to test the null hypothesis that fluorescence (AU) was equal in the *csrA*::*aph* mutant encoding *acrAB*, *tolC* and *ramA* promoters, compared to the wild-type, SL1344. As a *csrA* deletion had been associated with an increase in the transcription of *ramA* prior to this study (Ricci and Piddock, unpublished data), and increased *ramA* expression has been associated with an increase in *acrAB-tolC* expression (Nikaido, Yamaguchi et al. 2008), (Ricci and Piddock 2009), (O'Regan, Quinn et al. 2009), it was hypothesised that fluorescence was greater in the *csrA*::*aph* mutant, therefore a one-tailed distribution was assumed (two-sample assuming equal variance). A p-value of less than 0.05 = * significance, less than 0.01 = ** significance, and 0.001 = *** significance.

The *csrA*::*aph* mutant encoding pMW82-p*ramA* emitted fluorescence 2.1 fold higher compared to the wild-type strain (5956 AU vs 12504 AU, Figure 3.4), suggesting increased transcription of *ramA* in the *csrA*-deficient strain (n=6, p-value: 5.03×10^{-17}). Fluorescence in the *csrA*::*aph* mutant encoding pMW82-p*tolC* decreased by 1.9 fold compared to the wild-type strain (5600 AU vs 3097 AU, Figure 21) and the fluorescence generated by the *csrA*::*aph* mutant encoding pMW82-p*acrAB* decreased by 3.9 fold (18000 AU vs 4578 AU, Figure 3.4), suggesting decreased

transcription of *acrAB* and *tolC* in the *csrA*-deficient strain (n=6, p-values: 6.31 x 10^{-22} and 6.83 x 10^{-28} for *tolC* and *acrAB*, respectively.

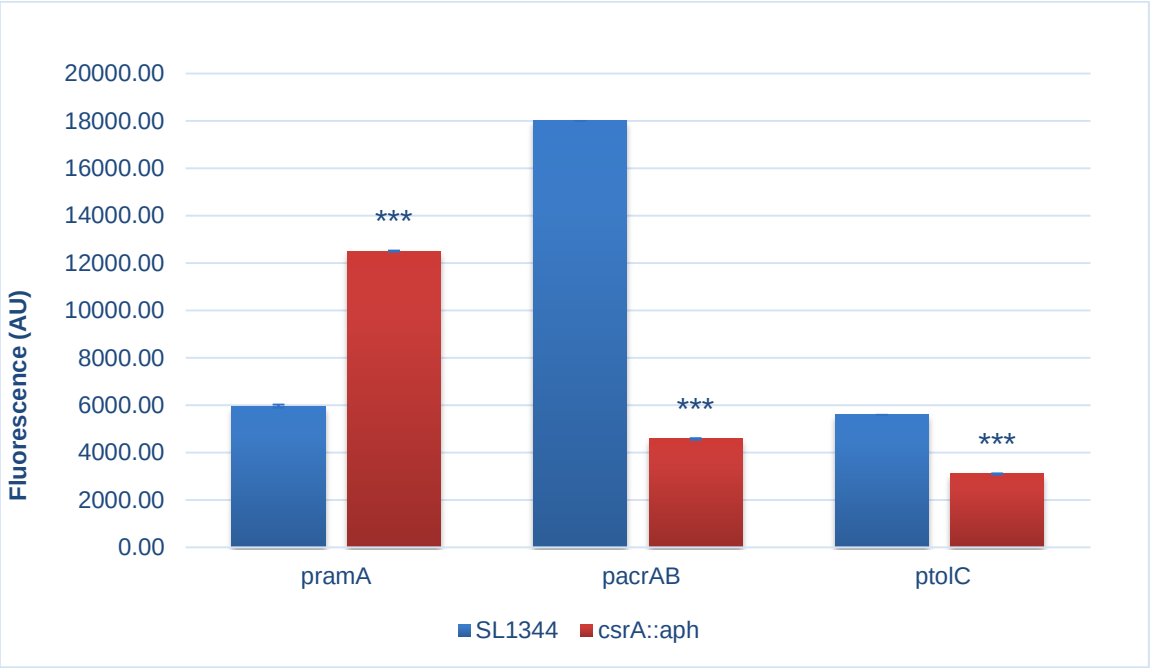

Figure 3.4: GFP was fused to DNA fragments carrying the promoter regions of *acrAB*, *tolC* and *ramA*. Fluorescence was used as an empirical measure of *acrAB*, *tolC* and *ramA* promoter activity in the *csrA*::*aph* mutant and the wild-type strain, SL1344. Fluorescence was measured in AU after 192 minutes (n=6, +/- SD).

3.4 The effect of *csrA*::*aph* on the expression of *acrA, acrB, tolC, ramA, marA, soxS*, *rob* & *ramR*

The global transcriptional activators of *acrAB* in Enterobacteriaceae are encoded by *ramA, marA, soxS and rob* (Perez, Poza et al. 2012), therefore RT PCR was used to investigate the expression of *acrA, acrB, tolC*, *ramA, marA, soxS, rob and ramR* in the *csrA*::*aph* mutant and compared to the wild-type, SL1344. *ramR* expression was interrogated in order to confirm whether the apparent high transcription rate of *ramA* (Figure 3.4) was due to a decrease in repression by RamR.

Consistent with fluorescence data (Figure 3.4), *ramA* expression increased in the *csrA*::*aph* mutant, compared to the wild-type strain (Figure 3.5) (n=6, p-value: 3.5 x 10^{-3}). The expression of the transcriptional activators *marA* and *soxS* also increased in the *csrA*-deficient strain (n=6, p-values: 6.5 x 10^{-3} and 8.8 x 10^{-5}, for *marA* and *soxS* respectively). *tolC* expression decreased modestly in the *csrA*::*aph* strain (n=6, p-value: 0.05), however *acrA* and *acrB* expression was not significantly different compared to the wild-type, SL1344 (n=6, p-values: 0.46 and 0.97, for *acrA* and *acrB* respectively.

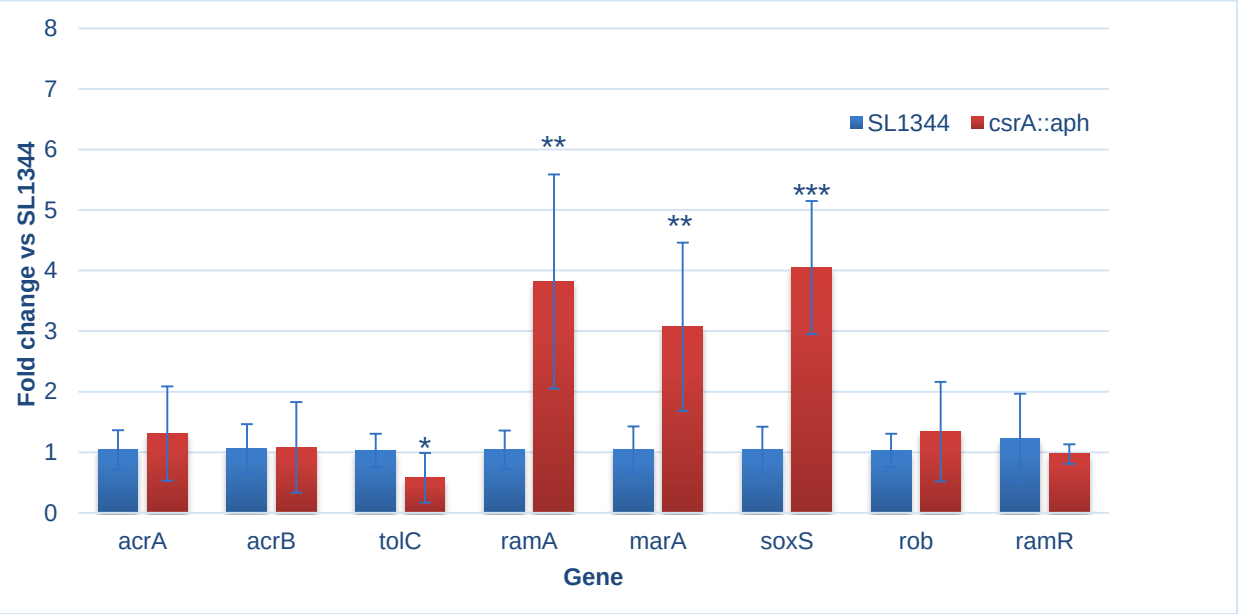

Figure 3.5: RT PCR was used to investigate the expression of *acrA, acrB, tolC, ramA, marA, soxS, rob* and *ramR* in the *csrA*::*aph* mutant and the wild-type strain, SL1344 (n=6, +/- SD). The time point of RT PCR was 93 minutes.

3.5 Biofilm formation & curli synthesis in the *csrA*::*aph* mutant

Inactivated *acrB* or *tolC* efflux components have been associated with a defect in biofilm formation (Baugh, Ekanayaka et al. 2012), in addition to an increase in *ramA* expression (Baugh, Phillips et al. 2013). Therefore, the observed increase in *ramA* expression in the *csrA*::*aph* mutant prompted the investigation of curli synthesis and the formation of competent biofilm, compared to the wild-type, SL1344.

S. enterica strain 14028S was used as a positive control for both biofilm formation and curli synthesis in this study, and the 14028S Δ*tolC* mutant was used as a negative control. Inactivation of the components of the AcrAB-TolC efflux pump has been shown to inhibit biofilm formation (Baugh, Ekanayaka et al. 2012), which is consistent with the results of this study. Biofilm formation decreased in the 14028S Δ*tolC* mutant (negative control), compared to the wild-type, 14028S (positive control), from OD_{600} 3.76 to 0.77 (Figure 23) (n=6, p-value: 2.52×10^{11}).

Biofilm formation (OD_{600}) decreased in the *csrA*::*aph* mutant, compared to the wild-type strain, SL1344, from OD_{600}: 0.29 to OD_{600}: 0.05 (Figure 3.6) (n=6, p-value: 6.5×10^{-5}). Consistently, the *csrA*::*aph* mutant did not appear to produce curli, based on the observed phenotype on Congo Red agar (Figure 3.7 D). Under a light microscope, the positive control strain curli morphology was red and rough, which is characteristic of a strain that produces curli (Figure 3.7 A). Curli production in the wild-type strain, SL1344, was not as prominent as the positive control strain, however cells appeared rough under a light microscope, suggesting some level of curli

synthesis (Figure 3.7 C). The negative control strain morphology was pale and smooth, reflecting an inability to synthesise curli (Figure 3.7 B).

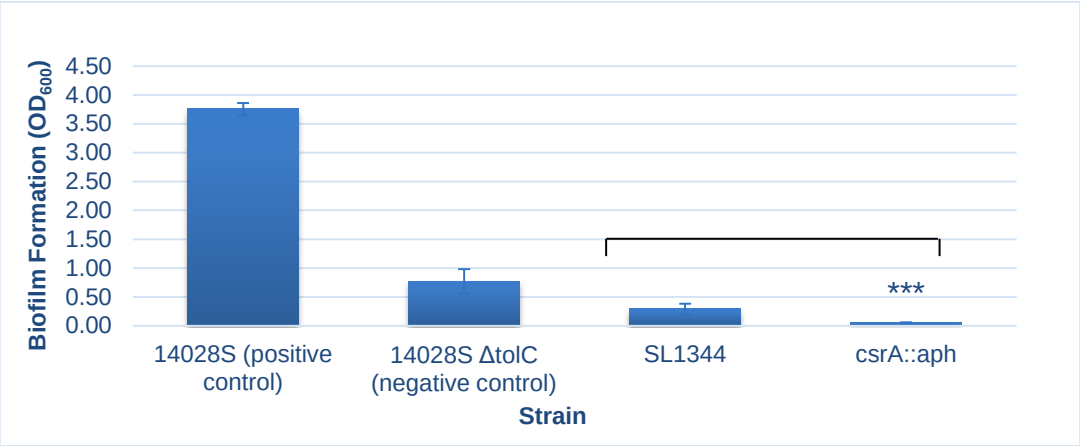

Figure 3.6: Average biofilm formation in the *csrA*::*aph* mutant (SL1344 background) compared to SL1344 and 14028S positive and negative controls. Absorbance (at 600nm) was used as a measure of biofilm formation. n=6, +/- SD.

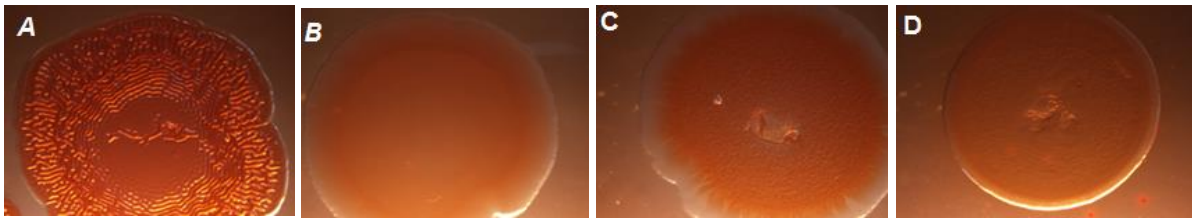

Figure 3.7: Curli biosynthesis in: 14028S positive control (A), 14028S Δ*tolC* negative control (B), SL1344 (C) and the *csrA*::*aph* mutant (D), n=4.

In order to confirm that *csrA* was required for competent biofilm formation and curli synthesis in a strain that synthesises and produces biofilm to a high level, P22 transduction was carried out to transduce the *csrA*::*aph* mutant into the positive control background (14028S). The *csrA*-tagged *aph* cassette in the 14028S background was confirmed by PCR (Figure 3.8). The *csrA*-tagged *aph* cassette

amplimer size was ~1500 bp (Figure 3.8, lanes 1-3), as expected by comparison with the control (Figure 3.8, lane 4).

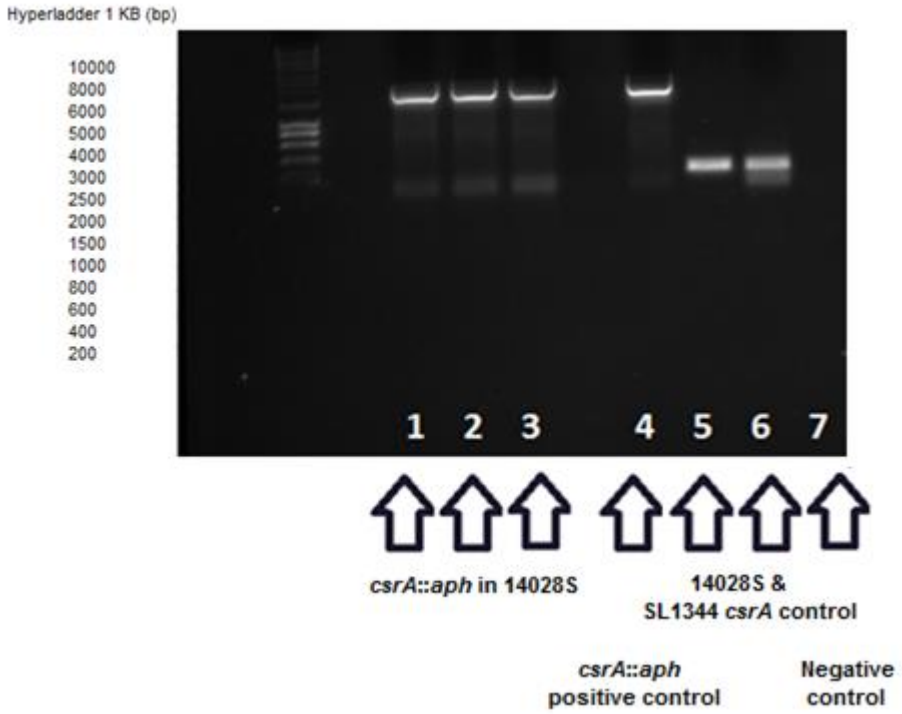

Figure 3.8: PCR confirmation following the transduction of the *csrA*::*aph* mutant into 14028S (lane 1, 2 and 3). HyperLadder 1KB was used and is annotated to the left of the figure.

Repeat biofilm and curli assays confirmed previous results; biofilm formation (OD_{600}) decreased in the 14028S *csrA*::*aph* mutant, compared to the wild-type strain, 14028S, from OD_{600}: 1.72 to OD_{600}: 0.06 (Figure 3.9) (n=6, p-value: 2.1×10^{-6}). Consistently, the 14028S *csrA*::*aph* mutant did not appear to produce curli, based on the observed phenotype on Congo Red agar (Figure 3.10 C).

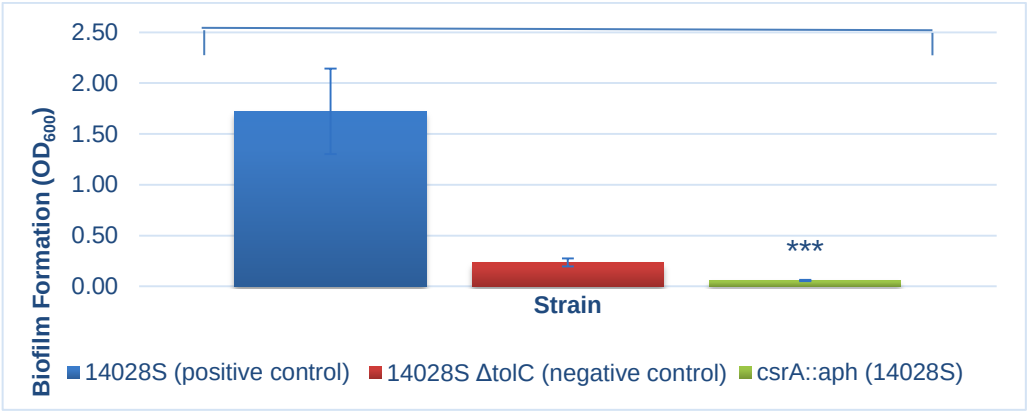

Figure 3.9: Average biofilm formation in the *csrA*::*aph* mutant (14028S background) compared to SL1344 and 14028S positive and negative controls. Absorbance (at 600nm) was used as a measure of biofilm formation. n=6, +/- SD.

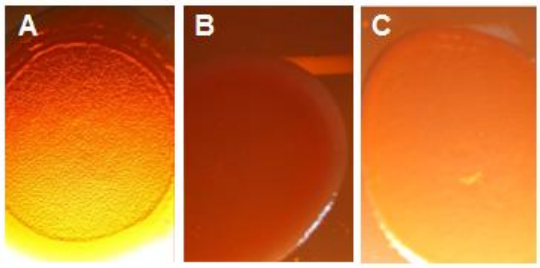

Figure 3.10: Curli biosynthesis in: 14028S (A), 14028S Δ*tolC* (B), and the *csrA*::*aph* mutant (14028S background) (C), n=4.

3.6 Antimicrobial susceptibility of the *csrA*::*aph* mutant

The overexpression of *acrAB* as a result of *ramA* overexpression correlates with MDR and decreases in susceptibility to substrates of the AcrAB-TolC efflux pump (van der Straaten, Janssen et al. 2004), (Ricci and Piddock 2009), (Bailey, Ivens et al. 2010). Therefore, the antimicrobial susceptibility of the *csrA*::*aph* mutant to structurally distinct quinolones (nalidixic acid), fluoroquinolones (ciprofloxacin), phenicols (chloremphenicol), tetracycline and ethidium bromide was investigated by determining the MIC of each compound, and compared to MICs for the wild-type

strain SL1344, SL1344 *ramR*::*aph* and *E. coli*. The compounds tested are known substrates of the AcrAB-TolC efflux pump (Giraud, Cloeckaert et al. 2000), (Piddock, White et al. 2000) (Baucheron, Imberechts et al. 2002), (Baucheron, Chaslus-Dancla et al. 2004), (Eaves, Ricci et al. 2004), (Bailey, Ivens et al. 2010).

The *csrA*::*aph* mutant did not display a MDR phenotype as MICs were +/- 1 dilution compared with SL1344 (Table 3.2); the tetracycline MIC range for the *csrA*::*aph* mutant and SL1344 at 1 x 10^6 cfu/mL, was 1, whereas the MIC range for the SL1344 *ramR*::*aph* mutant was 4-fold higher, an expected phenotype due to the deletion of *ramR* and the subsequent increase in expression of *ramA* and induction of AcrAB-TolC.

Final concentration of bacteria: 1 x10^6 cfu/mL					
	MIC µg/mL				
Strain	**CIP Range**	**NAL Range**	**CHL Range**	**TET Range**	**EtBr Range**
SL1344	0.0075 - 0.03	4 - 8	2 - 4	1	2048
E. coli	0.015	8	8 – 16	2 - 4	2048
SL1344 *ramR*::*aph*	0.06	16	8	4	2048
SL1344 *csrA*::*aph*	0.015	8	2 - 4	1	1024

Final concentration of bacteria: 1 x10^4 cfu/mL					
	MIC µg/mL				
Strain	**CIP Range**	**NAL Range**	**CHL Range**	**TET Range**	**EtBr Range**
SL1344	0.0075 - 0.015	2 - 4	2 - 4	1	1024
E. coli	0.0075	8	4	1	1024
SL1344 *ramR*::aph	0.03	16	8 - 16	4	2048
SL1344 *csrA*::*aph*	0.0075	4 - 8	2 - 4	0.5	512

Final concentration of bacteria: 1 x 10^2 cfu/mL					
	MIC µg/mL				
Strain	**CIP Range**	**NAL Range**	**CHL Range**	**TET Range**	**EtBr Range**
SL1344	0.0075 - 0.015	2 - 4	2 - 4	1	1024
E. coli	0.0075	4	4	1	64
SL1344 *ramR*::*aph*	0.03	16	8	4	2048
SL1344 *csrA*::*aph*	0.0075	2 - 4	1	0.5	128

Table 3.2: MIC results (n=2) for each compound at each cell concentration tested (cfu/mL). CIP = ciprofloxacin, NAL = nalidixic acid, CHL = chloremphenicol, TET = tetracycline and EtBr = ethidium bromide.

4.0 Discussion

4.1 Research hypothesis and experimental aims

The primary hypothesis that was investigated in this study was that CsrA may be involved in the regulation of RamA in *S. enterica* serovar Typhimurium SL1344, and therefore play a role in multi-drug resistance by bacterial efflux via AcrAB-TolC, which RamA is a known to be a transcriptional activator of. This hypothesis arose from experiments by Ricci & Piddock (unpublished data), in which pMW82-p*ramA*, a plasmid containing the cloned *ramA* promoter region fused to a gene encoding a green fluorescent protein (GFP) was introduced into the TraDIS library of SL1344. Flow cytometry revealed populations which had greater expression of *ramA* than the wild-type, SL1344. Subsequent experiments followed by DNA sequencing revealed that transposon disruption of the *csrA* gene resulted in a significant increase in GFP on two separate occasions. Therefore, it was proposed that CsrA may be involved in the regulation of RamA.

The experimental aims of this project were to create and characterise a *csrA::aph* mutant in SL1344 and investigate the effects of the gene disruption on the expression of *acrA, acrB, tolC, ramA, marA, soxS, rob* and *ramR*, the mutant's susceptibility to structurally distinct antimicrobials that are known substrates of the AcrAB-TolC efflux pump (Giraud, Cloeckaert et al. 2000), (Piddock, White et al. 2000) (Baucheron, Imberechts et al. 2002), (Baucheron, Chaslus-Dancla et al. 2004), (Eaves, Ricci et al. 2004), (Bailey, Ivens et al. 2010), and the mutant's ability to produce curli and competent biofilm, both known to be influenced by the expression of *acrB* and *tolC* (Baugh, Ekanayaka et al. 2012).

4.2 The effect of the *csrA* gene on the growth of *S. enterica* Serovar Typhimurium

The *csrA* gene was initially identified in *E. coli* K-12 by transposon mutagenesis, and first described as a negative regulator of glycogen biosynthesis during stationary phase (Romeo, Gong et al. 1993). The changes in gene expression of *csrA* and other stationary phase genes regulate bacterial physiology and metabolism in response to changes in environmental conditions. This enables bacteria to survive and adapt to suboptimal conditions, such as nutrient depletion and other poor growth conditions. Bacterial cells in the stationary growth phase are more efficient in utilising nutrients, and have an increased level of stress resistance compared to exponential phase cells, due to coordinated gene expression by global regulatory networks (Gottesman 1984).

csrA encodes an RNA-binding protein, CsrA, which binds to the mRNA sequences of its target molecules, preventing them from being accessible to the ribosome and ribosomal binding site (RBS). In this way, CsrA is able to modulate the translation of specific mRNA, either by altering the stability of the mRNA, or degrading the mRNA transcript before it is translated into protein by the ribosome (Romeo 1998), (Dubey, Baker et al. 2003).

CsrA has been shown to bind to specific sequences on mRNA molecules, containing GGA motifs and it is thought that CsrA blocks ribosome access to the Shine-Dalgarno sequence (Dubey, Baker et al. 2003), (Baker, Eory et al. 2007), a sequence found upstream of the start codon (AUG) that helps recruit the ribosome to the mRNA transcript. The Shine-Dalgarno sequence contains a conserved GGA sequence

(Baker, Eory et al. 2007), suggesting that CsrA envelopes this sequence when it is actively bound, preventing ribosome access.

A mutation in the *csrA* gene has previously been associated with an increase in the expression of two genes involved in glycogen synthesis, *glgB* (glycogen branching enzyme) and *glgC* (ADP glucose pyrophosphorylase), and the regulatory mechanism exerted by this gene was apparently independent of the other positive regulators of *glgC* expression (Romeo, Gong et al. 1993). The deletion of the *csrA* gene also resulted in an increase in the expression of genes involved in the gluconeogenesis pathway, such as *pckA* (phosphoenolpyruvate carboxykinase). *csrA* has also been shown to negatively regulate fructose-1,6-bisphosphatase and phospoenolpyruvate synthetase of the gluconeogenic pathway, and positively regulate glycolysis enzymes including enolase, triose-phosphate isomerase and glucose-6-phosphate isomerase (Sabnis, Yang et al. 1995).

The *csrA*::*aph* mutant created in this study had a growth defect, which is likely due to the effect of the gene deletion on the utilisation of carbon in SL1344. An investigation of the growth kinetics of the *csrA*::*aph* mutant and the wild-type, SL1344, revealed that in the absence of the *csrA* gene the strain struggled to reach mid-log phase in LB broth and minimal medium containing glucose or pyruvate. LB broth was the most nutritious media used and the growth of the *csrA*::*aph* mutant was optimal in this medium. LB broth contains tryptone, which provides an amino acid source, yeast extract, which provides a carbon source, and sodium chloride to maintain osmotic balance, whereas minimal medium contains only the minimal requirements for bacterial growth (inorganic salts and water), supplemented with a carbon source, which in this study was glucose or pyruvate. In *E. coli*, the *csrA* gene has been

proposed to be essential for the growth of bacteria in media containing glycolytic sources (Romeo, Gong et al. 1993), (Timmermans and Van Melderen 2009), likely due to the lack of repression of the enzymes involved in the cellular synthesis of glycogen, and the excess glycogen that accumulates in the media. The observations in this study, which found that the *csrA*::*aph* mutant displayed a long lag phase in minimal medium supplemented with glucose, was consistent with data previously published for *E. coli* (Romeo, Gong et al. 1993), (Timmermans and Van Melderen 2009).

Although the absence of the *csrA* gene has been linked to growth defects in glycolytic media, in *E. coli* it has been reported that growth is not affected in media containing pyruvate (Timmermans and Van Melderen 2009), as the pyruvate reduces the burden of the glycolysis pathway to convert glucose into pyruvate and therefore provides the intermediates for the Krebs Cycle or gluconeogenesis, the components of which are upregulated in an *E. coli csrA*::*aph* mutant (Sabnis, Yang et al. 1995). Previous data suggests that it is glycolysis which is impaired in the *csrA*::*aph* mutant in *E. coli*, and the accumulation of glycogen affects bacterial viability (Timmermans and Van Melderen 2009). However, in the present study the *csrA*::*aph* mutant in SL1344 was unable to grow in minimal medium supplemented with pyruvate and displayed similar growth in this medium compared to minimal media supplemented with glucose, therefore it is possible that the phenotype observed in the *csrA*::*aph* mutant in the presence of pyruvate could be due to some dysregulation in the Krebs cycle and gluconeogenic pathways caused by the disruption to the *csrA* gene in this strain.

As the *csrA*::*aph* mutant displayed optimal growth in LB broth, this medium was used for the duration of the study. Despite this, fresh aerobic cultures of the *csrA*::*aph* mutant at 37°C struggled to reach mid-log phase on the days of testing, so overnight cultures were used for aspects of the study that required the fresh growth of cells to mid-log phase. For the background strain, SL1344, overnight cultures were used to prepare a fresh culture on the days of testing, and these reached mid-log phase in ~2-3 hours.

4.3 The effect of the *csrA* gene on the expression of *ramA*

The *ramA* gene is a member of the AraC/XylS family of transcriptional activators (Gallegos, Schleif et al. 1997) and increased *ramA* expression is associated with an increase in the expression of *acrA*, *acrB* and *tolC*, which encode the components of the tripartite AcrAB-TolC MDR efflux complex, resulting in multi-drug resistance to structurally distinct antimicrobials that are expelled by this pump. RamA regulates efflux by AcrAB-TolC in most Enterobacteriaceae, except in *E. coli* and *Shigella* spp., which encode the homologue, *marA* (van der Straaten, Janssen et al. 2004), (Bailey, Paulsen et al. 2008).

To confirm data obtained by TraDIS sequencing, which identified that deletion of *csrA* in SL1344 resulted in a significant increase in *ramA* transcription, pMW82-p*ramA*, a plasmid containing a gene encoding a GFP fused to a DNA fragment carrying the *ramA* promoter region (290 bp) was used. Analysis of the fluorescence activity in the *csrA*::*aph* mutant with pMW82-p*ramA*, showed that the expression of GFP was over 2 fold higher, compared to the wild-type strain, SL1344 with pMW82-p*ramA*; these

data confirmed the TraDIS observation. RT-PCR showed that *ramA* expression was increased in the *csrA*::*aph* mutant, confirming the GFP data. Interestingly, expression of *marA* and *soxS* transcriptional activators was also increased, however as with *ramA*, to date there have been no studies to show that these genes have a binding site for, or are regulated by CsrA.

RamR, a member of the TetR family of transcriptional repressors, is the local repressor of RamA. Mutations in *ramR* are associated with an increase in the expression of *ramA,* the upregulation of the AcrAB-TolC efflux pump, and MDR (Abouzeed, Baucheron et al. 2008), (Ricci, Busby et al. 2012). The *ramR* gene is located in the opposite orientation to *ramA*, and lies upstream of it in *S. enterica* serovar Typhimurium. It is known that the RamR protein binds to the *ramA-ramR* intergenic region, which is located upstream of *ramA*, resulting in transcriptional repression (Abouzeed, Baucheron et al. 2008), (Baucheron, Coste et al. 2012), (Ricci, Busby et al. 2012), (Yamasaki, Nikaido et al. 2013).

RT-PCR data indicated that *ramR* expression was not significantly changed in the *csrA*::*aph* mutant, suggesting that the increase in *ramA* expression observed was not due to the depression of *ramR*. It is therefore hypothesised that CsrA binds to *ramA* and negatively regulates the gene at the post-transcriptional level, in a distinct mechanism to the transcriptional repression of *ramA* by RamR. Based on the fluorescence data obtained using pMW82-p*ramA* and data to support how CsrA interacts with its targets (Barnard, Loughlin et al. 2004), (Romeo, Gong et al. 1993), (Romeo, Vakulskas et al. 2013), (Seyll and Van Melderen 2013), CsrA may bind to a GGA motif in the *ramA* promoter sequence and so interferes with the translation of

RamA protein. However, it would be necessary to confirm that the *csrA*::*aph* mutant produces more RamA protein, as high gene expression does not always correlate with high protein expression. Unfortunately, due to the time constraints of this project, it was not possible to detect the RamA protein in the *csrA*::*aph* mutant by Western blotting.

4.4 The effect of the *csrA* gene on the expression of *acrAB-tolC*

Salmonella can be MDR as a consequence of the upregulation of efflux via AcrAB-TolC; this is typically characterised with increased expression of *ramA* (van der Straaten, Janssen et al. 2004), (Bailey, Paulsen et al. 2008). It was therefore hypothesized that the *csrA*::*aph* mutant constructed in this study would express the components of the AcrAB-TolC efflux pump at a higher level compared to the parental strain, SL1344, due to the increased *ramA* expression observed by fluorescence analysis. pMW82-p*acrAB* and pMW82-p*tolC* were plasmids that contained a gene encoding a GFP fused to DNA fragments carrying the *acrAB* and *tolC* promoter regions, respectively. The fluorescence data suggests that the transcription of these genes did not increase in the *csrA*::*aph* mutant, which is consistent with RT-PCR data. However, the fluorescence data suggests that promoter activity for *acrAB* genes significantly decreased compared to the wild-type strain, whereas RT-PCR data showed similar expression profiles of *acrA* and *acrB* in the *csrA*::*aph* mutant and the wild-type strain. The reason for this is unclear, although it could be a reflection of a regulatory mechanism affecting the transcription of both genes, as both *acrA* and *acrB* are required for AcrAB-TolC. However, RT PCR data presented in this study is limited by the variation between data points used to

calculate the mean fold change in gene expression, suggesting that it may be difficult to draw conclusions from this data without further repeats of the assay. MIC data provided further evidence that the *acrA, acrB* and *tolC* genes were not significantly upregulated in the *csrA*::*aph* mutant; MICs of a range of antibiotic classes, including quinolones, fluoroquinolones, phenicols and tetracycline were determined, in order to investigate the effects of the *csrA* deletion on a broad range of known substrates of the AcrAB-TolC efflux pump (Giraud, Cloeckaert et al. 2000), (Piddock, White et al. 2000), (Eaves, Ricci et al. 2004), (Baucheron, Chaslus-Dancla et al. 2004), (Bailey, Ivens et al. 2010), (Baucheron, Imberechts et al. 2002).

The inactivation of the *csrA* gene had no measurable effect on the susceptibility of SL1344 to the compounds tested and the MIC data obtained was similar to that for the parental strain, SL1344 (+/- 1 dilution). The *ramR::aph* mutant used as a control in this study was MDR, so it could be possible that MDR mediated by *ramR* inactivation is a distinct mechanism of antimicrobial resistance via the upregulation of AcrAB-TolC; however *csrA* may play a role in the regulation of *ramA* expression, separate to that of *ramR*. It would be useful to investigate the expression of *csrA* in the *ramR* mutant used in this study, to further explore whether there is a relationship between *csrA* and *ramR*. Alternatively, it could be possible that CsrA binds to *ramR*, inhibiting translation of the RamR protein and therefore leading to an increase in *ramA* expression. The detection of reduced RamR protein in the *csrA*::*aph* mutant should be confirmed by Western blotting to address this hypothesis further. It would also be interesting to overexpress *ramR* in the *csrA*::*aph* mutant, to investigate whether *ramA* is still overexpressed, using the pMW82-p*ramA* reporter and GFP expression analysis; *ramA* expression could increase even higher than that observed

in the *csrA*::*aph* mutant, suggesting two separate mechanisms of RamA regulation, and it would be interesting to investigate how the MICs changed in comparison with the *ramR*-deleted mutant used as a control for the MIC analyses in this study.

4.5 The effect of the *csrA* gene on pathogenicity

Previous studies have suggested that post-transcriptional regulators play significant roles in mediating the interactions between bacterial pathogens and host cells (Romeo 1998). These host-pathogen interactions include the ability to colonise and persist in host cells, as well as the secretion of various virulence factors that enable bacteria to cause infection (Johansson and Cossart 2003). Post-transcriptional regulation allows these mechanisms to be intricately controlled, through the mediation of cellular changes that lead to altered gene expression in pathogenic bacteria.

There is an association between AcrAB-TolC, pathogenicity and bacterial resistance (Buckley, Webber et al. 2006), as well as biofilm formation (Baugh, Ekanayaka et al. 2012). Cells in a biofilm consist of those which are actively growing and those which have very slow metabolic rates, and this complex association of cells makes them difficult targets for eradication, particularly on surfaces such as contaminated food, water supplies, and medical devices (Passerini, Lam et al. 1992).

CsrA has been proposed to globally regulate genes involved in biofilm synthesis in *E. coli* (Wang, Dubey et al. 2005). Its role in competent biofilm formation in SL1344 was investigated in this study and the results indicated that the *csrA*::*aph* mutant was unable to form competent biofilm in SL1344. When the *csrA*::*aph* mutant was

transduced into the background of a good biofilming strain of Salmonella, 14028S, a more prominent difference was seen between the strains when *csrA* was disrupted. In *E. coli*, the disruption of the *csrA* gene led to an increase in the synthesis of poly-beta-1,6-N-acetyl-d-glucosamine (PGA), so it has been proposed that CsrA competitively binds to the mRNA of PGA to block the access of the molecule to the 30S ribosomal subunit. Mutations in the sequences overlapping the Shine Dalgarno sequence of the target, proposed to be the CsrA binding site, also lead to a similar phenotype (Wang, Dubey et al. 2005).

The *S. enterica* serovar Typhimurium biofilm matrix is composed of cellulose and curli fibres. As curli are important for surface attachment and successful colonisation of a bacterial biofilm, the ability of the SL1344 *csrA*::*aph* mutant to synthesise curli was investigated; the *csrA*::a*ph* mutant did not produce curli and the observed phenotype on Congo Red correlates with the strains reduced ability to produce competent biofilm. When transduced into the strain, 14028S, the *csrA*::*aph* mutant was also unable to produce curli, which is consistent with the biofilm data.

High *ramA* expression has been associated with a decrease in curli production, and therefore an inability to form competent biofilm (Baugh, Phillips et al. 2013), which is consistent with the results of this study. The *csrA* gene could provide a link between increased *ramA* expression and decreased curli biosynthesis, however this would be difficult to conclude solely from the present study, and would require further investigation to elucidate the molecular mechanisms surrounding curli biosynthesis during biofilm formation.

4.6 Regulation of the *csrA* gene

In *E. coli*, CsrA is regulated by two small non-coding RNAs, CsrB and CsrC, that form large ribonucleoprotein complexes with CsrA (Romeo 1998). CsrB and CsrC contain binding sites for CsrA, which include conserved GGA amino acid sequences. The two small non-coding RNAs mimic CsrA targets, and therefore sequester CsrA activity by antagonising its regulatory effects. CsrB is a 366-nucleotide RNA molecule (Gudapaty, Suzuki et al. 2001), that can bind up to 18 subunits (9 dimers) of CsrA (Liu, Gui et al. 1997), (Romeo 1998). The CsrC protein is smaller and has a lower affinity for CsrA, being able to bind up to 6-8 subunits (3-4 dimers) of CsrA, however both molecules appear to use the same mechanism to sequester CsrA (Weilbacher, Suzuki et al. 2003). *csrC* disruption leads to an increase in *csrB* transcription and deletion of *csrB* leads to glycogen deficiency, a similar phenotype to that observed when *csrA* is over-expressed. When *csrA* was disrupted, CsrB RNA levels decreased (Gudapaty, Suzuki et al. 2001). It has been suggested that the level of CsrB is central to CsrA activity in the species (Romeo 1998), therefore it would be interesting to explore the association between *csrB* expression and *ramA* expression in the *csrA*::*aph* mutant in SL1344. If the expression of *csrB* decreases following disruption of the *csrA* gene, it is possible that the effects observed in the present study are not directly due to *csrA* disruption, but due to CsrB, and so this could be central to the regulation of RamA. One CsrB molecule has ~18 binding units for CsrA (Liu, Gui et al. 1997), (Romeo 1998), meaning that it is potentially likely that the remaining ~65-85% of the protein could interact with other RNA molecules (Gudapaty, Suzuki et al. 2001), potentially including *ramA*.

4.7 Conclusions of the study

The genes under the global control of CsrA are locally regulated; *ramA* is under the control of RamR, so CsrA, like other global regulators, might provide fine tuning of bacterial gene expression. Although the majority of studies have been done in *E. coli*, the *csrA* gene is evolutionarily conserved across distinct groups of bacteria, and there are homologues of the *csrA* gene amongst prokaryotes (Lapouge, Schubert et al. 2008).

The present study demonstrated that disruption of the *csrA* gene in *S. enterica* serovar Typhimurium led to a significant increase in the expression of *ramA, marA* and *soxS* (Figure 4.1 A), which are genes known to regulate bacterial efflux via the AcrAB-TolC tripartite efflux pump. However, an increase in the expression of these genes, did not lead to the increased expression of *acrA, acrB* and *tolC* (Figure 4.1 B), and the *csrA*::*aph* mutant was not MDR to a range of structurally-distinct substrates of the AcrAB-TolC efflux pump. The increase in *ramA* expression was not due to an a decrease in *ramR* expression, which has previously been demonstrated as a distinct mechanism of *ramA* regulation. Therefore the effect of *csrA* expression to *ramA* expression may be via a separate mechanism from its local repression by RamR.

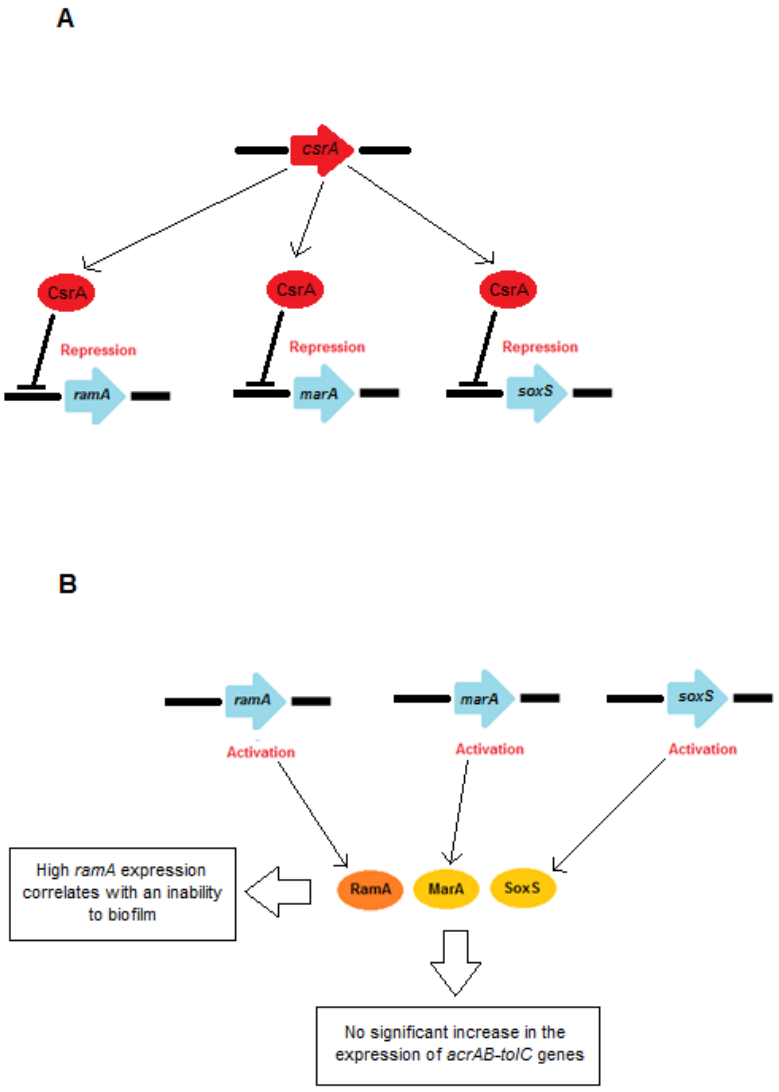

Figure 4.1: Proposed CsrA interactions. A: CsrA appears to be involved in the transcriptional repression of *ramA*, *marA* and *soxS*. B: In a *csrA*::*aph* mutant, the expression of the transcriptional activators *ramA*, *marA* and *soxS* increases, consistent with an inability to form competent biofilm. However, it is not yet clear why this does not lead to an increase in the expression of *acrAB-tolC* genes.

It is interesting to consider why *ramA* expression is increased in the *csrA*::aph mutant, without leading to an increase in the expression of *acrA, acrB* and *tolC* genes that encode the components of the AcrAB-TolC efflux pump. Due to the growth defects observed in the strain during this study, and previous data indicating the importance of *csrA* for growth in the presence of various carbon sources, it is possible that RamA

could also be involved in the stress response of *S. enterica* serovar Typhimurium, and the increase in *ramA* expression is a mechanism to compensate for the loss of the *csrA* gene. When the *csrA* gene was disrupted, the ability to synthesise curli and produce competent biofilm was impaired. Mutation in the *csrA* gene in *S. enterica* serovar Typhimurium has also been associated with an increase in the expression of the genes required for successful invasion or mammalian gastrointestinal mucosa (Jackson, Suzuki et al. 2002). This suggests that the genes necessary for survival may be upregulated in the absence of *csrA*, likely due to the central role of this gene in the global regulation of bacterial gene expression.

4.8 Limitations of the study

The present study was limited by the growth defect observed in the *csrA*::*aph* mutant, so it may be difficult to conclude that the increase in *ramA* expression was due to a *csrA* gene deletion, rather than the effects of poor growth in the strain. When preparing cultures of the *csrA*::*aph* mutant for testing, overnight cultures that had been aerobically incubated at 37°C with shaking for ~18-24 hours had only just reached mid-log phase, whereas diluted overnight cultures of SL1344 reached mid-log phase in ~2-3 hours. It is unclear how the growth kinetics of the *csrA*::*aph* mutant affected the gene expression of the strain, and the phenotype observed during biofilm and curli investigation. Additionally, RNA preparations of the *csrA*::*aph* mutant for RT-PCR were prepared in LB broth, with static aerobic incubation at 37°C, due to difficulties in replicating the growth conditions in minimal media. Therefore it may not be possible to directly compare the gene expression data obtained in the present

study with other laboratory data involving the expression of similar genes in other SL1344 strains.

The study is also limited by the lack of information about the interactions between CsrA, RamA, and potentially RamR, however the study presents novel data that may benefit further work.

4.9 Proposed future work

It would be interesting to investigate how the observations in this study are affected by *csrA* overexpression in *S. enterica* serovar Typhimurium, because other studies have shown that the expression of cell invasion genes remains constant when *csrA* is overexpressed or disrupted (Altier et al. 2000). It would be interesting to examine the effect of *csrA* overexpression on *ramA* expression, as this could provide further insight of the regulatory relationship between *csrA* and *ramA*. In a *csrA*-overexpressed mutant, it would also be interesting to consider how antimicrobial susceptibility and biofilm formation are affected; if the phenotypes of a *csrA*-deletion and *csrA*-overexpression mutant are similar, this may suggest that bacteria have a compensatory mechanism for the loss of *csrA,* likely because *csrA* is central to the intricate regulation of bacterial gene expression, so it would be necessary to keep CsrA levels constant in the cell.

Additionally, the *csrA*::*aph* mutant could be used to investigate how invasion is affected in SL1344 when the *csrA* gene is disrupted. In other studies, increased expression of *ramA* is associated with a significant decline in fitness and survival in macrophages (Bailey et al. 2010), so it may be possible to hypothesise that, similarly

to a *ramA* overexpressed strain, the *csrA*::*aph* mutant may invade cells poorly. This could further ascertain the role of *csrA* in the stress response in *S. enterica* serovar Typhimurium.

As previously mentioned, due to time constraints, it was not possible to produce data to indicate that the increased expression of *ramA* in the *csrA*::*aph* mutant was indicative of increased translation of the RamA protein. Therefore, I propose that the confirmation of the RamA protein in this strain would be the primary objective in the continuation of the study.

5.0 References

Abouzeed, Y. M., S. Baucheron, et al. (2008). "ramR mutations involved in efflux-mediated multidrug resistance in Salmonella enterica serovar Typhimurium." Antimicrobial Agents and Chemotherapy 52(7): 2428-2434.

Adamson, D. N. and H. N. Lim (2013). "Rapid and robust signaling in the CsrA cascade via RNA-protein interactions and feedback regulation." Proceedings of the National Academy of Sciences of the United States of America 110(32): 13120-13125.

Agaras, B., P. Sobrero, et al. (2013). "A CsrA/RsmA translational regulator gene encoded in the replication region of a Sinorhizobium meliloti cryptic plasmid complements Pseudomonas fluorescens rsmA/E mutants." Microbiology-Sgm 159: 230-242.

Altier, C., M. Suyemoto, et al. (2000). "Regulation of Salmonella enterica serovar typhimurium invasion genes by csrA." Infection and Immunity 68(12): 6790-6797.

Bailey, A. M., A. Ivens, et al. (2010). "RamA, a Member of the AraC/XylS Family, Influences Both Virulence and Efflux in Salmonella enterica Serovar Typhimurium." Journal of Bacteriology 192(6): 1607-1616.

Bailey, A. M., I. T. Paulsen, et al. (2008). "RamA confers multidrug resistance in Salmonella enterica via increased expression of acrB, which is inhibited by chlorpromazine." Antimicrobial Agents and Chemotherapy 52(10): 3604-3611.

Baker, C. S., L. A. Eory, et al. (2007). "CsrA inhibits translation initiation of Escherichia coli hfq by binding to a single site overlapping the Shine-Dalgarno sequence." Journal of Bacteriology 189(15): 5472-5481.

Barnard, F. M., M. F. Loughlin, et al. (2004). "Global regulation of virulence and the stress response by CsrA in the highly adapted human gastric pathogen Helicobacter pylori." Molecular Microbiology 51(1): 15-32.

Baucheron, S., E. Chaslus-Dancla, et al. (2004). "Role of TolC and parC mutation in high-level fluoroquinolone resistance in Salmonella enterica serotype Typhimurium DT204." Journal of Antimicrobial Chemotherapy 53(4): 657-659.

Baucheron, S., F. Coste, et al. (2012). "Binding of the RamR Repressor to Wild-Type and Mutated Promoters of the ramA Gene Involved in Efflux-Mediated Multidrug Resistance in Salmonella enterica Serovar Typhimurium." Antimicrobial Agents and Chemotherapy 56(2): 942-948.

Baucheron, S., H. Imberechts, et al. (2002). "The AcrB multidrug transporter plays a major role in high-level fluoroquinolone resistance in Salmonella enterica serovar typhimurium phage type DT204." Microbial Drug Resistance-Mechanisms Epidemiology and Disease 8(4): 281-289.

Baucheron, S., S. Tyler, et al. (2004). "AcrAB-TolC directs efflux-mediated multidrug resistance in Salmonella enterica serovar Typhimurium DT104." Antimicrobial Agents and Chemotherapy 48(10): 3729-3735.

Baugh, S., A. S. Ekanayaka, et al. (2012). "Loss of or inhibition of all multidrug resistance efflux pumps of Salmonella enterica serovar Typhimurium results in impaired ability to form a biofilm." Journal of Antimicrobial Chemotherapy 67(10): 2409-2417.

Baugh, S., CR Phillips, et al. (2014). "Inhibition of multidrug efflux as a strategy to prevent biofilm formation."
Journal of Antimicrobial Chemotherapy 69(3): 673-81.

Buckley, A. M., M. A. Webber, et al. (2006). "The AcrAB-TolC efflux system of Salmonella enterica serovar Typhimurium plays a role in pathogenesis." Cellular Microbiology 8(5): 847-856.

Casin, I., J. Breuil, et al. (2003). "Fluoroquinolone resistance linked to GyrA, GyrB, and ParC mutations in Salmonella enterica Typhimurium isolates in humans." Emerging Infectious Diseases 9(11): 1455-1457.

Chopra, I. and M. Roberts (2001). "Tetracycline antibiotics: Mode of action, applications, molecular biology, and epidemiology of bacterial resistance." Microbiology and Molecular Biology Reviews 65(2): 232-+.

Costerton, J. W., K. J. Cheng, et al. (1987). "Bacterial Biofilms in Nature and Disease." Annual Review of Microbiology 41: 435-464.

Costerton, J. W., P. S. Stewart, et al. (1999). "Bacterial biofilms: A common cause of persistent infections." Science 284(5418): 1318-1322.

Datsenko, K. A. and B. L. Wanner (2000). "One-step inactivation of chromosomal genes in Escherichia coli K-12 using PCR products." Proceedings of the National Academy of Sciences of the United States of America 97(12): 6640-6645.

Donlan, R. M. (2001). "Biofilms and device-associated infections." Emerging Infectious Diseases 7(2): 277-281.

Dubey, A. K., C. S. Baker, et al. (2003). "CsrA regulates translation of the Escherichia coli carbon starvation gene, cstA, by blocking ribosome access to the cstA transcript." Journal of Bacteriology 185(15): 4450-4460.

Eaves, D. J., V. Ricci, et al. (2004). "Expression of acrB, acrF, acrD, marA, and soxS in salmonella enterica serovar typhimurium: Role in multiple antibiotic resistance." Antimicrobial Agents and Chemotherapy 48(4): 1145-1150.

Fey, P. D., T. J. Safranek, et al. (2000). "Ceftriaxone-resistant salmonella infection acquired by a child from cattle." New England Journal of Medicine 342(17): 1242-1249.

Fierer, J. and D. G. Guiney (2001). "Diverse virulence traits underlying different clinical outcomes of Salmonella infection." Journal of Clinical Investigation 107(7): 775-780.

Finlay, B. B., S. Ruschkowski, et al. (1991). "Cytoskeletal Rearrangements Accompanying Salmonella Entry into Epithelial-Cells." Journal of Cell Science 99: 283-&.

Fralick, J. A. (1996). "Evidence that TolC is required for functioning of the Mar/AcrAB efflux pump of Escherichia coli." Journal of Bacteriology 178(19): 5803-5805.

Gallegos, M. T., R. Schleif, et al. (1997). "AraC/XylS family of transcriptional regulators." Microbiology and Molecular Biology Reviews 61(4): 393-&.

Giraud, E., A. Cloeckaert, et al. (2000). "Evidence for active efflux as the primary mechanism of resistance to ciprofloxacin in Salmonella enterica serovar typhimurium." Antimicrobial Agents and Chemotherapy 44(5): 1223-1228.

Glynn, M. K., C. Bopp, et al. (1998). "Emergence of multidrug-resistant Salmonella enterica serotype typhimurium DT104 infections in the United States." New England Journal of Medicine 338(19): 1333-1338.

Goodman, A.L, Kulasekara, B, Rietsch A, Boyd, D, Smith, R.S, Lory, S. (2004). "A signalling network reciprocally regulates genes associated with acute infection and chronic persistence in Pseudomonas aeruginosa." Developmental Cell 7(5): 745-754.

Gottesman, S. (1984). "Bacterial Regulation - Global Regulatory Networks." Annual Review of Genetics 18: 415-441.

Gudapaty, S., K. Suzuki, et al. (2001). "Regulatory interactions of Csr components: the RNA binding protein CsrA activates csrB transcription in Escherichia coli." Journal of Bacteriology 183(20): 6017-6027.

Horiyama, T., A. Yamaguchi, et al. (2010). "TolC dependency of multidrug efflux systems in Salmonella enterica serovar Typhimurium." Journal of Antimicrobial Chemotherapy 65(7): 1372-1376.

Jackson, D. W., K. Suzuki, et al. (2002). "Biofilm formation and dispersal under the influence of the global regulator CsrA of Escherichia coli." Journal of Bacteriology 184(1): 290-301.

Johansson, J. and P. Cossart (2003). "RNA-mediated control of virulence gene expression in bacterial pathogens." Trends in Microbiology 11(6): 280-285.

Jordan, D. C. (1961). "Effect of Vancomycin on Synthesis of Cell Wall Mucopeptide of Staphylococcus Aureus." Biochemical and Biophysical Research Communications 6(3): 167-&.

Keeney, D., A. Ruzin, et al. (2008). "MarA-mediated overexpression of the AcrAB efflux pump results in decreased susceptibility to tigecycline in Escherichia coli." Journal of Antimicrobial Chemotherapy 61(1): 46-53.

Keyhani, N. O. and S. Roseman (1997). "Wild-type Escherichia coli grows on the chitin disaccharide, N,N '-diacetylchitobiose, by expressing the cel operon." Proceedings of the National Academy of Sciences of the United States of America 94(26): 14367-14371.

Kikuchi, T., Y. Mizunoe, et al. (2005). "Curli fibers are required for development of biofilm architecture in Escherichia coli K-12 and enhance bacterial adherence to human uroepithelial cells." Microbiology and Immunology 49(9): 875-884.

Lapouge, K., M. Schubert, et al. (2008). "Gac/Rsm signal transduction pathway of gamma-proteobacteria: from RNA recognition to regulation of social behaviour." Molecular Microbiology 67(2): 241-253.

Levy, S. B. (1998). "The challenge of antibiotic resistance." Scientific American 278(3): 46-53.

Li, X. Z., D. M. Livermore, et al. (1994). "Role of Efflux Pump(S) in Intrinsic Resistance of Pseudomonas-Aeruginosa - Resistance to Tetracycline, Chloramphenicol, and Norfloxacin." Antimicrobial Agents and Chemotherapy 38(8): 1732-1741.

Liu, M. Y., G. J. Gui, et al. (1997). "The RNA molecule CsrB binds to the global regulatory protein CsrA and antagonizes its activity in Escherichia coli." Journal of Biological Chemistry 272(28): 17502-17510.

Ma, D., D. N. Cook, et al. (1993). "Molecular-Cloning and Characterization of Acra and Acre Genes of Escherichia-Coli." Journal of Bacteriology 175(19): 6299-6313.

Mather, A. E., S. W. J. Reid, et al. (2013). "Distinguishable Epidemics of Multidrug-Resistant Salmonella Typhimurium DT104 in Different Hosts." Science 341(6153): 1514-1517.

Mcmurry, L., R. E. Petrucci, et al. (1980). "Active Efflux of Tetracycline Encoded by 4 Genetically Different Tetracycline Resistance Determinants in Escherichia-Coli." Proceedings of the National Academy of Sciences of the United States of America-Biological Sciences 77(7): 3974-3977.

Nikaido, E., A. Yamaguchi, et al. (2008). "AcrAB multidrug efflux pump regulation in Salmonella enterica serovar typhimurium by RamA in response to environmental signals." Journal of Biological Chemistry 283(35): 24245-24253.

Nikaido, H. (2003). "Molecular basis of bacterial outer membrane permeability revisited." Microbiology and Molecular Biology Reviews 67(4): 593-+.

Nikaido, H. and M. Vaara (1985). "Molecular-Basis of Bacterial Outer-Membrane Permeability." Microbiological Reviews 49(1): 1-32.

Nilsson, M. R. (2004). "Techniques to study amyloid fibril formation in vitro." Methods 34(1): 151-160.

Nishino, K., T. Latifi, et al. (2006). "Virulence and drug resistance roles of multidrug efflux systems of Salmonella enterica serovar Typhimurium." Molecular Microbiology 59(1): 126-141.

Nishino, K., E. Nikaido, et al. (2009). "Regulation and physiological function of multidrug efflux pumps in Escherichia coli and Salmonella." Biochimica Et Biophysica Acta-Proteins and Proteomics 1794(5): 834-843.

O'Regan, E., T. Quinn, et al. (2009). "Multiple Regulatory Pathways Associated with High-Level Ciprofloxacin and Multidrug Resistance in Salmonella enterica Serovar Enteritidis: Involvement of ramA and Other Global Regulators." Antimicrobial Agents and Chemotherapy 53(3): 1080-1087.

Oethinger, M., W. V. Kern, et al. (2000). "Ineffectiveness of topoisomerase mutations in mediating clinically significant fluoroquinolone resistance in Escherichia coli in the absence of the AcrAB efflux pump." Antimicrobial Agents and Chemotherapy 44(1): 10-13.

Olliver, A., M. Valle, et al. (2004). "Role of an acrR mutation in multidrug resistance of in vitro-selected fluoroquinolone-resistant mutants of Salmonella enterica serovar Typhimurium." Fems Microbiology Letters 238(1): 267-272.

Parker, L. L. and B. G. Hall (1990). "Characterization and Nucleotide-Sequence of the Cryptic Cel Operon of Escherichia-Coli K12." Genetics 124(3): 455-471.

Passerini, L., K. Lam, et al. (1992). "Biofilms on Indwelling Vascular Catheters." Critical Care Medicine 20(5): 665-673.

Pawar, D. M., M. L. Rossman, et al. (2005). "Role of curli fimbriae in mediating the cells of enterohaemorrhagic Escherichia coli to attach to abiotic surfaces." Journal of Applied Microbiology 99(2): 418-425.

Perez, A., M. Poza, et al. (2012). "Effect of Transcriptional Activators SoxS, RobA, and RamA on Expression of Multidrug Efflux Pump AcrAB-TolC in Enterobacter cloacae." Antimicrobial Agents and Chemotherapy 56(12): 6256-6266.

Piddock, L. J. V. (2006). "Multidrug-resistance efflux pumps - not just for resistance." Nature Reviews Microbiology 4(8): 629-636.

Piddock, L. J. V., D. G. White, et al. (2000). "Evidence for an efflux pump mediating multiple antibiotic resistance in Salmonella enterica serovar Typhimurium." Antimicrobial Agents and Chemotherapy 44(11): 3118-3121.

Pos, K. M. (2009). "Trinity revealed: Stoichiometric complex assembly of a bacterial multidrug efflux pump." Proceedings of the National Academy of Sciences of the United States of America 106(17): 6893-6894.

Pradel, E. and J. M. Pages (2002). "The AcrAB-TolC efflux pump contributes to multidrug resistance in the nosocomial pathogen Enterobacter aerogenes." Antimicrobial Agents and Chemotherapy 46(8): 2640-2643.

Prouty, A. M., I. E. Brodsky, et al. (2004). "Bile-salt-mediated induction of antimicrobial and bile resistance in Salmonella typhimurium." Microbiology-Sgm 150: 775-783.

Ramos, J. M., J. M. Ales, et al. (1996). "Changes in susceptibility of Salmonella enteritidis, Salmonella typhimurium, and Salmonella virchow to six antimicrobial agents in a Spanish hospital, 1980-1994." European Journal of Clinical Microbiology & Infectious Diseases 15(1): 85-88.

Ricci, V., S. J. W. Busby, et al. (2012). "Regulation of RamA by RamR in Salmonella enterica Serovar Typhimurium: Isolation of a RamR Superrepressor." Antimicrobial Agents and Chemotherapy 56(11): 6037-6040.

Ricci, V. and L. J. V. Piddock (2009). "Ciprofloxacin selects for multidrug resistance in Salmonella enterica serovar Typhimurium mediated by at least two different pathways." Journal of Antimicrobial Chemotherapy 63(5): 909-916.

RichterDahlfors, A., A. M. J. Buchan, et al. (1997). "Murine salmonellosis studied by confocal Microscopy: Salmonella typhimurium resides intracellularly inside macrophages and exerts a cytotoxic effect on phagocytes in vivo." Journal of Experimental Medicine 186(4): 569-580.

Romeo, T. (1998). "Global regulation by the small RNA-binding protein CsrA and the non-coding RNA molecule CsrB." Molecular Microbiology 29(6): 1321-1330.

Romeo, T., M. Gong, et al. (1993). "Identification and Molecular Characterization of Csra, a Pleiotropic Gene from Escherichia-Coli That Affects Glycogen Biosynthesis, Gluconeogenesis, Cell-Size, and Surface-Properties." Journal of Bacteriology 175(15): 4744-4755.

Romeo, T., C. A. Vakulskas, et al. (2013). "Post-transcriptional regulation on a global scale: form and function of Csr/Rsm systems." Environmental Microbiology 15(2): 313-324.

Romling, U., Z. Bian, et al. (1998). "Curli fibers are highly conserved between Salmonella typhimurium and Escherichia coli with respect to operon structure and regulation." Journal of Bacteriology 180(3): 722-731.

Sabnis, N. A., H. H. Yang, et al. (1995). "Pleiotropic Regulation of Central Carbohydrate-Metabolism in Escherichia-Coli Via the Gene Csra." Journal of Biological Chemistry 270(49): 29096-29104.

Seyll, E. and L. Van Melderen (2013). "The Ribonucleoprotein Csr Network." International Journal of Molecular Sciences 14(11): 22117-22131.

Steele-Mortimer, O., J. H. Brumell, et al. (2002). "The invasion-associated type III secretion system of Salmonella enterica serovar Typhimurium is necessary for intracellular proliferation and vacuole biogenesis in epithelial cells." Cellular Microbiology 4(1): 43-54.

Sterzenbach, T., K. T. Nguyen, et al. (2013). "A novel CsrA titration mechanism regulates fimbrial gene expression in Salmonella typhimurium." Embo Journal 32(21): 2872-2883.

Stewart, P. S. (2002). "Mechanisms of antibiotic resistance in bacterial biofilms." International Journal of Medical Microbiology 292(2): 107-113.

Su, L. H., C. H. Chiu, et al. (2004). "Antimicrobial resistance in nontyphoid Salmonella serotypes: A global challenge." Clinical Infectious Diseases 39(4): 546-551.

Suzuki, K., P. Babitzke, et al. (2006). "Identification of a novel regulatory protein (CsrD) that targets the global regulatory RNAs CsrB and CsrC for degradation by RNase E." Genes & Development 20(18): 2605-2617.

Thanassi, D. G., L. W. Cheng, et al. (1997). "Active efflux of bile salts by Escherichia coli." Journal of Bacteriology 179(8): 2512-2518.

Threlfall, E. J. (2000). "Epidemic Salmonella typhimurium DT 104 - a truly international multiresistant clone." Journal of Antimicrobial Chemotherapy 46(1): 7-10.

Timmermans, J. and L. Van Melderen (2009). "Conditional Essentiality of the csrA Gene in Escherichia coli." Journal of Bacteriology 191(5): 1722-1724.

Vakharia, H., G. J. German, et al. (2001). "Isolation and characterization of Escherichia coli tolC mutants defective in secreting enzymatically active alpha-hemolysin." Journal of Bacteriology 183(23): 6908-6916.

van der Straaten, T., R. Janssen, et al. (2004). "Salmonella gene rma (ramA) and multiple-drug-resistant Salmonella enterica serovar Typhimurium." Antimicrobial Agents and Chemotherapy 48(6): 2292-2294.

Wang, X., A. K. Dubey, et al. (2005). "CsrA post-transcriptionally represses pgaABCD, responsible for synthesis of a biofilm polysaccharide adhesin of Escherichia coli." Molecular Microbiology 56(6): 1648-1663.

Webber, M. A., A. M. Bailey, et al. (2009). "The Global Consequence of Disruption of the AcrAB-TolC Efflux Pump in Salmonella enterica Includes Reduced Expression of SPI-1 and Other Attributes Required To Infect the Host." Journal of Bacteriology 191(13): 4276-4285.

Wei, B. D. L., A. M. Brun-Zinkernagel, et al. (2001). "Positive regulation of motility and flhDC expression by the RNA-binding protein CsrA of Escherichia coli." Molecular Microbiology 40(1): 245-256.

Weilbacher, T., K. Suzuki, et al. (2003). "A novel sRNA component of the carbon storage regulatory system of Escherichia coli." Molecular Microbiology 48(3): 657-670.

White, A. P., D. L. Gibson, et al. (2006). "Thin aggregative fimbriae and cellulose enhance long-term survival and persistence of Salmonella." Journal of Bacteriology 188(9): 3219-3227.

Chaudhuri, R.R., Loman, N.J, et al. (2008). "xBASE2: a comprehensive resource for comparative bacterial genomics." Nucleic Acids Research 36: D543-D546.

Yamasaki, S., E. Nikaido, et al. (2013). "The crystal structure of multidrug-resistance regulator RamR with multiple drugs." Nature Communications 4.

Zhao, S., S. Qaiyumi, et al. (2003). "Characterization of Salmonella enterica serotype Newport isolated from humans and food animals." Journal of Clinical Microbiology 41(12): 5366-5371.

UNIVERSITY OF BIRMINGHAM

Project 2: Exploring the dynamics of *Pseudomonas aeruginosa* attachment to host cells during anti-adhesion therapy

by

Victoria Attah

Supervisor: Dr Anne-Marie Krachler

A research thesis submitted to the University of Birmingham as part of the requirements for the degree of MRes in Molecular and Cellular Biology

Host and Pathogen Interactions Group

Institute of Microbiology and Infection

School of Biosciences

University of Birmingham

Abstract

There is an urgent need for alternative therapeutics to treat bacterial infections and limit the transmission of resistance. One promising approach is to target bacterial virulence, allowing the host immune system to clear the infection. So-called anti-virulence therapies are thought to generate little selective pressure for the development of resistance.

The attachment of bacteria to host cells is considered a prerequisite for bacteria to establish and propagate infection. Anti-attachment therapies are well-documented, however clinical treatments are currently unavailable. Mathematical modelling is a useful tool to model the efficacy of anti-virulence therapies *in silico*, particularly in combination with standard antibiotics. However, computer simulations based on theoretical values may limit the specificity of dosing regimens.

The aims of this study were to generate experimental data in support of *in silico* modelling for anti-virulence therapy. This was achieved by exploring the attachment of 6 clinical *Pseudomonas aeruginosa* strains from the Queen Elizabeth Hospital in Birmingham to HeLa cells (0 to 5 hours post-infection). Baseline attachment data was compared to attachment in the presence of 4-methylumbelliferyl α-D-mannopyranoside and recombinant GST-MAM7 beads, which present two distinct approaches to inhibit bacterial adhesion. Whilst 4-methylumbelliferyl α-D-mannopyranoside resulted in modest inhibition to attachment, GST-MAM7 beads generated interesting data for further study.

Acknowledgements

I am grateful to my supervisor, Dr Anne-Marie Krachler, for giving me the opportunity to undertake my research project in the Host and Pathogen Interactions (HAPI) group, and her help, advice and feedback during my time in the laboratory and during the writing of my thesis.

I would like to thank all other members of the HAPI lab for their help and kindness throughout my time with the group.

Contents

List of figures used in the study

List of tables used in the study

1.0 Introduction

1.1 Multiple drug resistance and *Pseudomonas aeruginosa*

The growing phenomenon of bacterial resistance to antimicrobials poses a key problem for the treatment of bacterial infections, due to the limitations for infection management (Swartz 1994), (Harris, Torres-Viera et al. 1999). Multi-drug resistant (MDR) bacteria are capable of surviving in the presence of distinct structural classes of therapeutic drugs, at concentrations high enough to eradicate susceptible cells from the population, exerting a selective pressure on these bacteria. This selective pressure allows resistant cells to proliferate and dominate in the population, through the transfer of genetic material, and therefore infection persists with very few treatment options available, particularly for bacteria resistant to multiple therapeutic agents (Alonso, Campanario et al. 1999).

Since the discovery of antimicrobials in the 1940s, a combination of mismanagement, overuse and exploitation as growth promoters in livestock, are all factors that have thought to contribute to the emergence and spread of resistance (Arason, Kristinsson et al. 1996), (Kummerer 2004). As a result, the management of antimicrobial resistance is a scientific challenge of global significance and as described in a report published by The World Health Organisation in April 2014, a “post-antibiotic era” could follow, where once treatable bacterial infections will eventually become untreatable (WHO, 2014). Consequently, since resistant bacteria were first documented in the literature, scientific research has tried to understand the molecular and cellular mechanisms of bacterial resistance as well as exploring novel treatments for bacterial infections, aimed at preventing its spread.

Pseudomonas aeruginosa is a coccobacillus, gram-negative bacterium that is ubiquitous in water, soil and most artificial environments and surfaces (Green, Schroth et al. 1974). It is also thought that *P. aeruginosa* makes up the normal skin flora of up to 20% of the human population. The organism was first described in 1872 (Schroeter 1872) and the first pure culture was isolated from human skin wounds in 1882 (Gessard 1882). Morphological identification of *P. aeruginosa* involves the observation of pearlescent blue-green colonies on nutrient agar, attributed to pyocyanin toxins secreted by the organism.

P. aeruginosa is considered to be an opportunistic pathogen of humans and animals that is capable of causing infection when host immune defences are low. *P. aeruginosa* infection of healthy tissues is rare, however, nosocomial risk groups for *P. aeruginosa* infection include patients undergoing bone marrow transplants, patients with cystic fibrosis or AIDS, and patients with severe burns (Bodey, Bolivar et al. 1983), (Govan and Nelson 1992), (Mendelson, Gurtman et al. 1994). Strains of *P. aeruginosa* associated with infections are considered toxigenic and tissue-invasive, and can gain access to the host through wounds and abrasions in the skin, leading to the invasion and colonisation of tissues and organ sites. Specific clinical manifestations of infection where *P. aeruginosa* is the causative agent depend on the strain; however, general symptoms include localised inflammation of infected body sites and sepsis - leading to chronic illness, which can be fatal if left untreated.

P. aeruginosa is considered to be the most-common gram-negative causative agent of hospital-acquired infections, and is associated with 8% of wound infections, 10%

of blood stream infections, 12% of urinary tract infections, and 16% of pneumonia, therefore is considered a serious pathogen leading to potentially-fatal complications caused by secondary infections in immunocompromised and debilitated patients (Van Delden and Iglewski 1998).

The ability of *P. aeruginosa* to cause infection is attributed to surface and secreted virulence factors, including those involved in attachment to host cells, colonisation of body sites and invasion, as well as those which are involved in tissue damage or stimulating an immune response (Feldman, Bryan et al. 1998), (Ran, Hassett et al. 2003), (Lau, Ran et al. 2004), (Kipnis, Sawa et al. 2006). *P. aeruginosa* pyocyanin toxins cause oxidative stress when administered to *Caenorhabditis elegans*, which is thought to be due to the disturbance of cellular mechanisms in competing cells to promote the survival of the organism in niche environments (Ran, Hassett et al. 2003), (Lau, Ran et al. 2004). *P. aeruginosa* is able to proliferate in aerobic and partial oxygen-depleted conditions, and at temperatures up to 42°C, which may additionally enhance its ability to survive and proliferate in the host, as observed in the lungs of cystic fibrosis patients, which are coated in thick mucus that may otherwise limit the diffusion of oxygen to bacterial cells (Alvarez-Ortega and Harwood 2007).

P. aeruginosa is a frequent coloniser of moist artificial environments, including catheters and other medical equipment in hospitals and clinical healthcare environments, and the organism has been isolated from hospital sinks, drains, floors, and vessels containing lotions and creams (Noble and Savin 1966), (Ayliffe, Babb et

al. 1974). In 2012, sink taps were identified as the source of a *P. aeruginosa* outbreak in a neonatal intensive care unit, highlighting its ubiquitous presence in diverse environments and the potential sources of bacterial contamination that may lead to secondary bacterial infections (Breahnach, Cubbon et al. 2012). Additionally, *P. aeruginosa* is capable of surviving and proliferating in distilled water for a prolonged amount of time, so has the potential to cause infection in patients undergoing respiratory therapies (Carson, Favero et al. 1973). Cross infections can occur through direct environmental contact or through carriers, confirming the importance of implementing strict disinfection regimes in hospitals. However, despite improved hospital practises, including hand hygiene to prevent cross-contamination, strict isolation of infected patients and improved wound treatments, up to 60% of deaths in hospital burns units are still caused by outbreaks of *P. aeruginosa* (Van Delden and Iglewski 1998).

In 2000, the first wild-type *P. aeruginosa* strain was sequenced. The complete genome, which still remains one of the largest prokaryotic genomes sequenced to date, indicated that *P. aeruginosa* ability to adapt to niche environments is likely attributed to the high number of encoded proteins that are involved in virulence, transport and regulation (Stover, Pham et al. 2000). Additionally, 0.3% of the *P. aeruginosa* genome encodes genes which are involved in resistance to antimicrobials and around 10% of the *P. aeruginosa* genome encodes genes located in pathogenicity islands (PAIs). PAIs are encoded chromosomally or extrachromosomally in pathogenic gram-positive and gram-negative bacteria, but are generally absent from non-pathogenic species, and enable *P. aeruginosa* to acquire

genes, termed mobile genetic elements, including those that confer resistance to multiple antimicrobial compounds. These mobile elements are acquired through horizontal gene transfer, including phage, plasmid or transposon transfer events, and can occur between bacteria of the same species and bacteria of different species (Frost, Leplae et al. 2005).

The most widely used therapeutic compounds used to treat bacterial infections, including those caused by *P. aeruginosa*, are classed as either bactericidal or bacteriostatic, based upon their mechanism of action. Bactericidal compounds eradicate bacteria by interfering in essential pathways and include antiseptics, disinfectants and antibiotics, whereas bacteriostatic compounds inhibit cell growth and proliferation by interfering with cellular metabolism, protein synthesis or DNA replication, impaired for as long as the compound is present. The antibiotic class known as the beta-lactam antibiotics are considered bactericidal, because they target the cross-linking mechanism of gram-positive cell walls, leading to lysis of the bacterial cell (Tomasz 1979), whereas the tetracyclines are considered bacteriostatic, as they bind to ribosomes to prevent the translation of specific proteins targeted for their virulence (Chopra and Roberts 2001).

P. aeruginosa has both intrinsic and acquired antimicrobial resistance determinants, and their simultaneous expression contributes to MDR, and to the failure of antimicrobial treatments (Hancock 1998). Acquired bacterial resistance may arise from a spontaneous mutation, which is passed on via horizontal or vertical transfer, leading to a dominant resistant phenotype at sites of infection. Acquired resistance

determinants include antibiotic-inactivating enzymes such as aminoglycoside modifying enzymes (AMEs), metallo-beta-lactamases (MBLs), extended spectrum-beta-lactamases (ESBLs), and cephalosporinases, and confer high levels of resistance to aminoglycosides, beta-lactamases and cephalosporins, respectively (Doi, Ogura et al. 1968), (Tomasz 1979), (Rodriguez-Martinez, Poirel et al. 2009). Resistance to the fluoroquinolone antibiotics is also mediated by mutations in the DNA gyrase target enzyme, *gyrA*, and topoisomerase IV enzyme, parC (Nakano, Deguchi et al. 1997).

P. aeruginosa intrinsic bacterial resistance can be mediated by the constitutive expression of efflux pumps, which span the inner and outer bacterial membranes. Studies have shown that efflux pumps are expressed at a low, baseline level in wild-type *P. aeruginosa* strains, and expression significantly increases when the bacteria are exposed to antibiotics (Poole 2001). *P. aeruginosa* resistance is associated with the expression of MexAB-OprM and MexXY-OprA efflux pumps, which form part of the Resistance Nodulation Division (RND) family of transporters. The role of RND efflux pumps in bacterial resistance has been well-characterised in many gram-negative bacteria (Poole 2004), (Piddock 2006). It is interesting to consider that overexpression of one efflux pump, as a result of exposure to one antibiotic, additionally offers bacteria resistance to other antibiotics that are substrates of the same pump. For example, quinolone antibiotics are the substrate for all Mex efflux pumps, and therefore resistance to this compound may indirectly affect the susceptibility of bacteria to other compounds (Kohler, MicheaHamzehpour et al. 1997). This is likely to affect the range of treatments available to treat resistant *P.*

aeruginosa infections, and may further enable additional target mutations to develop against specific antibiotics. Reduced expression of outer membrane porins, which alter membrane permeability to substrates, also confers a low level of antimicrobial resistance, such as a decrease in the expression of the OprD porin, which is involved in the uptake of hydrophilic carbapenems. OprD and MexEF are oppositely regulated by a common regulatory mechanism, therefore increased efflux pump expression is associated with decreased porin expression, highlighting the complexity of resistance gene regulation in bacteria (Kohler, MicheaHamzehpour et al. 1997).

Due to intrinsic and acquired resistance, treatments for resistant *P. aeruginosa* infections may be limited and depend on frontline antimicrobials, including imipenem and meropenem (Kesado, Hashizume et al. 1980), (Edwards, Turner et al. 1989). Imipenem is a broad-spectrum antibiotic that targets and inhibits the synthesis of the bacteria cell wall, and is usually given as a combinational therapy with cilastatin, which prevents its degradation by dehydropeptidase 1 in the stomach. Imipenem forms part of a subgroup of beta-lactams, called carbapenems and is effective against many bacteria that are resistant to other beta-lactams, including *P. aeruginosa*. Meropenem has a similar mechanism of action to Imipenem, however is not deactivated by dehydropeptidase 1, so can be administered alone.

1.2. *Pseudomonas aeruginosa* biofilms

P. aeruginosa is capable of forming competent biofilm, which likely contributes to the success of the pathogen in causing device-associated infections in healthcare environments. A biofilm is defined as an organised structure of different bacterial

species suspended in an extracellular matrix, initiated by attachment to a surface (Costerton, Stewart et al. 1999). Biofilms are much more efficient at colonising surfaces, and due to the close proximity of bacteria within a biofilm, increased communication is thought to occur via a phenomenon known as quorum sensing, which allows the bacterial population to respond to extracellular signals, by secreting small molecules that enable them to rapidly adapt to their environment (Davies, Parsek et al. 1998). Biofilms are difficult to remove, particularly the bacteria within the body of the biofilm, as the structure offers a higher level of protection for the cells within. Higher concentrations of antimicrobials are generally needed to eradicate bacteria within a biofilm, compared with planktonic bacteria, therefore biofilms likely act as reservoirs of infection (Donlan 2001). Although there are instances were bacterial biofilm is considered symbiotic for the bacteria and the host, as has been explored in *Escherichia coli* in the large intestine, which produces vitamin K, biofilm becomes a problem of clinical-relevance when it is implicated in the colonisation of medical devices. In this way, biofilm formation is often considered a prerequisite for device-associated complications and secondary infections. Biofilm may enhance the spread of resistance between bacterial species, as it is thought that resistance genes can be transferred more readily between bacteria within a biofilm (Savage, Chopra et al. 2013), which is particularly important when considering the treatment of biofilm with low concentrations of antimicrobial compounds that may select for resistance. Due to the complexity, little is known about the molecular mechanisms surrounding the trigger for *P. aeruginosa* to switch to a biofilm phenotype, which would likely impact on future approaches to treat biofilms (Sauer, Camper et al. 2002).

1.3 *Pseudomonas aeruginosa* virulence and pathogenicity

The genome of *P. aeruginosa* encodes a number of genes which play a role in the virulence and pathogenicity of the organism. For example, genes encoding flagella make *P. aeruginosa* strains more virulent than non-flagellated strains (Montie, Doylehuntzinger et al. 1982). Virulence factors may be intrinsically encoded on the bacterial chromosome, or acquired from mobile genetic elements, and in order to evade the host immune response many bacteria deliver extracellular toxins and effector proteins to the host cytosol that can damage or change the cellular activities to benefit the pathogen. These proteins are transported into host cells by type III, type IV and type VI secretion systems and the process is dependent on bacterial contact with the host cell (Galan and Collmer 1999).

Toxin A is encoded by more than 85% of *P. aeruginosa* clinical isolates (Pollack, Taylor et al. 1977), and *in vivo*, injection of Toxin A into mice has been shown to prevent protein synthesis from occurring in host tissues. Strains of Pseudomonas lacking this toxin injected into a mouse infection model caused a reduced amount of tissue damage, compared to those strains where Toxin A was intact (Ohman, Sadoff et al. 1980). However, Blackwood et al (1983) demonstrated that Toxin A is not required to establish bacterial infection, suggesting that Pseudomonas hosts an array of strategies to colonise, establish and propagate infection (Blackwood, Stone et al. 1983). For example, cell surface polysaccharides including lipopolysaccharide (LPS) are important for outer membrane integrity and maintaining a barrier between the bacterial cell and the environment, and may play additional roles in host-pathogen interactions and biofilm formation.

Gene expression of a number of bacterial genes is known to occur via quorum sensing (Whiteley, Lee et al. 1999), whereby bacteria are able to respond to stimuli in their environment. The phenomenon is dependent on reaching a critical threshold of signalling molecule, referred to as an autoinducer. Various autoinducers have been identified in bacteria, including small peptides and organic molecules such as the N-acylhomoserine lactones in gram negative bacteria (Williams, Bainton et al. 1992). Typically, as the cell density of the bacterial population increases, the concentration of the autoinducer signalling molecule increases, triggering a co-ordinated response resulting in the induction or inhibition of specific protein synthesis. Quorum sensing is known to mediate bacterial defence against other competing organisms in niche environments, enhance nutrient access under stress conditions, as well as signal the escape of cellular populations from survival risks (Williams, Winzer et al. 2007). This suggests that quorum sensing provides fine tuning of transcriptional regulation, enabling bacteria to sense and respond to their environment rapidly. Quorum sensing has been shown to be involved in the regulation of a number of bacterial virulence genes, including proteases, elastases and pyocyanin, as well as those required for competent biofilm formation (Table 1.1).

Acylated homoserine lactone
Alkaline protease
Catalase
Elastase
Toxin A
Hydrogen cyanide
Lectins
Pyocyanin
Rhamnolipid
Secretion protein
Superoxide dismutase

Table 1.1: Known *P. aeruginosa* quorum sensing-regulated virulence genes (Gambello, Kaye et al. 1993), (Hassett, Ma et al. 1999), (Toder, Ferrell et al. 1994), (Pessi and Haas 2000), (Winzer, Falconer et al. 2000), (Brint and Ohman 1995), (Ochsner and Reiser 1995), (Chapon-Herve, Akrim et al. 1997).

1.4 *Pseudomonas aeruginosa* attachment to host cells

In order to persist in the harsh environment within a human host, bacteria must be able to withstand being cleared from the body. The ability of bacteria to attach to host cells has long been known to be an important initial step in the colonisation and the establishment of infection, as attachment allows the bacteria to deploy their repertoire of virulence factors into the host cytosol (Galan and Collmer 1999), (Hayes, Aoki et al. 2010), (Krachler and Orth 2013). Uropathogenic *E. coli* (UPEC), a primary cause of urinary tract infections, interacts with cells in the urinary tract to facilitate attachment (Leffler and Svanborgeden 1981), and oral and respiratory bacteria must adhere to host cells strongly, in order to withstand sheer forces and mechanisms of mucosal flow.

Bacteria attach to host cells via cell surface proteins, called adhesins. Adhesins are one of many virulence factors that facilitate attachment by acting as surface recognition molecules, anchoring the bacteria to other cells or surfaces (Figure 1.1). Attachment allows pathogens to overcome shear forces and remain in the environment they benefit from. Adhesins are species-specific and different adhesins may target different receptors on particular cells or surfaces, and may have different receptor specificities. Inhibition of specific adhesins has been shown to alter the virulence of bacteria (Hahn 1997); therefore it is likely that these molecules play an important role in the establishment of bacterial infection. Furthermore, exploring the dynamics of adhesin gene expression has revealed that specific adhesins are expressed at different phases of infection, therefore, bacteria secrete multiple adhesins to facilitate efficient attachment, emphasising the sophistication of this

complex process. Adhesins play a significant role in bacterial virulence, as initial host cell attachment is required for the delivery of secreted toxins and effector proteins to disarm host defences and propagate infection. *Neisseria gonorrhoeae* attachment to polymophonuclear neutrophils enables the bacteria to escape from phagocytosis, and therefore allows the spread of the bacterium in the host (Densen and Mandell 1978).

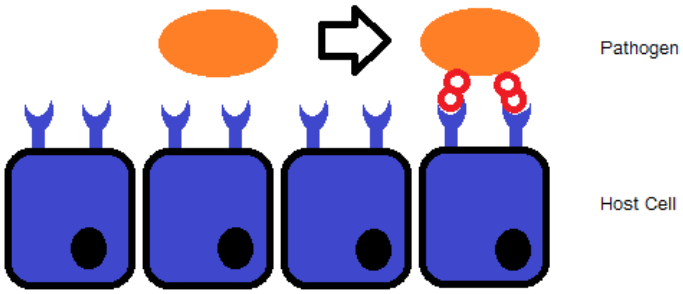

Figure 1.1: Host-pathogen attachment: bacterial cells (orange) synthesise adhesive proteins (red), which bind to specific receptors on host cells (purple), facilitating attachment.

In gram-negative bacteria, bacterial adhesion to host cells is mediated by the expression of lectins, which are proteins found at the tips of bacterial fimbriae or pili. These carbohydrate-specific proteins allow bacteria to recognise mannose-containing glycoproteins on host cell surfaces (Sharon and Lis 1989). Around 90% of UPEC strains encode fimbriae that recognise receptors on the bladder epithelium, which initiates host-cell binding. *In vivo*, lectin binding to seromucinous glands in the lungs and epithelial cells in the pancreas has also been observed (Kirkeby, Wimmerova et al. 2007).

FimH is a D-mannose sensitive adhesin that has been best characterised by extensive study in a number of bacteria, found at the fibrial tip of Type 1 fimbriae (Figure 1.2). FimH is a 29 kDa protein, composed of 279 amino acids, and subunits are localised according to the chaperone/usher pathway (Sauer, Remaut, et al. 2004). FimH facilitates binding to host cells which contain mannose residues, involved in human metabolism, including intestinal epithelial cells, red blood cells, and neutrophils. The FimH protein forms carbohydrate-protein complexes through the recognition and reversible binding to specific carbohydrates containing mannose, forming tight receptor-ligand bonds (Sharon and Lis 1989).

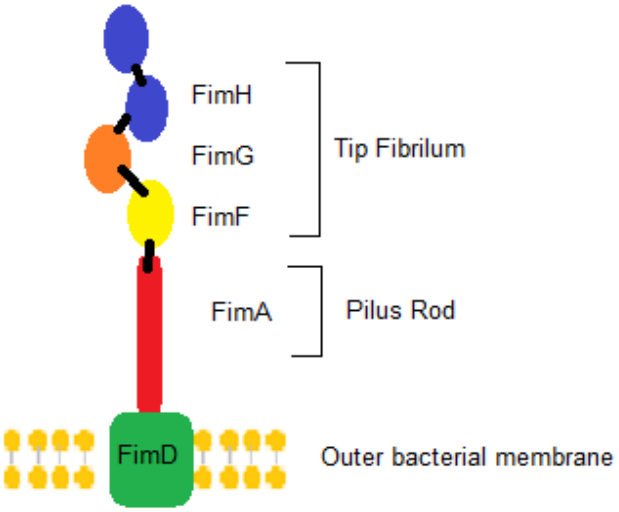

Figure 1.2: Assembly of Type 1 fimbriae. The bacterial membrane is composed of a lipid bilayer (yellow), in which FimD is anchored. Adapted from (Crespo, Puorger et al. 2012).

As FimH is not stable in its pure form, it was first crystallised in complex with FimC, a protein required for the biogenesis of type 1 fimbriae, in 1999 (Choudhury, Thompson et al. 1999). The crystal structure of the complex revealed that FimH is composed of two domains, a lectin domain and a pilin domain, composing amino acids 1 to 156 and 160 to 279, respectively, and connected via a tetra-peptide loop. It was later shown that the interaction of the two domains resulted in two possible conformations

of FimH. The C-terminal pilin domain is responsible for anchoring FimH to the pilus, whereas the N-terminal lectin domain consists of a mannose binding pocket, facilitating surface recognition and reversible binding of the protein to host cells. Depending on the interaction of the two domains, binding efficiency to mannose residues changes; tight domain interaction result in a mannose binding pocket with a greater affinity for mannose, compared with loose domain interaction via a short linker chain, which results in a mannose binding pocket that is more closed, therefore reducing the binding efficacy to carbohydrates. It has been shown that FimH mannose affinity increases during conditions of increased mechanical force (Yakovenko, Sharma et al. 2008), which is unlike other receptor-ligand binding that generally becomes weaker during the onset of force. This phenomenon is referred to as “catch bond” and likely enhances the survival of pathogenic bacteria in the host, due to the harsh environmental conditions at various body sites. Therefore, high mannose-binding enables bacteria to anchor onto host cells to avoid clearance.

Many adhesion factors identified in pathogenic bacteria are expressed during different phases of infection and from different environmental triggers, and therefore may not be required during the early attachment of bacteria to host cells (Boekema, Van Putten et al. 2004), (Lebreton, Riboulet-Bisson et al. 2009). Krachler et al., hypothesised that all bacteria share a common mechanism for attachment, which allows further specific expression and secretion of other adhesins and virulence factors to initiate the spread of infection (Krachler, Ham et al. 2011).

Mammalian cell entry (mce) domains were first identified in the genome of *Mycobacterium tuberculosis* and are expressed on the bacterial cell surface. Although there is currently no crystal structure available for mce, the role of mce domains in enhancing virulence was observed when cloned into non-pathogenic *E. coli,* which enabled the bacterium to invade HeLa cells, evade phagocytosis, and survive inside human macrophages for at least 24 hours (Arruda, Bomfim et al. 1993). The genome of *M. tuberculosis* encodes 4 homologous mce domains: mce1, mce2, mce3 and mce4 (Chitale, Ehrt et al. 2001), which are expressed differently depending on the bacterial growth phase. It was suggested that mce1 is expressed dominantly during early growth phases, evidenced by the inability of recombinant mce2 alone to cause invasion of HeLa cells, despite a 67% homology to mce1 (Chitale, Ehrt et al. 2001). However, multiple mce operons have been shown to be expressed in animal tissue infected with *M. tuberculosis*, suggesting that multiple mce domains may contribute to successful bacterial infection (Kumar, Bose et al. 2003).

Multivalent adhesion molecule 7 (MAM7) is an outer membrane protein containing 7 mce domains (Krachler, Ham et al. 2011). The C-terminal is localised to the extracellular space and the first 44 N-terminal amino acids are predicted to form a transmembrane helix, thought to be important in anchoring MAM7 to the outer membrane of bacteria. Deletion of MAM7 in non-cytotoxic *V. parahemolyticus* resulted in a reduction of attachment to epithelial cells and macrophages *in vitro*, from 80% to 35-45%, suggesting the protein is involved in bacterial attachment to host cells, further evidenced by heterologous expression of non-native MAM7 in a

poorly-adherent *V. parahemolyticus* strain, which resulted in greater attachment to these cells. *In vivo*, deletion of MAM7 in *V. parahemolyticus* resulted in a non-pathogenic phenotype following infection of *C. elegans*, whereas infection with the wild-type bacterium resulted in worm death within 13 days (Krachler, Ham et al. 2011). Taken together, the data suggests that MAM7 contributes to bacterial virulence by enhancing adhesion to host cells. Furthermore, Krachler et al., suggest that there is a positive correlation between the number of mce domains that MAMs have in bacteria, and the efficiency of host cell attachment, determined by the competitive index (CI). The CI for strains containing 1 mce domain was 0.27, whereas the CI for strains containing 6 or 7 mce domains was 0.8, implying a greater attachment potential of bacterial strains with more than one mce domain (Krachler, Ham et al. 2011). It is interesting to consider that all bacteria have at least 1 mce domain, whereas gram-negative bacteria have evolved 6 or more mce domains. It is likely that those bacteria which depend on host cell attachment for survival and proliferation can compete with other organisms in harsh environments with high efficiency adhesion to host cells. Examples of these bacterial species may include those that colonise the oral and respiratory tracts.

MAM7 is thought to bind to fibronectin and phosphatidic acid receptors on host cells, with the interaction being much stronger for the latter, although binding affinity for phosphatidic acid significantly decreases when there are 5, 6 or 7 mce domains (Krachler, Ham et al. 2011). This suggests other mechanisms may mediate tight host cell binding during bacterial adhesion to host cells.

1.5 Anti-attachment therapy

The rapid spread of antimicrobial resistance draws attention to the requirement for alternative treatments for bacterial infections. It has been suggested that a promising novel strategy is one that will not select for resistant bacteria. One of the potential approaches includes attenuating bacteria by targeting virulence, including the prevention of cell adhesion or the delivery of toxins to the host cell.

Attachment of bacteria to host cells is a fundamental process for bacteria to establish infection (Galan and Collmer 1999), (Hayes, Aoki et al. 2010), (Krachler and Orth 2013), therefore presents a potential target for a universal range of bacterial species. Approaches include inhibitors that mimic host cell receptors, which bind to bacteria, and those that mimic bacterial ligands, which bind to host cells, competitively reducing the bacterial-host cell interaction potential (Figure 1.3). Natural compounds with anti-adhesive properties, including cranberry juice, are effective in preventing UTIs, therefore engineered treatments may be beneficial for the treatment of a number of bacterial infections. It is thought that anti-attachment-based therapies may limit the spread of bacterial resistance because bacterial viability would remain unaffected, therefore the urgency to develop resistance diminishes. Furthermore, targeting bacterial attachment to host cells aims to promote the clearance of non-attached bacteria by the host immune system, causing no harm towards the host or the bacteria.

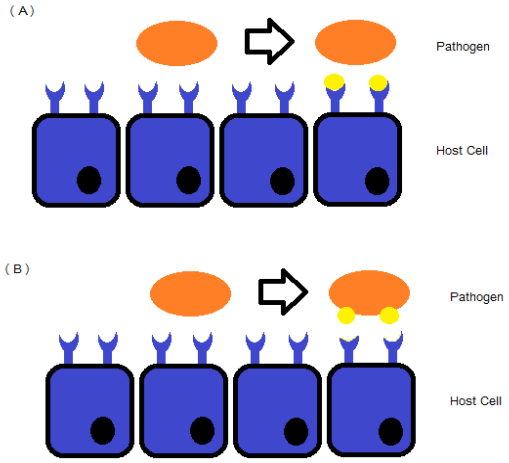

Figure 1.3: Strategies for inhibiting pathogen attachment to host cells. (A): bacterial cells (orange) are unable to attach to host cells (purple) due to the presence of recombinant proteins (yellow) that bind to the host cells, (B): bacterial cells (orange) are unable to attach to host cells (purple) due to the presence of proteins that mimic host cell receptors (yellow).

Anti-adhesin antibodies have been successful in generating acquired in-host immunity and reducing infection of UPEC strains (Bidhendi, Sattari et al. 2007), and as adhesins are located on the bacterial cell surface, they are readily accessible to antibodies and therefore may be effective targets for vaccines. The primary structure of FimH is 99% conserved amongst bacteria, therefore FimH is thought to be a promising target for anti-adhesion therapy; vaccinations using FimH to immunise the host have been explored and *in vivo,* FimH immunisation was shown to prevent *E. coli* UTI (Langermann, Palaszynski et al. 1997), (Langermann, Mollby et al. 2000). Furthermore, it has been suggested that a novel anti-adhesion strategy could be an inhibitor which binds to FimH to maintain the protein in its low affinity state. Rodriguez et al., used X-ray crystallography and site-directed mutagenesis to explore mutations in the lectin domain of FimH that would allow the protein to remain in its low affinity state (Rodriguez, Kidd, et al. 2013). However, other studies have shown that *E. coli*

FimH conversion from a high affinity to a low affinity state may be beneficial for infection by shedding antibodies from the immune response that are bound to it (Tchesnokova, Aprikian et al. 2011), which highlights the complexity of FimH interactions in the host.

Low molecular weight carbohydrates have been shown to inhibit the interaction between the bacterial lectin, FimH, and the host cell. X-ray crystallography and substrate binding studies have shown that α-D-mannosides bind to bacterial FimH with high affinity (Fitos, Heremans et al. 1979), (Kotter, Krallmann-Wenzel et al. 1998), (Bouckaert, Berglund et al. 2005), (Sperling, Fuchs et al. 2006). The highest binding affinity is associated with long chain mannosides**,** thought to be because the ligands interact more strongly with the hydrophobic amino acid residues that line the mannose-binding pocket (Han, Pinkner et al. 2010). Furthermore, such aromatic α-glycosides are more effective inhibitors of attachment of *E. coli* to guinea pig ileal epithelial cells than methyl α-mannosides (Firon, Ashkenazi et al. 1987), suggesting a promising strategy for FimH inhibition.

1.6 Mathematical model of resistance and anti-attachment therapy

Anti-virulence treatments are not available clinically, therefore mathematical modelling is a practical tool to assess their viability *in silico*. One such model has been developed in the Department of Chemistry, at the University of Birmingham (Ternent, unpublished). Initial simulations explore the conditions required for the emergence of resistant bacteria in a bacterial population of susceptible and resistant cells, typical of localised bacterial infections. The model simulation is based on four variables: the number of susceptible bacteria in the population, the number of

resistant bacteria in the population, the antibiotic selected for a single-dose treatment, and the immune cells recruited to the site of infection (considered to be proportional to the number of bacteria at the site of infection). The model allows the determination of the conditions required for resistant bacteria to become dominant in the infection population, and therefore the conditions required for current treatment failure due to the development of bacterial resistance. Further simulations present a model for the clearance of an infection using an anti-virulence treatment only, which successfully eliminates the resistant population of bacteria at the site of infection, due to the fitness cost associated with maintaining a resistant phenotype. The final simulation presents a model for a combinational treatment approach, whereby dosing with an antibiotic and an anti-virulence, competitive-replacement compound, is able to successfully eliminate both the susceptible and resistant bacterial population at an infection site. However, the simulated data suggests that the limiting factor is the dose of the anti-virulence compound in removing the resistant population of bacteria, because every bacterial strain, infection and patient are different. A high dose of an anti-virulence treatment would flood the infection site, however is likely to be expensive, and potentially harmful to the host. Therefore dosing regimens must be tailor-made so they are strain and site-specific. Many of the parameters described for the model are estimated values, and therefore may not be accurate; experimental values should therefore be determined, in order to establish when treatment would be effective in an individual, and at what concentration and doses the anti-virulence therapy would be successful.

1.7 Research hypothesis and experimental aims

The primary aim of this project was to generate experimental data in support of *in silico* modelling for anti-virulence therapy at the University of Birmingham (Ternent, unpublished). Six clinical isolates of *P. aeruginosa* were obtained from an outbreak at the Queen Elizabeth hospital in Birmingham (laboratory strain numbers: 985, 992, 1004, 1007, 1008 and 1009); isolates 992 and 1004 were isolated from the water supply in the outbreak ward, and isolates 985, 1007, 1008 and 1009 were isolated from a patient at various times during a two week antibiotic treatment. Attachment of the strains to HeLa cells was explored from 0 to 5 hours, and baseline attachment data was compared to attachment in the presence of 4-methylumbelliferyl α-D-mannopyranoside and recombinant GST-MAM7 beads, which present two distinct approaches to inhibit bacterial adhesion.

Prior to beginning this project, there was no significant difference between the growth rates of all six isolates, all six isolates were resistant to imipenem (>8 µg/mL) and sensitive to meropenem, with the exception of isolate 1004, which was resistant to meropenem (>8 µg/mL). Interestingly, isolate 1004 showed a significant increase in attachment to the macrophage cell line J774 *in vitro*, although the assay itself was not able to discriminate between bacterial attachment and macrophage phagocytosis (unpublished data).

2.0 Materials and Methods

Table 2.1: Bacterial strains used in the study.

Laboratory Reference	Bacteria	Source and Description	Growth
985	*Pseudomonas aeruginosa*	Burns Unit, Queen Elizabeth Hospital, Birmingham (clinical, patient)	LB media not supplemented
992	*Pseudomonas aeruginosa*	Burns Unit, Queen Elizabeth Hospital, Birmingham (clinical, water)	LB media not supplemented
1004	*Pseudomonas aeruginosa*	Burns Unit, Queen Elizabeth Hospital, Birmingham (clinical, water)	LB media not supplemented
1007	*Pseudomonas aeruginosa*	Burns Unit, Queen Elizabeth Hospital, Birmingham (clinical, patient)	LB media not supplemented
1008	*Pseudomonas aeruginosa*	Burns Unit, Queen Elizabeth Hospital, Birmingham (clinical, patient)	LB media not supplemented
1009	*Pseudomonas aeruginosa*	Burns Unit, Queen Elizabeth Hospital, Birmingham (clinical, patient)	LB media not supplemented

Table 2.2: Mammalian cells used in the study.

Cell Line	Source and Description	Growth
HeLa	Mammalian (human) epithelial cells	Dulbeccos modified Eagle Medium, supplemented with 10% foetal bovine serum, 5% L-glutamine and 5% penicillin-streptomycin

2.1 Bacterial strains used in this study

All bacterial strains used in this study are listed in Table 2.1.

All bacterial strains were recovered from storage at -80°C in liquid cyoprotectant. A sterile 1 µL inoculation loop was used to streak each strain to purity onto Luria Bertani (LB) agar plates, which were then incubated in a static aerobic incubator for 24 hours at 37°C. Plates were checked to ensure they were free from contamination.

LB agar was prepared by autoclaving 25 g of LB power (Sigma) and 12g (1.2%) of agar (Sigma) in 1000 mL sterile distilled water (SDW), and once cooled, agar plates were poured aseptically and air dried. Unused plates were stored at 4°C for up to two weeks.

Overnight cultures of the bacterial strains used in this study were prepared by aliquoting 5 mL of sterile LB into sterile 15 mL tubes. A single bacterial colony was picked from a LB agar plate, into each tube. The tubes were incubated in a shaking aerobic incubator for 24 hours at 37°C.

LB broth was prepared by autoclaving 12.5 g of powder (Sigma), dissolved in 500 mL SDW.

All bacterial cultures used in this study were used to prepare Multiplicity of Infection (MOI) stocks of 10 and 1. MOI refers to the ratio of bacterial cells to the cells under study. For the duration of this study, an MOI of 10 denotes a stock preparation of 10 bacterial cells for every HeLa cell.

Overnight cultures were diluted 1:10 in colourless, non-supplemented Dulbeccos Modified Eagle Medium (DMEM) (Sigma) and the OD_{600} was measured using a

spectrophotometer (Eppendorf), by aliquoting 1 mL of each diluted culture into a plastic cuvette. The optical density was measured against 1 mL of colourless DMEM only (blank). The dilution factor required for an MOI of 10 was calculated using the formula 3 / OD_{600}, which gave the volume of bacteria required in µL, per mL of colourless DMEM. The dilution factor required for an MOI of 1 was calculated as above, with the volume of bacteria in µL divided by 10.

2.2 Mammalian cells used in this study

All mammalian cells used in this study are listed in Table 2.2.

All mammalian cells used in this study were handled in a class II biosafety cabinet.

HeLa cells were recovered from storage in liquid nitrogen in DMSO (Sigma), and quickly thawed by placing the cryovial into a water bath set at 37°C. The outside of the cryovial was sprayed with 70% ethanol and wiped with a paper towel. The thawed HeLa cells were resuspended in 9 mL of pre-warmed DMEM, supplemented with 10% Fetal Bovine Serum (FBS), 1% L-glutamine and 1% penicillin-streptomycin (all Sigma), in a sterile 50 mL tube (BD Falcon). The tube was centrifuged at 500 x g for 5 minutes at room temperature to separate the DMSO from the HeLa cells. The supernatant from each tube was discarded and the pellet containing the HeLa cells was resuspended in 10 mL of pre-warmed DMEM. The cells were inoculated into a 9 cm tissue culture dish (BD Falcon) and incubated in a static incubator for 24 hours at 37°C, 5% CO_2. After 24 hours, the culture dish was checked using a light microscope to ensure the cells had attached and formed a monolayer on the culture surface. The DMEM was removed from the culture dish and replaced with 10 mL of fresh, pre-warmed DMEM. The dish was incubated as previously described and checked daily

using a light microscope until the cells reached the desired confluency for sub-culturing and preparation for study (~70-80%).

When HeLa cells in culture reached the desired confluency for splitting, the serine protease Trypsin (Sigma) was used to detach HeLa cells from the surface of the tissue culture dish. DMEM was removed from the tissue culture dish using an automated aspirator vacuum fitted with a sterile glass pipette, and 1 mL of phosphate buffered saline (PBS) (Oxoid) was inoculated onto the edge of the dish by tilting, to wash the cell monolayer. The dish was gently agitated to ensure the PBS covered the cell surface, and was immediately removed. One mL of Trypsin was inoculated onto the edge of the dish by tilting and the dish was gently agitated to ensure complete coverage of the cell surface. The dish was incubated in a static incubator for 5-10 minutes at 37°C, 5% CO_2. The dish was checked during the incubation period using a light microscope to ensure the Trypsin had caused detachment of cells from the tissue culture surface. Once detached, 9 mL of fresh, pre-warmed DMEM was inoculated onto the dish using an automatic pipette and a disposable 10 mL stripette (Costar), to stop the Trypsin reaction.

For maintenance: HeLa cells were split using the ratio 1:10. One mL of HeLa cells were inoculated into 9 mL of pre-warmed DMEM in a new sterile 9 cm tissue culture dish labelled with the appropriate passage number. For the duration of this study, the HeLa cell passage number did not exceed 20. The cells were incubated in a static incubator at 37°C, 5% CO_2 and checked daily until ~70-80% confluency was reached, after which the cells were split as previously described.

For testing: Following Trypsin treatment, resuspended HeLa cells were transferred to a 50 mL tube for counting using a haemocytometer (BS.748, Hawksley, Improved Neubauer). Before use, the haemocytometer and cover slide were sterilised by spraying with 70% ethanol and wiping with a paper towel. Once assembled, 15 µL of HeLa cells were inoculated into the haemocytometer. Each large square in the chamber holds a volume of 0.1 µL, therefore the number of cells in 4 chambers was counted, divided by 4 to obtain an average cell count per large square, and multiplied by 10^4 in order to calculate the number of HeLa cells per mL (1000 µL) of DMEM. Unless otherwise stated, the seeding density of HeLa cells used for the duration of this study was 1.5 x 10^5 / mL. The dilution factor was calculated using the formula $C_s \times V_s = C_f \times V_f$ (where **C** is the concentration, **V** is the volume, **s** is the start and **f** is the final). A HeLa cell stock of 1.5 x 10^5 / mL was prepared using pre-warmed DMEM in a sterile 50 mL tube. Unless otherwise stated, 1 mL of 1.5 x 10^5 / mL HeLa cells was inoculated into each well of a 24-well microtitre tray (MTT) (Greiner bio-one) using an automatic pipette and a disposable 10 mL stripette. MTTs were incubated in a static incubator at 37°C, 5% CO_2 for 24 hours.

2.3 Bacterial infection and attachment assays

Overnight bacterial cultures were prepared as previously described, and an MOI of 1 or 10 was prepared. HeLa cells were seeded into 24-well MTTs, as previously described and following 24 hours incubation, cells were checked using a light microscope to ensure they reached the desired confluency for testing. Existing DMEM was removed from MTTs using an automated aspirator vacuum fitted with a sterile glass pipette, and 1 mL of PBS was inoculated into each well using an

automatic pipette and a disposable 10 mL stripette, to remove residual DMEM from the HeLa cells. The MTTs were incubated for 5-10 minutes at room temperature, before removing the PBS. Each bacterial strain (1 mL) at MOI 10 or 1 was inoculated into the wells of the MTTs, as shown in Figure 2.1. The plates were centrifuged at 1000 x g for 5 minutes at room temperature, and the infection assay was carried out immediately at time points of 1, 0.5, 1, 1.5, 2, 3, 4 and 5 hours.

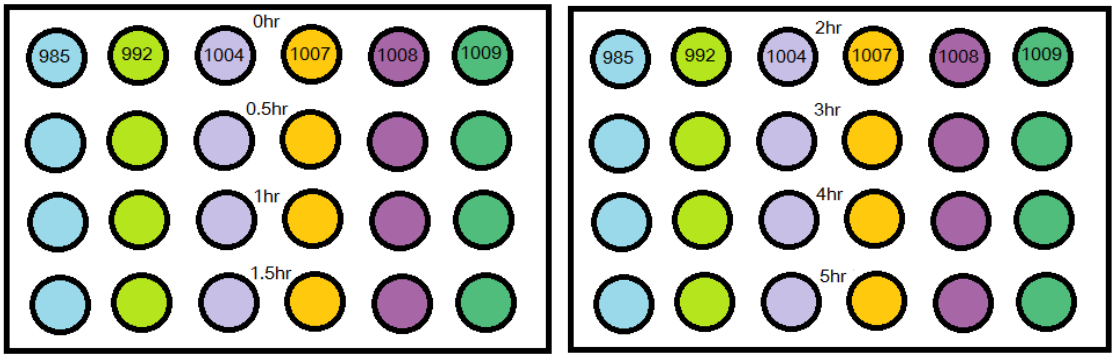

Figure 2.1: MTT layout for investigating the dynamics of *P. aeruginosa* attachment to HeLa cells. The attachment of six *P. aeruginosa* strains was investigated over 5 hours.

At each time point, bacteria that were attached to the HeLa cell monolayer were recovered and enumerated: Non-adherent bacteria were removed from the wells using a manual pipette set to 1000 µL, and the wells were washed three times with 1 mL of sterile PBS. This was added and removed using a manual pipette set to 1000 µL, ensuring the HeLa cell monolayer was not disturbed by gently tilting the MTT. To recover attached bacteria, the HeLa cells were lysed using 1 mL of 0.05% Triton x 100, by repeated pipetting. A stock solution of 0.1% Triton x 100 (Sigma) was prepared in sterile PBS and diluted 1:2 for study. To enumerate attached bacteria, serial 1:10 dilutions were prepared by removing 20 µL from each lysed well of the

MTT, into 180 µL of sterile PBS in sterile 0.8 mL tubes (Sarstedt). Optimal bacterial dilutions were derived experimentally in order to enumerate the bacteria accurately and obtain colonies in the countable range (depending on MOI and time point, generally 1:100 – 1:10,000). The appropriate bacterial dilution (100 µL) was inoculated onto a labelled LB agar plate and spread evenly using an L-shaped etilever (Sarstedt). Once dry, the LB agar plates were inverted and incubated in a static aerobic incubator for 24 hours at 37°C. Plates were checked to ensure they were free from contamination and colonies were counted either by eye, or using an automated colony counter. Colony forming units (CFUs) per mL were calculated by multiplying the number of colonies on each plate by the dilution factor, and as 100 µL was enumerated, this number was then multiplied by 10.

All bacterial cultures used in this study were tested at an MOI of 10 and 1.

Input Controls: In order to calculate the concentration of bacteria added to HeLa cell monolayers at Time = 0, the stock solution of each strain (at MOI 10 or MOI 1) was diluted and plated onto LB agar as described above, in order to calculate the input concentration for each experiment.

4-methylumbelliferyl α-D-mannopyranoside

Low molecular weight carbohydrates have been shown to inhibit the interaction between the bacterial lectin, FimH, and the host cell, particularly α-D-mannosides which have been shown to bind to bacterial FimH with high affinity (Fitos, Heremans et al. 1979), (Kotter, Krallmann-Wenzel et al. 1998), (Bouckaert, Berglund et al. 2005), (Sperling, Fuchs et al. 2006).

In this study, 4-methylumbelliferyl α-D-mannopyranoside was used to explore the dynamics of bacterial attachment to HeLa cells, as it has previously been shown to be a potent inhibitor of bacterial adhesion mediated by FimH (Firon, Ashkenazi et al. 1987), (Nagahori, Lee et al. 2002). It was hypothesised that this compound would bind to the *P. aeruginosa* FimH molecule with high affinity, and compromise attachment to HeLa cells via this mechanism. As a result, the approach was intended to reduce the attachment of bacteria to HeLa cells in comparison to baseline attachment.

A 0.01 mg / mL stock of 4-methylumbelliferyl α-D-mannopyranoside was prepared from powder (stored at 4°C) in Dimethyl sulfoxide (DMSO) (Sigma). A final 100 µM concentration of 4-methylumbelliferyl α-D-mannopyranoside was prepared directly in bacterial MOI 10 and 1 stocks, with the infection and attachment assays carried out as previously described (Figure 2.2). The 0.01 mg / mL stock was stored at 4°C in foil to protect it from the light. Data was compared to attachment in the absence of 4-methylumbelliferyl α-D-mannopyranoside using the Student T-Test (1-tailed distribution, 2-sample equal variance). Bacterial input controls were included as previously described.

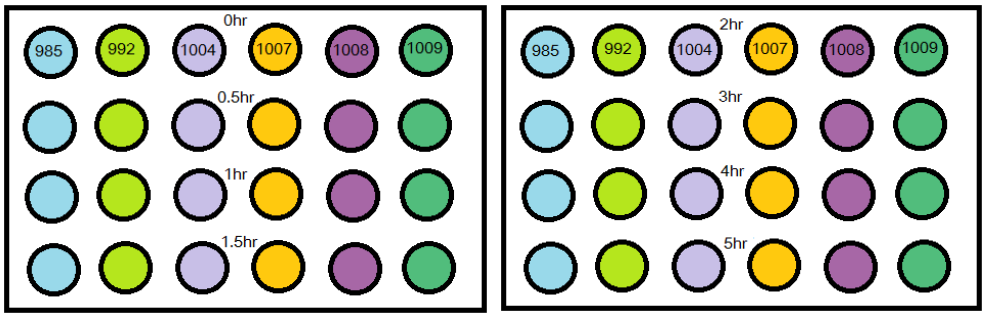

Figure 2.2: MTT layout for investigating the dynamics of *P. aeruginosa* attachment to HeLa cells in the presence of 4-methylumbelliferyl α-D-mannopyranoside. The attachment of six *P. aeruginosa* strains was investigated over 5 hours.

Multivalent adhesion molecule 7 (GST-MAM7 beads)

MAM7 is a small protein expressed by many bacteria, and hypothesised to be a common initial binding factor for many gram-negative pathogens. Recombinant MAM7 tagged with gluthathione S-transferase (GST), immobilised and coupled to the surface of inert polymer beads has been shown to be effective in reducing bacterial attachment to host cells, through competitive binding to phosphatidic acid and fibronectin host receptors (Krachler, Ham et al. 2012). Therefore, this approach was used to explore the changes in *P. aeruginosa* attachment to HeLa cells, compared to GST-only-coupled polymer beads. It was hypothesised that recombinant MAM7 would bind to target receptors and reduce bacterial attachment to the HeLa cells.

GST-MAM7 and GST beads were aliquoted into sterile 0.8 mL tubes and stored at -20°C. A final concentration of 500 nM peptide was prepared directly in bacterial MOI 10 and 1 stocks, using 2 µL of beads per 1 mL bacterial stock, with the infection and attachment assays carried out as previously described (Figure 2.3). GST-MAM7 and GST attachment data were compared using the Student T-Test (1-tailed distribution, 2-sample equal variance). Bacterial input controls were included as previously described.

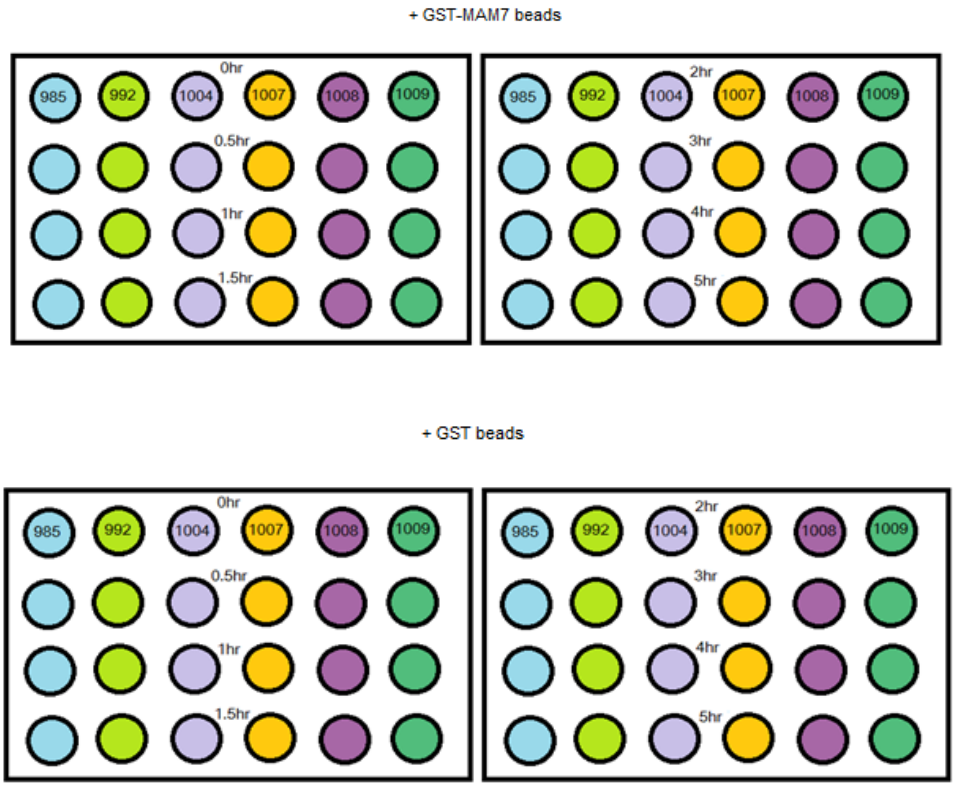

Figure 2.3: MTT layout for investigating the dynamics of *P. aeruginosa* attachment to HeLa cells in the presence of GST-MAM7 beads and GST beads. The attachment of six *P. aeruginosa* strains was investigated over 5 hours.

2.4 Immunostaining

To investigate HeLa cell morphology during infection with *P. aeruginosa*, Immunostaining and fluorescence microscopy were used to explore the HeLa phenotype at 1 hour and 5 hours post-infection, in the presence of GST-MAM7 and GST beads.

Immunostaining: Coverslips (VWR International) were sterilised by spraying both sides with 70% ethanol and allowed to dry on a paper towel. Each coverslip was placed into the well of a sterile 6-well MTT (Greiner bio-one) using forceps. Confluent HeLa cells were detached from tissue culture dishes and counted, as described in 2.2, and 2 mL of HeLa cells at a concentration of 1.5 x 10^5 / mL was inoculated into each well of the MTT containing a coverslip. MTTs were incubated in a static

incubator at 37°C, 5% CO_2 for 24 hours. Following incubation, DMEM was removed from each well using an automated aspirator vacuum fitted with a sterile glass pipette, and 1 mL of phosphate buffered saline (PBS) was inoculated onto the edge of the dish by tilting, to wash the cell monolayer. The infection assay was carried out as previously described, at time points of 1 and 5 hours (Figure 2.4).

At each time point, non-adherent bacteria were removed from the wells using a pipette and washed three times using 1 mL of sterile PBS. The coverslip was washed by tilting the plate and adding the PBS away from the coverslip. The cells on the coverslip were fixed by pipetting 1 mL of 3.2% formaldehyde solution directly onto each coverslip and storing the MTTs at 4°C overnight. A 50 mL solution of 3.2% formaldehyde was prepared from a 37% stock solution (stored at 4°C) (Sigma) by adding 5 mL to 5 mL of sterile PBS and 40 mL of deionised water ($_d$H2O).

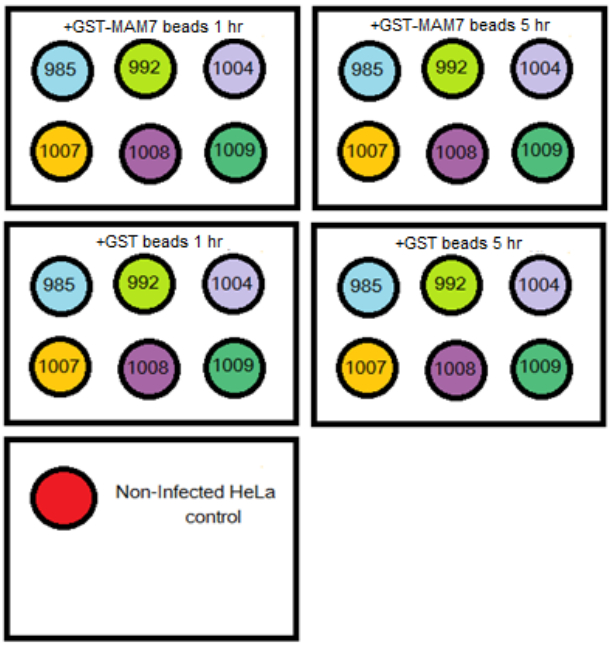

Figure 2.4: MTT layout for immunostaining preparation of *P. aeruginosa* attachment to HeLa cells in the presence of GST-MAM7 and GST beads.

Following incubation, the formaldehyde was removed from each well and the HeLa cell monolayer on each coverslip was permeabilised to allow the uptake of fluorescent stains for imaging, by inoculating 1 mL of 0.1% Triton X-100 into each well. The plates were incubated for 5 minutes at room temperature. The Triton X-100 was removed from each well, and each coverslip was washed once by tilting the plate and adding 1 mL sterile PBS away from the coverslip, which was removed.

Hoechst and phalloidin cell-permeable stains were used for fluorescence microscopy. Hoechst is typically used to stain DNA and nucleic acids in mammalian cells, whilst phalloidin is typically used to stain actin fibres in mammalian cells. A dye solution was prepared in the ratio of 0.1% Hoechst and 1% phalloidin (Biotium) in sterile PBS and 200 µL was inoculated directly onto each coverslip. The MTTs were incubated for 10 minutes at room temperature to allow the uptake of the dyes. Each coverslip was washed twice by tilting the plate and adding 1 mL of sterile PBS away from the coverslip. The coverslips were washed a third time with $_{d}H2O$, which was not removed from the wells until mounting, to prevent the coverslips from drying.

For mounting; a glass slide (Thermoscientific) was labelled and one drop of mounting solution was added to the centre. The corresponding coverslip was removed from the 6-well MTT using forceps and gently blotted onto a paper towel, avoiding the disturbance of the HeLa monolayer. The coverslip was placed over the mounting solution, ensuring that the HeLa cell monolayer was inserted between the coverslip and the glass slide. The process was repeated until all coverslips had been mounted. The slides were kept inside a dark box prior to microscopy to prevent light damage.

Fluorescence microscopy

NIS Elements Imaging Software was used to image each coverslip prepared as described. Before opening the computer programme, the Nikon Eclipse Ti-S microscope, camera and light source (Nikon Intensilight C-HGFI) were switched on. A 60 x 1.40 Oil Lens was used for microscopy, requiring each coverslip to be immersed in one drop of non-drying immersion oil (Cargille Laboratories) before mounting onto the microscope. Representative areas of each coverslip were selected for imaging using hoechst (UV filter) and phalloidin (green filter) stains, in addition to Differential Interference Contrast (DIC). Exposure was adjusted appropriately between filters. Images were exported and Image J software was used to overlay hoechst and phalloidin images.

3.0 Results

3.1 Attachment of *P. aeruginosa* to HeLa cells in the presence and absence of 4-methylumbelliferyl α-D-mannopyranoside

P. aeruginosa attachment to HeLa cells was explored at 0, 0.5, 1, 1.5, 2, 3, 4 and 5 hours, at baseline and in the presence of 100 μM of 4-methylumbelliferyl α-D-mannopyranoside, a low molecular weight carbohydrate that has been shown to inhibit the interaction between bacterial FimH and host cells (Firon, Ashkenazi et al. 1987), (Nagahori, Lee et al. 2002).

At a ratio of bacterial cells to HeLa cells of 10:1 (MOI 10), *P. aeruginosa* attachment to HeLa cells at baseline increased positively from 0 to 5 hours in all bacterial strains tested (for strain 985 (n=3): bacterial attachment at 0 hours = 5.67 x 10^5/mL and bacterial attachment at 5 hours = 1.36 x 10^7/mL) (Figure 3.1). In the presence of 4-methylumbelliferyl α-D-mannopyranoside, *P. aeruginosa* attachment to HeLa cells appeared reduced at each time-point compared to the baseline, in all bacterial strains tested (for strain 985 (n=3): baseline bacterial attachment at 0 hours = 5.67 x 10^5/mL and bacterial attachment in the presence of 4-methylumbelliferyl α-D-mannopyranoside at 0 hours = 1.70 x 10^5/mL) (Figure 3.1).

The student T-Test was used to test the null hypothesis that the attachment of *P. aeruginosa* to HeLa cells was equal in the presence and absence of 4-methylumbelliferyl α-D-mannopyranoside, at each time point. It was predicted that bacterial attachment in the presence of 4-methylumbelliferyl α-D-mannopyranoside would be lower than in its absence, therefore a one-tailed distribution was assumed (two-sample assuming equal variance). A p-value of less than 0.05 = * significance, less than 0.01 = ** significance, and 0.001 = *** significance.

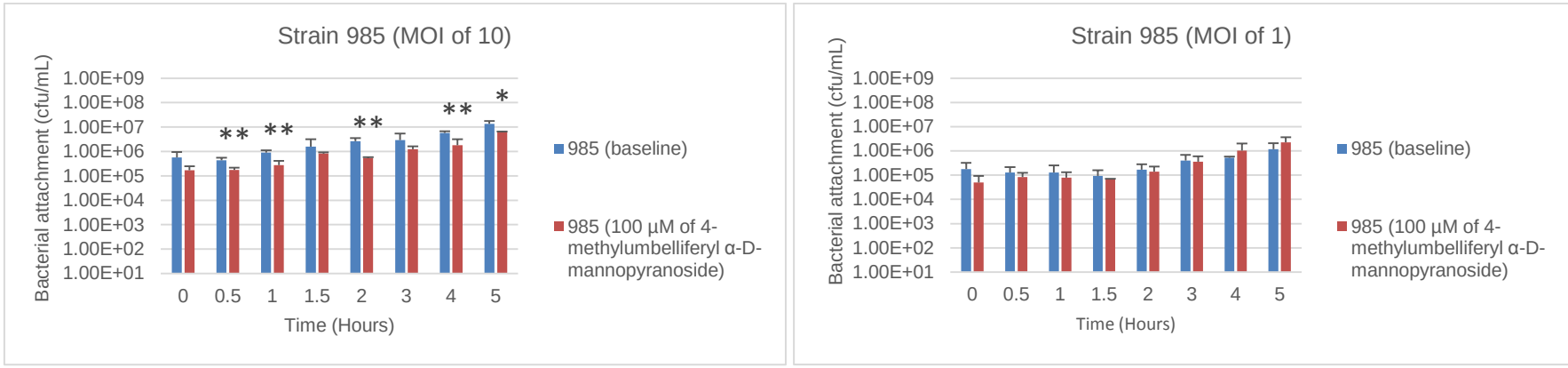

Figure 3.1: Attachment in colony forming units (CFUs) per mL, of *P. aeruginosa* strain 985 at an MOI of 10 (left) and an MOI of 1 (right) to HeLa cells over 5 hours, in the presence and absence of 100 µM of 4-methylumbelliferyl α-D-mannopyranoside (n=3, +SD).
Mean input (MOI 10): 1.70 x 10^6/mL, (MOI 1): 6.30 x 10^5/mL.

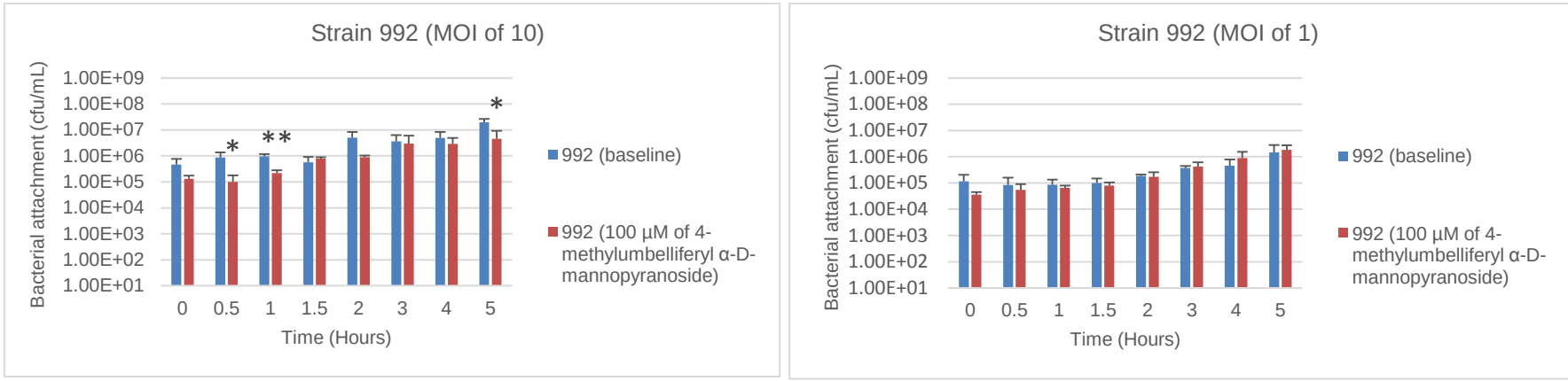

Figure 3.2: Attachment in colony forming units (CFUs) per mL, of *P. aeruginosa* strain 992 at an MOI of 10 (left) and an MOI of 1 (right) to HeLa cells over 5 hours, in the presence and absence of 100 µM of 4-methylumbelliferyl α-D-mannopyranoside (n=3, +SD).
Mean input (MOI 10): 3.37 X 10^6/mL, (MOI 1): 1.93 x 10^5/mL.

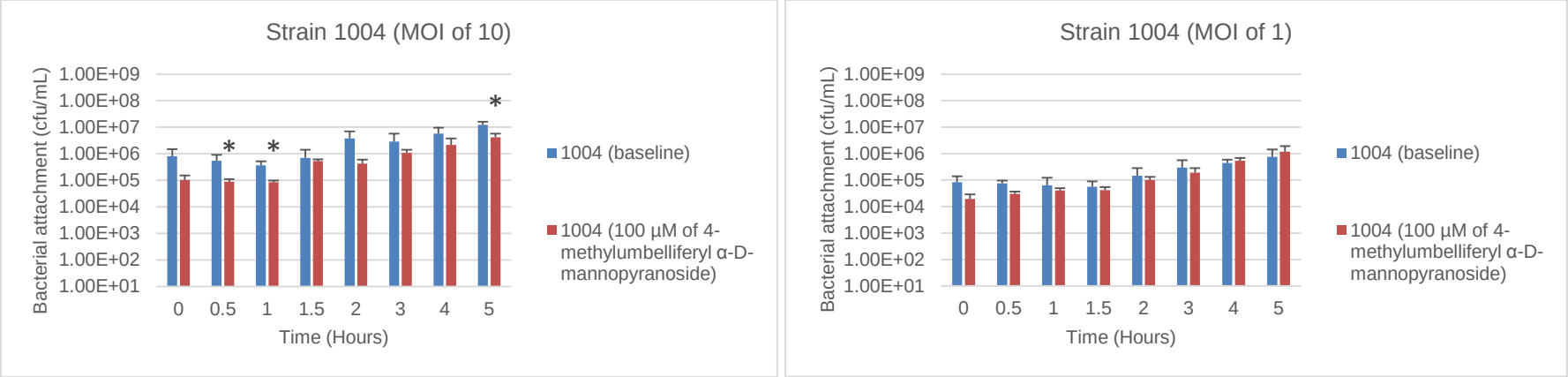

Figure 3.3: Attachment in colony forming units (CFUs) per mL, of *P. aeruginosa* strain 1004 at an MOI of 10 (left) and an MOI of 1 (right) to HeLa cells over 5 hours, in the presence and absence of 100 µM of 4-methylumbelliferyl α-D-mannopyranoside (n=3, +SD).
Mean input (MOI 10): 5.77 x 10^6/Ml, (MOI 1): 3.70 x 10^5/mL.

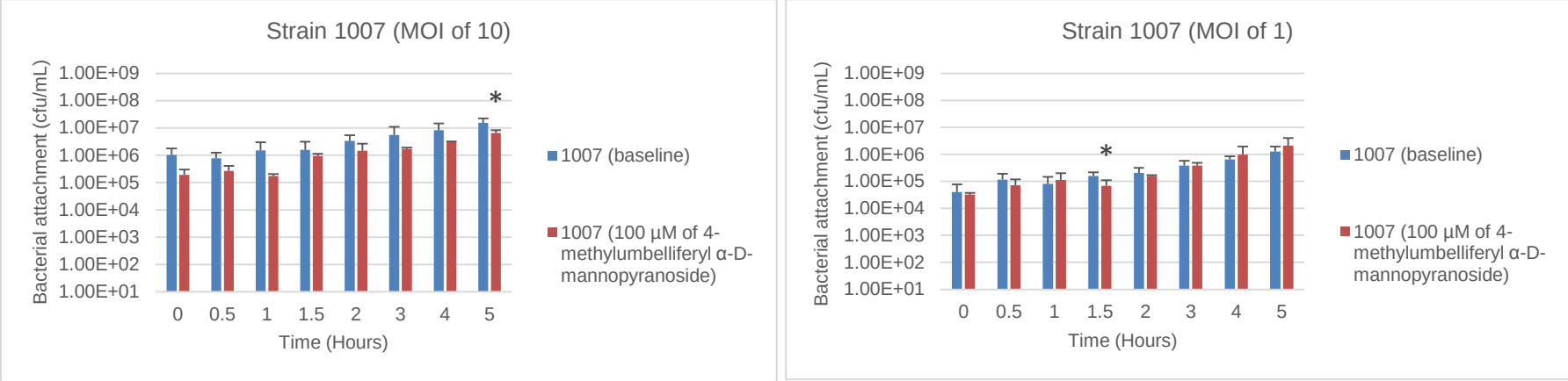

Figure 3.4: Attachment in colony forming units (CFUs) per mL, of *P. aeruginosa* strain 1007 at an MOI of 10 (left) and an MOI of 1 (right) to HeLa cells over 5 hours, in the presence and absence of 100 µM of 4-methylumbelliferyl α-D-mannopyranoside (n=3, +SD).
Mean input (MOI 10): 1.12 x 10^7/mL, (MOI 1): 2.13 x 10^5/mL.

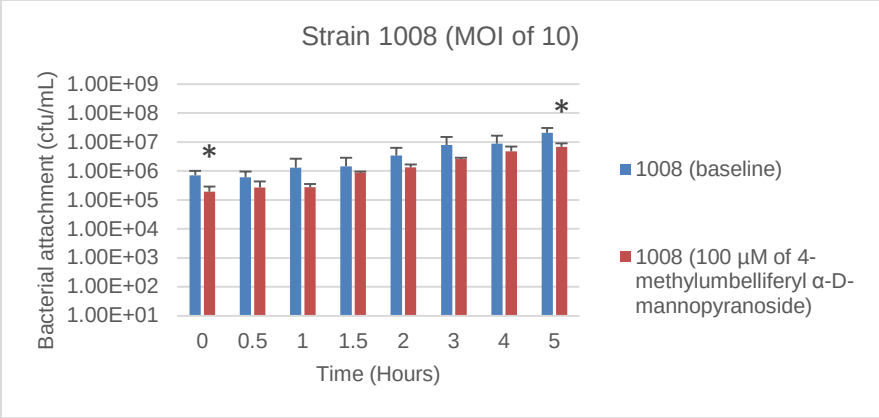

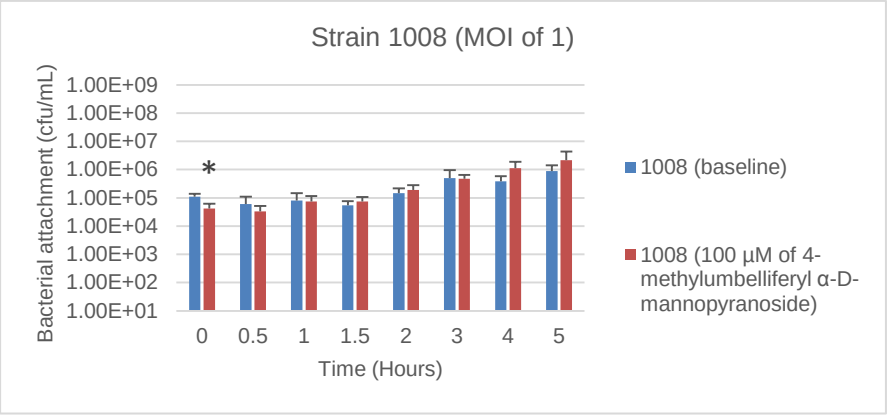

Figure 3.5: Attachment in colony forming units (CFUs) per mL, of *P. aeruginosa* strain 1008 at an MOI of 10 (left) and an MOI of 1 (right) to HeLa cells over 5 hours, in the presence and absence of 100 µM of 4-methylumbelliferyl α-D-mannopyranoside (n=3, +SD).
Mean input (MOI 10): 8.93 x 10^6/Ml, (MOI 1): 2.03 x 10^5/mL.

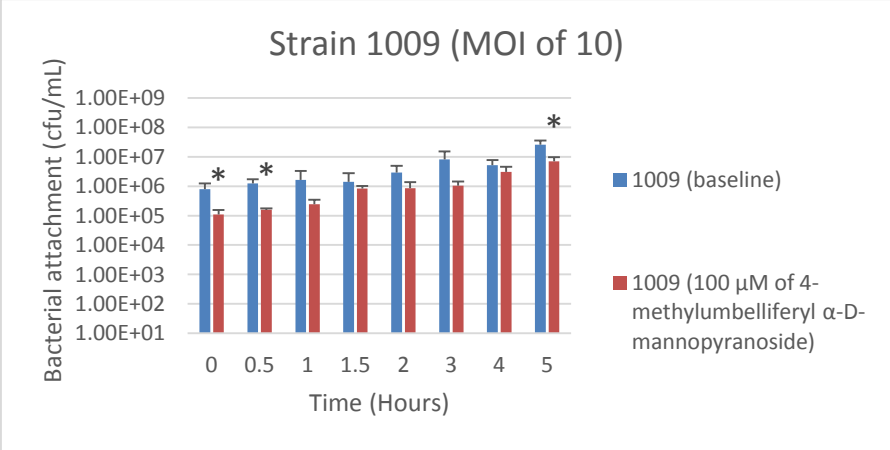

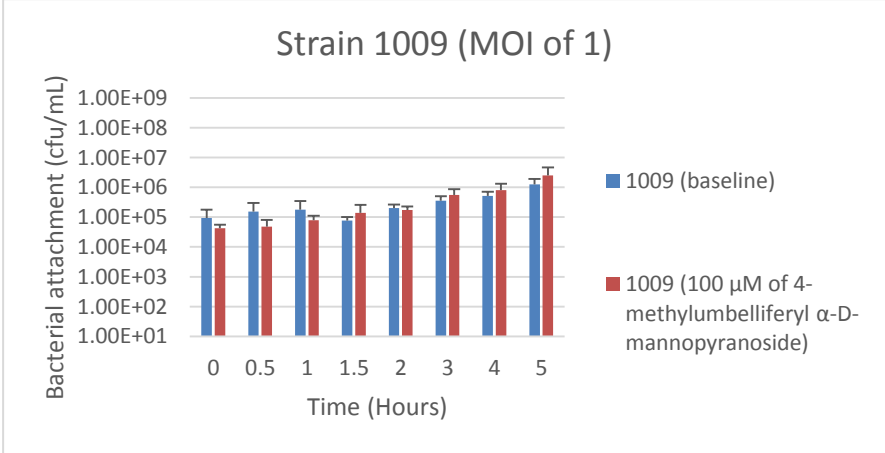

Figure 3.6: Attachment in colony forming units (CFUs) per mL, of *P. aeruginosa* strain 1009 at an MOI of 10 (left) and an MOI of 1 (right) to HeLa cells over 5 hours, in the presence and absence of 100 µM of 4-methylumbelliferyl α-D-mannopyranoside (n=3, +SD).
Mean input (MOI 10): 1.01 x 107/Ml, (MOI 1): 2.72 x 10^5/mL.

Strain 985 showed the most significant decreases in attachment at multiple time points ((n=3): 0.5 hours p = 0.01, 1 hour p = 0.01, 2 hours p = 0.01, 4 hours p = 0.01 and 5 hours p = 0.02) (Figure 3.1). Other strains showed modest decreases in attachment at few time points (strain 992 (n=3): 0.5 hours p = 0.05, 1 hour p = 0.02 and 5 hours p = 0.02 (Figure 3.2), strain 1004 (n=3): 0.5 hours p = 0.05, 1 hour p = 0.02, 5 hours p = 0.02 (Figure 3.3), strain 1007 (n=3): 5 hours p = 0.05 (Figure 3.4), strain 1008 (n=3): 0 hours p = 0.02, 5 hours p = 0.03 (Figure 3.5), strain 1009 (n=3): 0 hours p = 0.03, 0.5 hours p = 0.03 and 5 hours p = 0.02 (Figure 3.7)).

At MOI 1, *P. aeruginosa* attachment to HeLa cells at baseline increased positively from 0 to 5 hours in all bacterial strains tested, as previously described (for strain 985 (n=3): bacterial attachment at 0 hours = 1.77 x 10^5/mL and bacterial attachment at 5 hours = 1.18 x 10^6/mL) (Figure 3.1). At this MOI, the presence of 4-methylumbelliferyl α-D-mannopyranoside appeared to have a more modest effect on *P. aeruginosa* attachment to HeLa cells, and at some time points studied, attachment increased in its presence (strain 985 (n=3): baseline bacterial attachment at 5 hours = 1.18 x 10^6/mL and bacterial attachment in the presence of 4-methylumbelliferyl α-D-mannopyranoside = 2.24 x 10^6/mL) (Figure 3.1).

Using the student T-Test to determine significance, only two data points were deemed statistically significant (strain 1007 (n=3): baseline bacterial attachment at 1.5 hours = 1.57 x 10^5/mL and bacterial attachment in the presence of 4-methylumbelliferyl α-D-mannopyranoside = 6.8 x 10^4/mL, with a p-value of 0.05 (Figure 3.4), and strain 1008 (n=3): baseline bacterial attachment at 0 hours = 1.10 x

10^5/mL and bacterial attachment in the presence of 4-methylumbelliferyl α-D-mannopyranoside = 4.23 x 10^4/mL, with a p-value of 0.05) (Figure 3.5).

Input Controls: In order to calculate the concentration of bacteria added to HeLa cell monolayers at Time = 0, the stock solution of each strain (at MOI 10 or MOI 1) was enumerated in order to calculate the input concentration for each experiment. For each bacterial strain tested, input controls were consistently lower than bacteria enumerated at 5 hours (for strain 985 (MOI 10): Input = 1.70 x 10^6/mL, baseline bacterial attachment at 5 hours = 1.36 x 10^7/mL, (MOI 1): Input = 6.30 x 10^5/mL, baseline bacterial attachment at 5 hours = 1.18 x 10^6/mL (Figure 3.1).

3.2 Attachment of *P. aeruginosa* to HeLa cells in the presence of GST-MAM7 and GST beads

P. aeruginosa attachment to HeLa cells was explored at 0, 0.5, 1, 1.5, 2, 3, 4 and 5 hours, at baseline (GST beads), and in the presence of GST-MAM7 beads, which have been shown to inhibit the interaction between bacterial MAM7 and host cells through competitive binding of recombinant MAM7 (Krachler, Ham et al. 2012).

At MOI 10, *P. aeruginosa* attachment to HeLa cells at baseline (GST beads) increased positively from 0 to 5 hours in all bacterial strains tested (for strain 985 (n=2-3): bacterial attachment at 0 hours = 1.40 x 10^5/mL and bacterial attachment at 5 hours = 7.40 x 10^6/mL) (Figure 3.7). In the presence of GST-MAM7 beads, *P. aeruginosa* attachment to HeLa cells between 0 hours and 1.5 hours was not

significantly changed (strain 985 (n=2-3): bacterial attachment at 0 hours = 1.70 x 10^5/mL, 0.5 hours = 1.42 x 10^5/mL, 1 hour = 1.21 x 10^5/mL and 1.5 hours = 2.45 x 10^5/mL. However, attachment decreased between 1.5 hours and 5 hours in all bacterial strains tested (for strain 985 (n=2-3): bacterial attachment at 2 hours = 8.61 x 10^3/mL, 3 hours = 1.70 x 10^3/mL, 4 hours = 1.27 x 10^3/mL and 5 hours = 2.78 x 10^3/mL (Figure 3.7).

The student T-Test was used to test the null hypothesis that the attachment of *P. aeruginosa* to HeLa cells was equal in the presence and absence of GST-MAM7 beads, at each time point. It was predicted that bacterial attachment in the presence of GST-MAM7 would be lower than in the presence of control GST beads, therefore a one-tailed distribution was assumed (two-sample assuming equal variance). A p-value of less than 0.05 = * significance, less than 0.01 = ** significance, and 0.001 = *** significance.

Strains 985, 1008 and 1009 showed statistically significant decreases in attachment at all time-points between 1.5 and 5 hours (for strain 985 (n=2-3): 2 hours p = 0.01, 3 hours p = 0.05, 4 hours p = 0.05 and 5 hours = 0.01 (Figure 3.7), for strain 1008 (n=2-3): 2 hours p = 0.01, 3 hours p = 0.05, 4 hours p = 0.05 and 5 hours p = 0.001 (Figure 3.11), for strain 1009 (n=2-3): 2 hours p = 0.05, 3 hours p = 0.01, 4 hours p = 0.05 and 5 hours p = 0.001 (Figure 3.12). Other strains showed a decrease in attachment that was not significant at all time points (Figures 3.8-3.10).

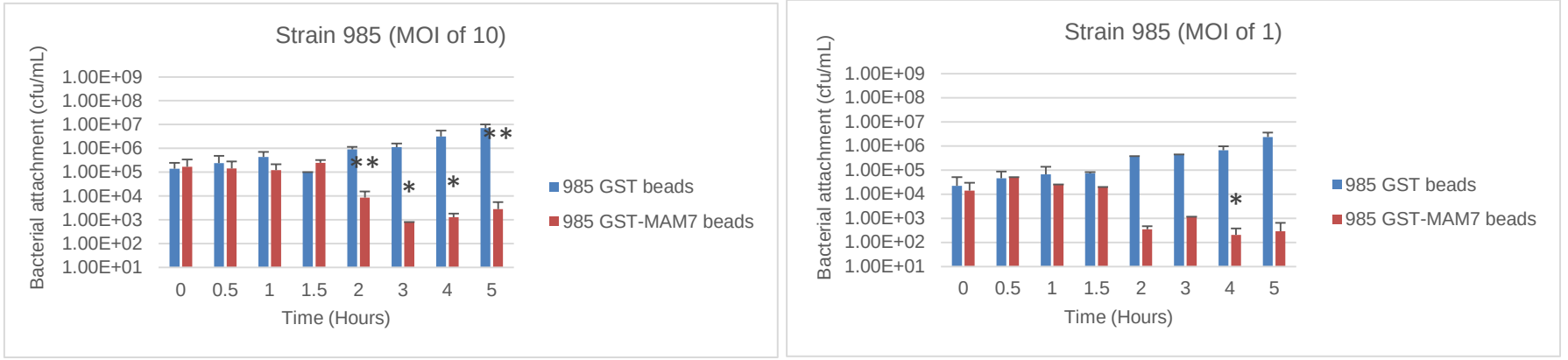

Figure 3.7: Attachment in colony forming units (CFUs) per mL, of *P. aeruginosa* strain 985 at an MOI of 10 (left) and an MOI of 1 (right) to HeLa cells over 5 hours, in the presence of GST-MAM7 beads and GST beads (n=1-3, +SD).
Mean input (MOI 10): 1.10 x 10^6/mL, (MOI 1): 2.89 x 10^5 /mL

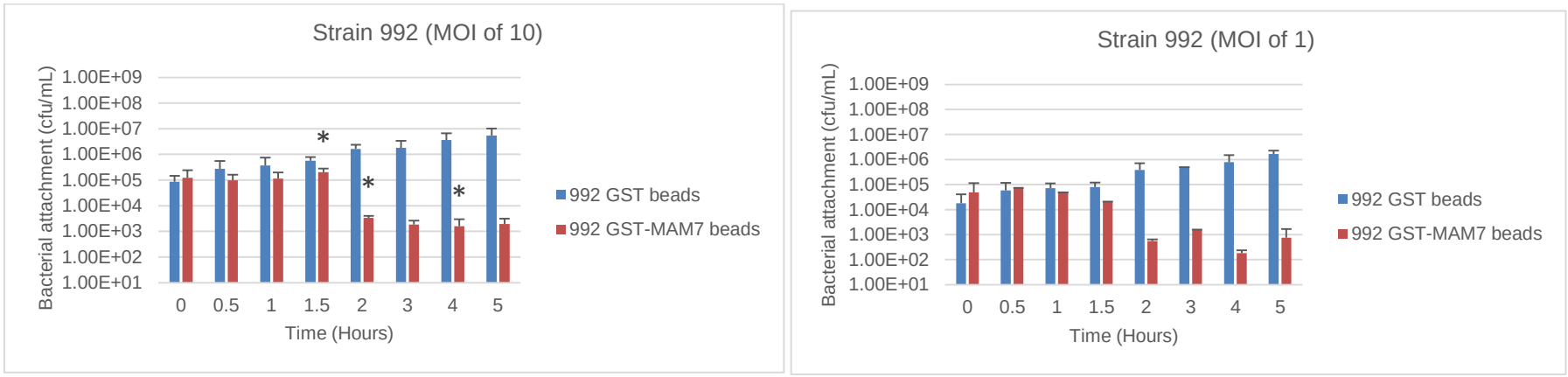

Figure 3.8: Attachment in colony forming units (CFUs) per mL, of *P. aeruginosa* strain 992 at an MOI of 10 (left) and an MOI of 1 (right) to HeLa cells over 5 hours, in the presence of GST-MAM7 beads and GST beads (n=1-3, +SD).
Mean input (MOI 10):1.39 x 10^6/mL, (MOI 1): 2.74 x 10^5/mL

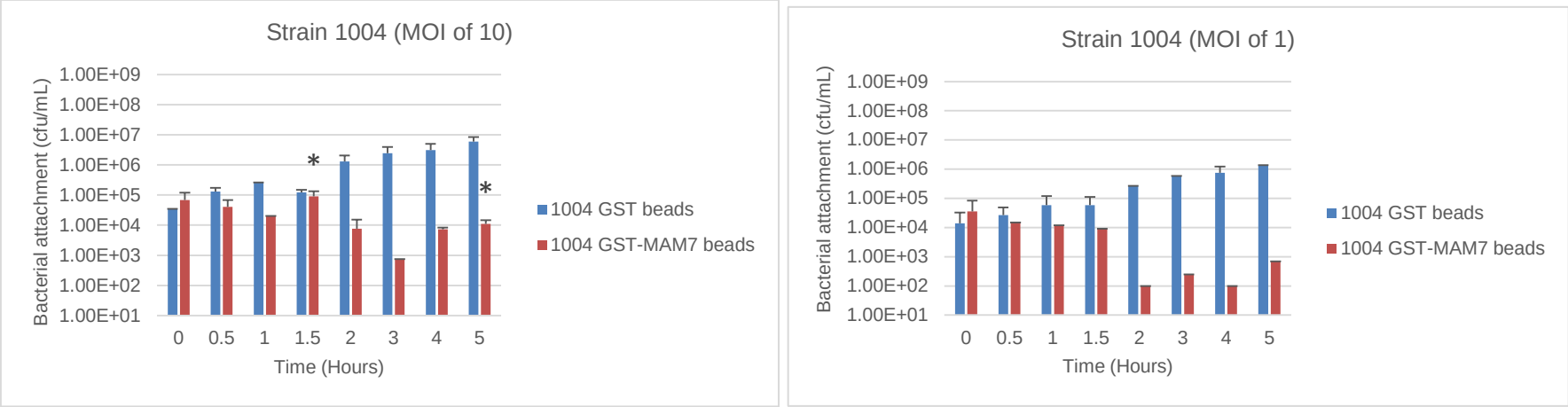

Figure 3.9: Attachment in colony forming units (CFUs) per mL, of *P. aeruginosa* strain 1004 at an MOI of 10 (left) and an MOI of 1 (right) to HeLa cells over 5 hours, in the presence of GST-MAM7 beads and GST beads (n=1-3, +SD).
Mean input (MOI 10): 1.76 x 10^6/mL, (MOI 1): 4.60 x 10^5/mL

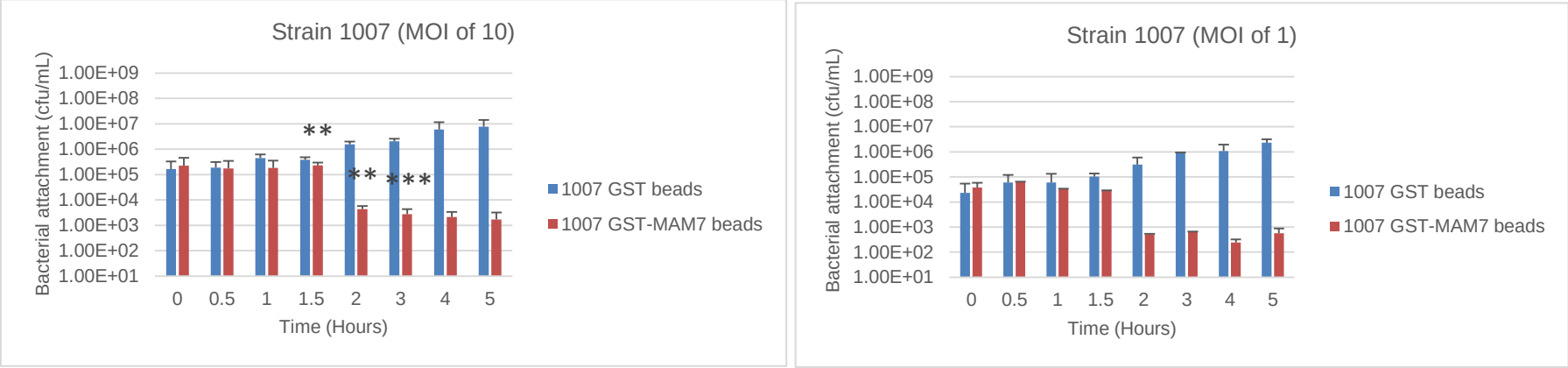

Figure 3.10: Attachment in colony forming units (CFUs) per mL, of *P. aeruginosa* strain 1007 at an MOI of 10 (left) and an MOI of 1 (right) to HeLa cells over 5 hours, in the presence of GST-MAM7 beads and GST beads (n=1-3, +SD).
Mean input (MOI 10): 1.50 x 10^6/mL, (MOI 1): 2.22 x 10^5/mL

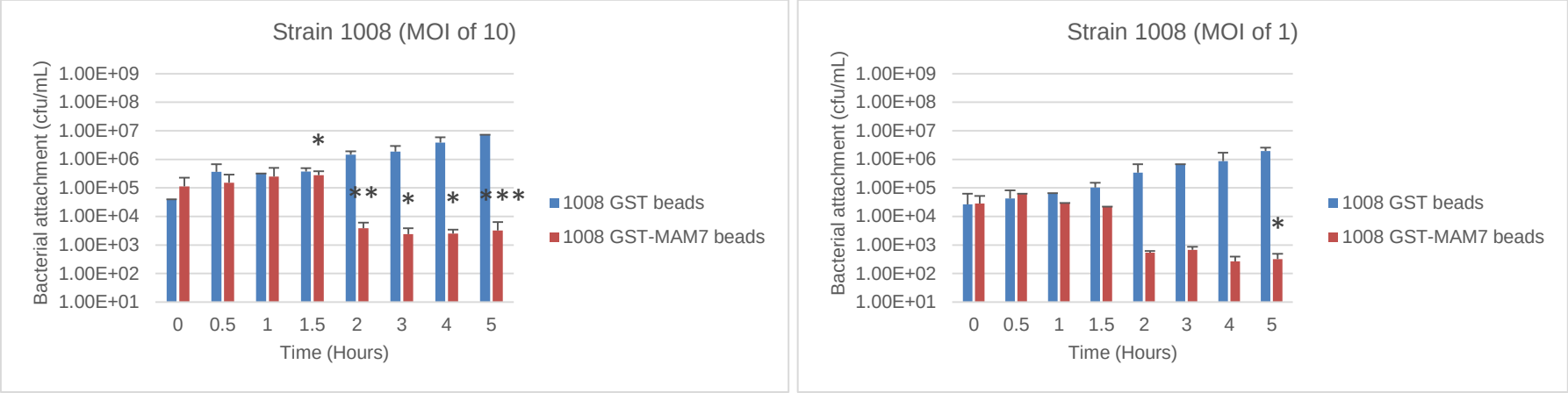

Figure 3.11: Attachment in colony forming units (CFUs) per mL, of *P. aeruginosa* strain 1008 at an MOI of 10 (left) and an MOI of 1 (right) to HeLa cells over 5 hours, in the presence of GST-MAM7 beads and GST beads (n=1-3, +SD).
Mean input (MOI 10): 1.36 x 10^6/mL, (MOI 1): 1.60 x 10^5/mL

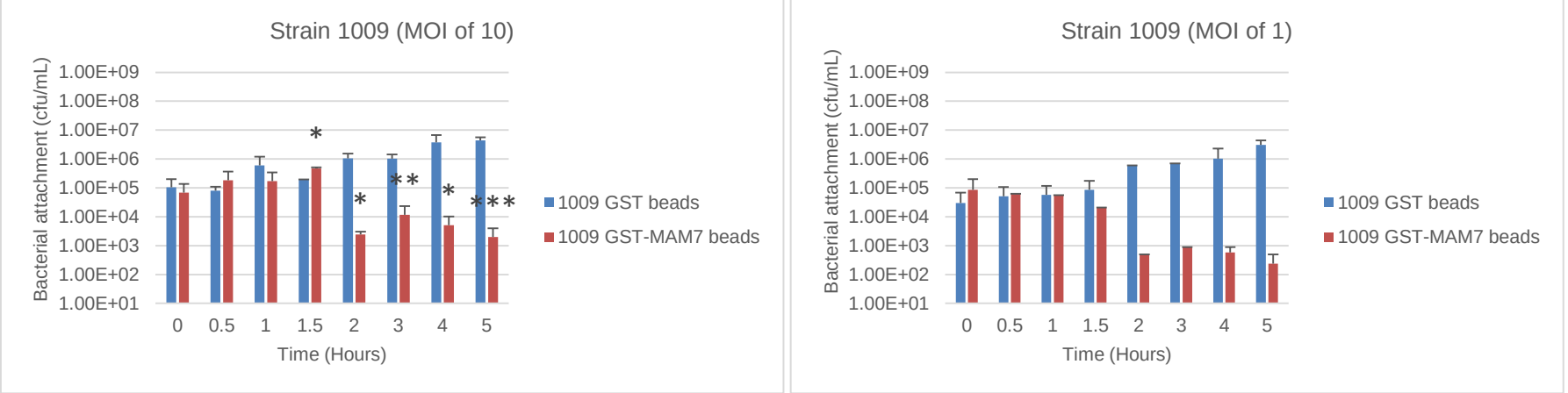

Figure 3.12: Attachment in colony forming units (CFUs) per mL, of *P. aeruginosa* strain 1009 at an MOI of 10 (left) and an MOI of 1 (right) to HeLa cells over 5 hours, in the presence of GST-MAM7 beads and GST beads (n=1-3, +SD).
Mean input (MOI 10): 3.40 x 10^5/mL, (MOI 1): 2.02 x 10^5/mL

At MOI 1, *P. aeruginosa* attachment to HeLa cells at baseline (GST beads) increased positively from 0 to 5 hours in all bacterial strains tested, as previously described (for strain 985 (n=1-2): bacterial attachment at 0 hours = 2.20 x 10^4/mL and bacterial attachment at 5 hours = 2.34 x 10^6/mL) (Figure 3.7). At this MOI, the presence of GST-MAM7 beads had a similar effect on *P. aeruginosa* attachment to HeLa cells as has been described for MOI 10 (for strain 985 (n=1-2): bacterial attachment at 2 hours = 3.45 x 10^2/mL, 3 hours = 1.17 x 10^3/mL, 4 hours = 2.05 x 10^2/mL and 5 hours = 2.90 x 10^2/mL (Figure 3.7).

The student T-Test was used to determine significance where 2 data points were available (strain 985 (n=2): 4 hours p = 0.05 (Figure 3.7) and strain 1008 (n=2): 5 hours p =0.05 (Figure 3.11).

Input Controls: for each bacterial strain tested, input controls were consistently lower than bacteria enumerated at 5 hours at baseline (GST beads) (for strain 985 (MOI 10): Input = 1.10 x 10^6/mL, baseline bacterial attachment at 5 hours = 7.10 x 10^6/mL, (MOI 1): Input = 2.89 x 10^5/mL, baseline bacterial attachment at 5 hours = 2.34 x 10^6/mL (Figure 3.7).

3.3 Immunostaining and fluorescence microscopy of *P. aeruginosa* attachment to HeLa cells in the presence of GST-MAM7 and GST beads

Immunostaining and fluorescence microscopy were used to explore the changes in HeLa cell morphology at 1 and 5 hours post-infection with *P. aeruginosa* strains, in the presence of GST-MAM7 and GST beads. This was carried out to investigate the decrease in *P. aeruginosa* attachment in the presence of GST-MAM7 beads (Figures 3.7-3.12). The hoechst cell-permeable stain was used to stain DNA (blue) and the phalloidin cell-permeable stain was used to stain actin fibres (red).

Non-infected HeLa cells were included for comparison (Figure 3.13). In all strains tested during the study, *P. aeruginosa* infection in the presence of GST-only beads led to modest actin stress-fibre formation in HeLa cells at 1 and 5 hours post-incubation, compared to the non-infected HeLa cells (phalloidin red stain, figures 3.14-3.15, 3.18-3.19, 3.22-3.23, 3.26-3.27, 3.30-3.31 and 3.33-3.34). For strains 985 and 992 in the presence of GST beads, stress fibre formation appeared increased at 5 hours post-infection, compared to 1 hour post-infection (Figures 3.14-3.15 and 3.18-3.19).

HeLa cell morphology during *P. aeruginosa* infection in the presence of GST-MAM7 beads was not significantly changed compared to GST-only beads, however actin stress fibre formation visualised at 5 hours appeared modestly decreased in some strains compared to the observed phenotype at 5 hours in the presence of GST beads (Figures 3.16-3.17, 3.20-3.21, 3.24-3.25 and 3.28-3.29).

In all strains tested in the presence of GST beads, the proportion of bacterial cells attached to the HeLa cell monolayer increased between 1 and 5 hours, however in

the presence of GST-MAM7 beads, fewer bacteria were seen attached to the HeLa monolayer at 5 hours (DIC images), which is consistent with attachment data (Figures 3.7-3.12). No significant changes in hoechst DNA-binding was observed in the presence of GST-MAM7 and GST beads, suggesting that the GST-MAM7 beads had no significant effect on the HeLa cell phenotype during attachment inhibition.

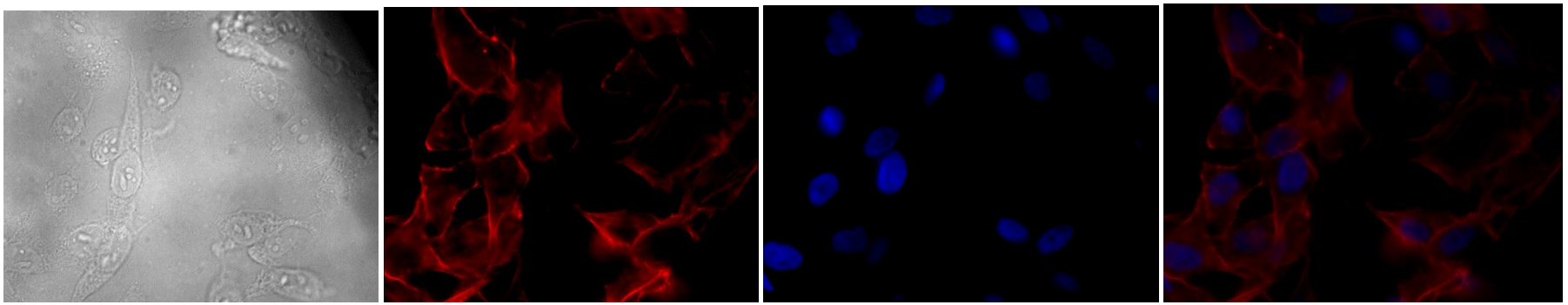

Figure 3.13: Non-infected HeLa cells and immunostaining with hoechst (DNA) and phalloidin (actin). Left to right: DIC image, phalloidin-stained image, hoechst-stained image, and overlaid phalloidin & hoechst-stained images.

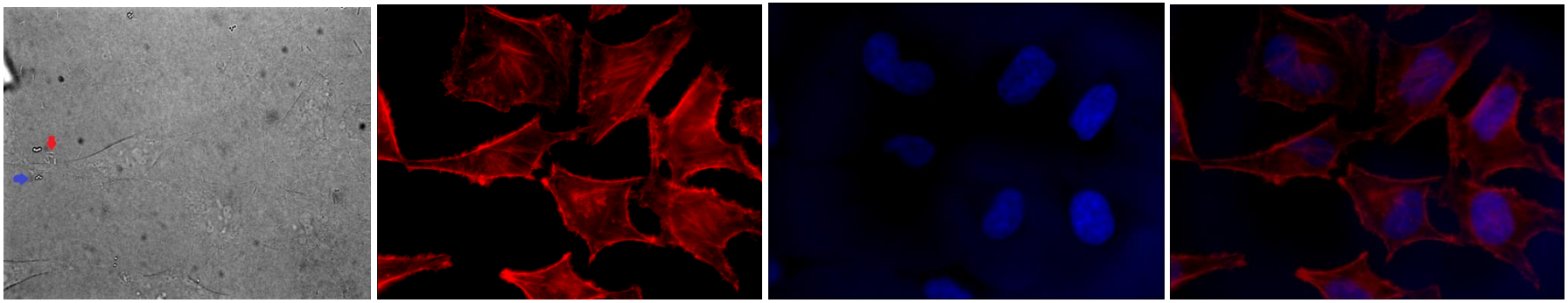

Figure 3.14: Infection of HeLa cells with *P. aeruginosa* strain 985 (MOI 10) containing GST beads for 1 hour and Immunostaining with hoechst (DNA) and phalloidin (actin). Left to right: DIC image, phalloidin-stained image, hoechst-stained image, and overlaid phalloidin & hoechst-stained images. Red arrow indicates visible bacterial cells and blue arrow indicates the GST beads. 60 x magnification.

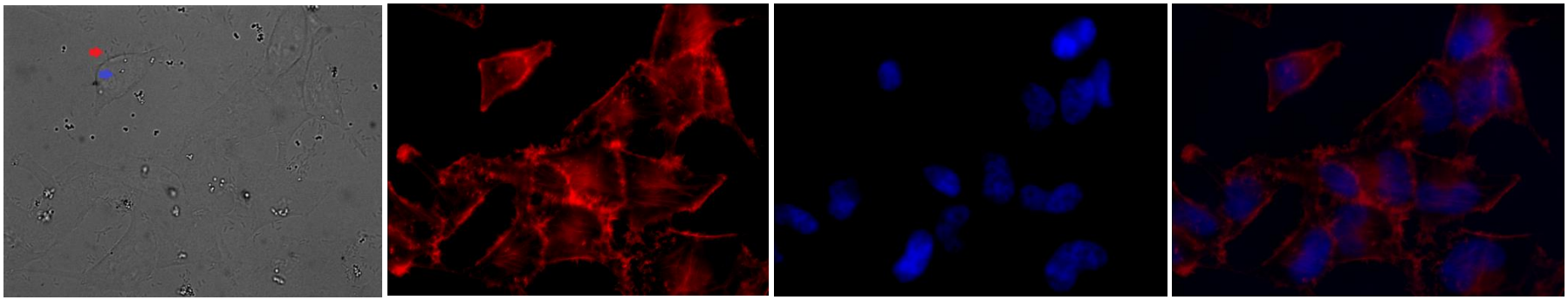

Figure 3.15: Infection of HeLa cells with *P. aeruginosa* strain 985 (MOI 10) containing GST beads for 5 hours and Immunostaining with hoechst (DNA) and phalloidin (actin). Left to right: DIC image, phalloidin-stained image, hoechst-stained image, and overlaid phalloidin & hoechst-stained images. Red arrow indicates visible bacterial cells and blue arrow indicates the GST beads. 60 x magnification.

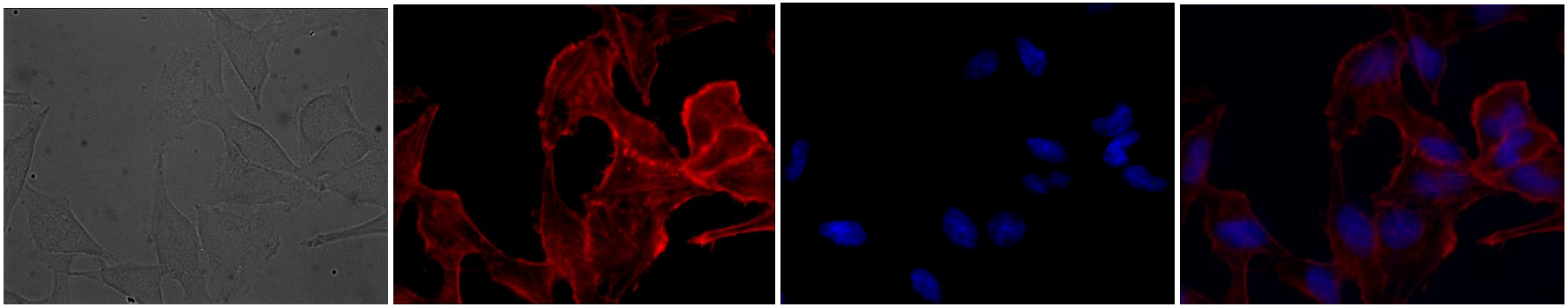

Figure 3.16: Infection of HeLa cells with *P. aeruginosa* strain 985 (MOI 10) containing GST-MAM7 beads for 1 hour and Immunostaining with hoechst (DNA) and phalloidin (actin). Left to right: DIC image, phalloidin-stained image, hoechst-stained image, and overlaid phalloidin & hoechst-stained images. 60 x magnification.

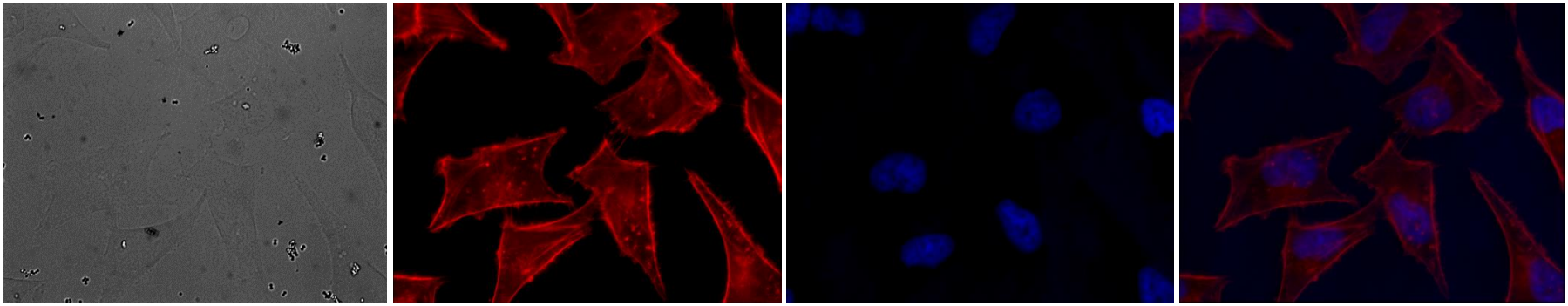

Figure 3.17: Infection of HeLa cells with *P. aeruginosa* strain 985 (MOI 10) containing GST-MAM7 beads for 5 hours and Immunostaining with hoechst (DNA) and phalloidin (actin). Left to right: DIC image, phalloidin-stained image, hoechst-stained image, and overlaid phalloidin & hoechst-stained images. 60 x magnification.

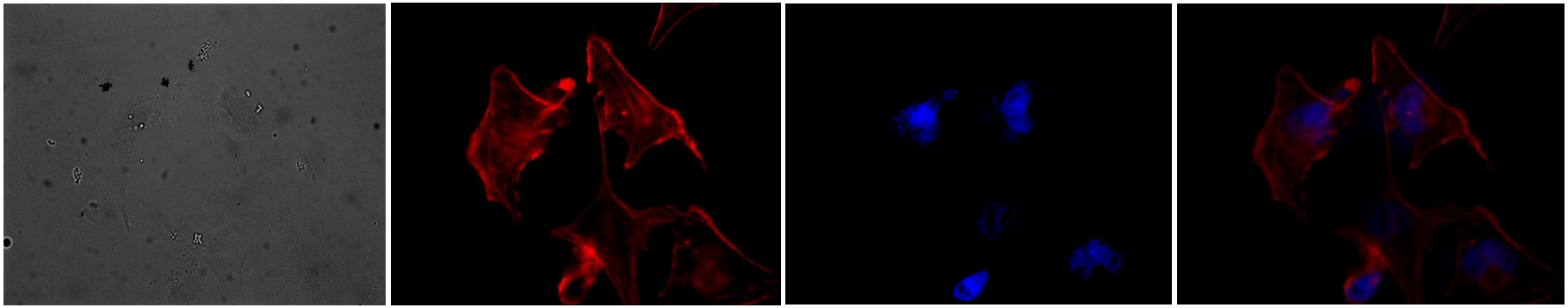

Figure 3.18: Infection of HeLa cells with *P. aeruginosa* strain 992 (MOI 10) containing GST beads for 1 hour and Immunostaining with hoechst (DNA) and phalloidin (actin). Left to right: DIC image, phalloidin-stained image, hoechst-stained image, and overlaid phalloidin & hoechst-stained images. 60 x magnification.

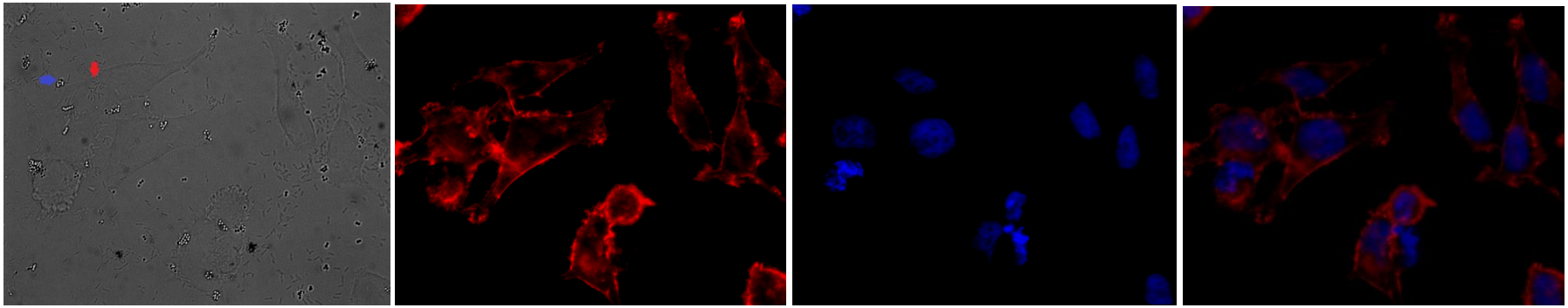

Figure 3.19: Infection of HeLa cells with *P. aeruginosa* strain 992 (MOI 10) containing GST beads for 5 hours and Immunostaining with hoechst (DNA) and phalloidin (actin). Left to right: DIC image, phalloidin-stained image, hoechst-stained image, and overlaid phalloidin & hoechst-stained images. Red arrow indicates visible bacterial cells and blue arrow indicates the GST beads. 60 x magnification.

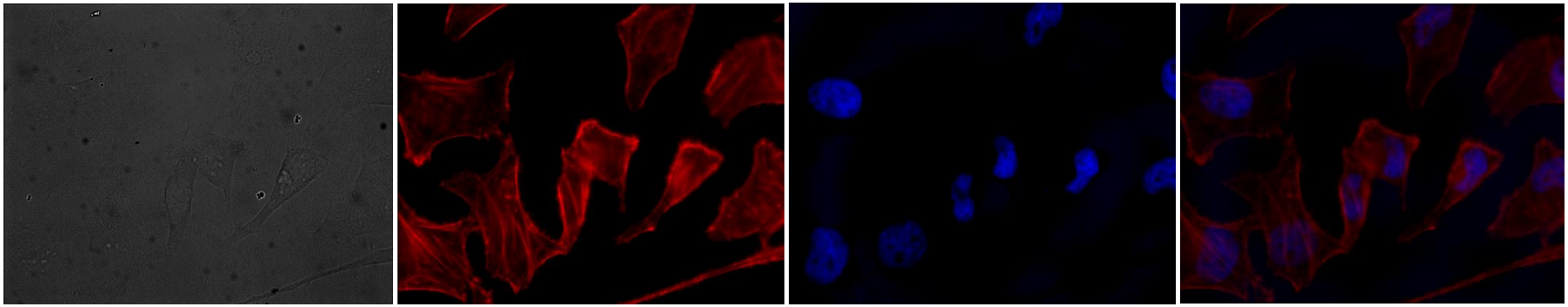

Figure 3.20: Infection of HeLa cells with *P. aeruginosa* strain 992 (MOI 10) containing GST-MAM7 beads for 1 hour and Immunostaining with hoechst (DNA) and phalloidin (actin). Left to right: DIC image, phalloidin-stained image, hoechst-stained image, and overlaid phalloidin & hoechst-stained images. 60 x magnification.

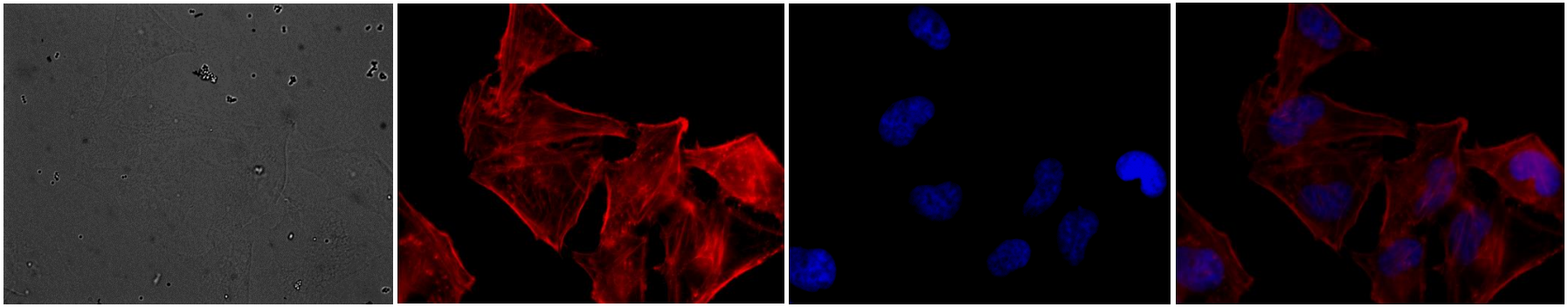

Figure 3.21: Infection of HeLa cells with *P. aeruginosa* strain 992 (MOI 10) containing GST-MAM7 beads for 5 hours and Immunostaining with hoechst (DNA) and phalloidin (actin). Left to right: DIC image, phalloidin-stained image, hoechst-stained image, and overlaid phalloidin & hoechst-stained images. 60 x magnification.

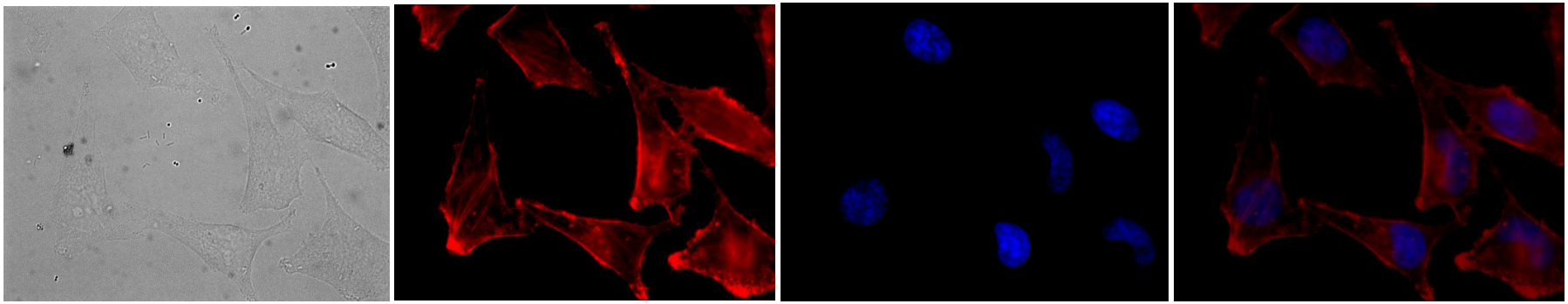

Figure 3.22: Infection of HeLa cells with *P. aeruginosa* strain 1004 (MOI 10) containing GST beads for 1 hour and Immunostaining with hoechst (DNA) and phalloidin (actin). Left to right: DIC image, phalloidin-stained image, hoechst-stained image, and overlaid phalloidin & hoechst-stained images. 60 x magnification.

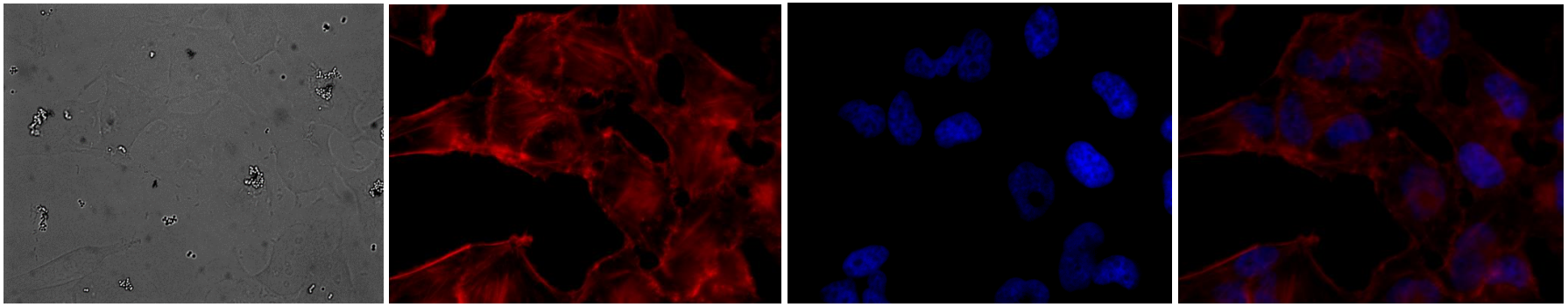

Figure 3.23: Infection of HeLa cells with *P. aeruginosa* strain 1004 (MOI 10) containing GST beads for 5 hours and Immunostaining with hoechst (DNA) and phalloidin (actin). Left to right: DIC image, phalloidin-stained image, hoechst-stained image, and overlaid phalloidin & hoechst-stained images. 60 x magnification.

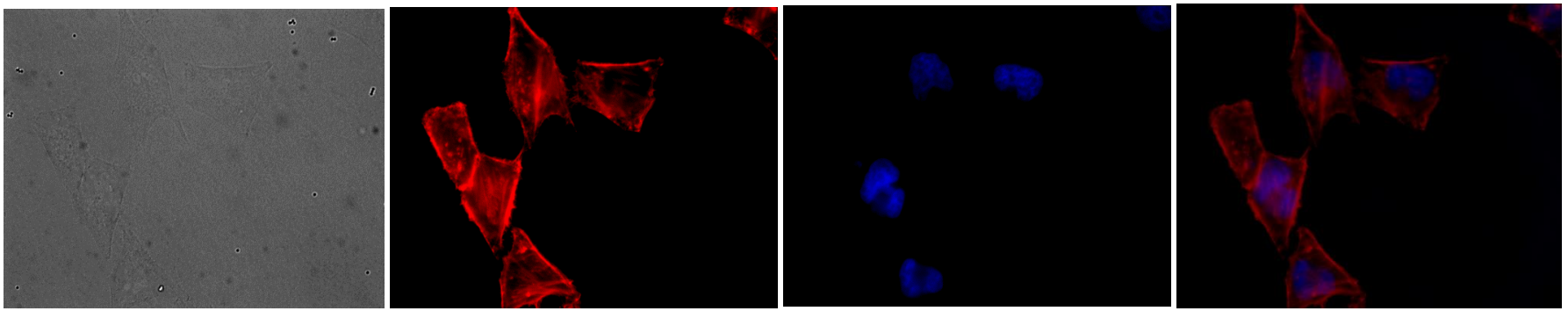

Figure 3.24: Infection of HeLa cells with *P. aeruginosa* strain 1004 (MOI 10) containing GST-MAM7 beads for 1 hour and Immunostaining with hoechst (DNA) and phalloidin (actin). Left to right: DIC image, phalloidin-stained image, hoechst-stained image, and overlaid phalloidin & hoechst-stained images. 60 x magnification.

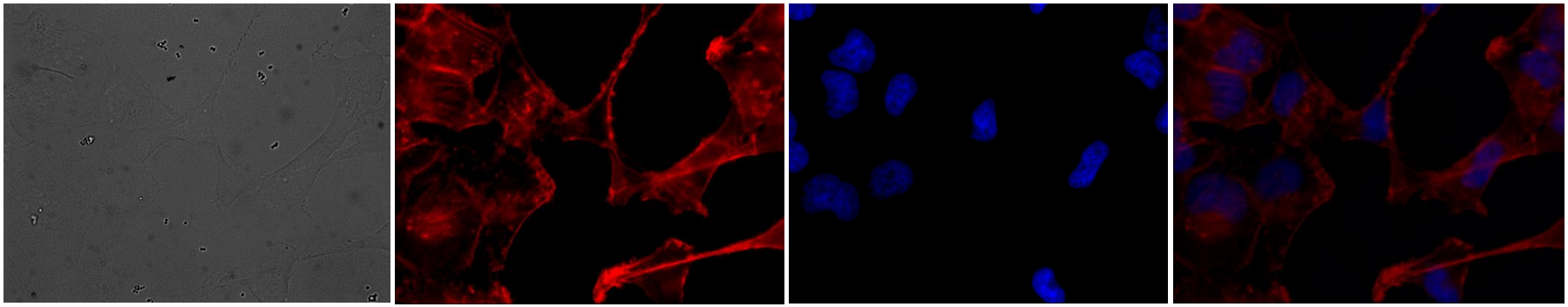

Figure 3.25: Infection of HeLa cells with *P. aeruginosa* strain 1004 (MOI 10) containing GST-MAM7 beads for 5 hours and Immunostaining with hoechst (DNA) and phalloidin (actin). Left to right: DIC image, phalloidin-stained image, hoechst-stained image, and overlaid phalloidin & hoechst-stained images. 60 x magnification.

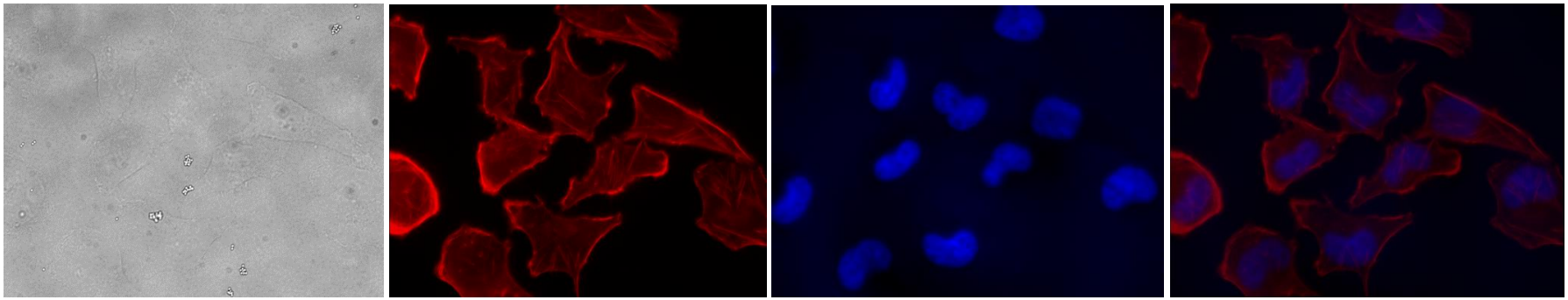

Figure 3.26: Infection of HeLa cells with *P. aeruginosa* strain 1007 (MOI 10) containing GST beads for 1 hour and Immunostaining with hoechst (DNA) and phalloidin (actin). Left to right: DIC image, phalloidin-stained image, hoechst-stained image, and overlaid phalloidin & hoechst-stained images. 60 x magnification.

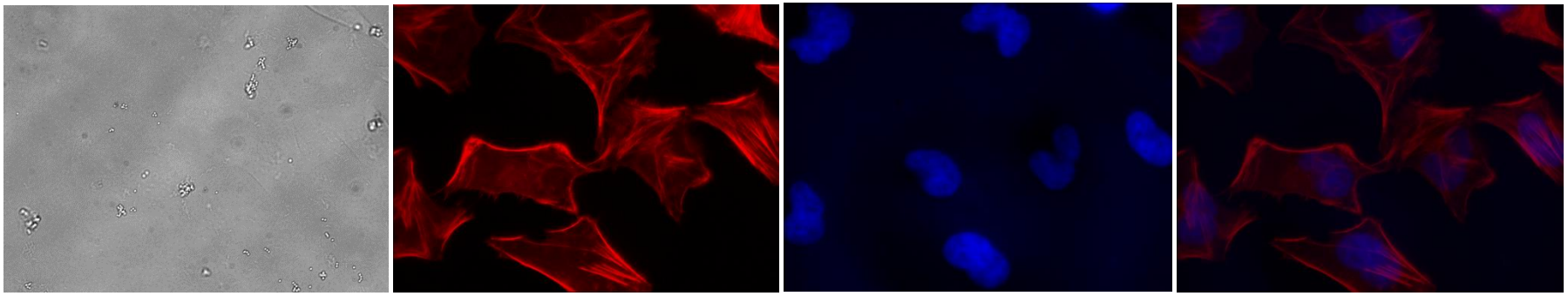

Figure 3.37: Infection of HeLa cells with *P. aeruginosa* strain 1007 (MOI 10) containing GST beads for 5 hours and Immunostaining with hoechst (DNA) and phalloidin (actin). Left to right: DIC image, phalloidin-stained image, hoechst-stained image, and overlaid phalloidin & hoechst-stained images. 60 x magnification.

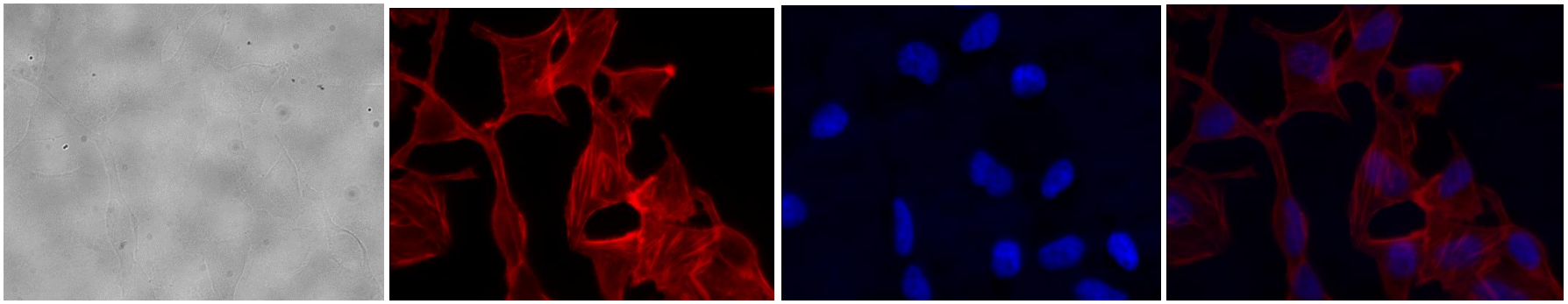

Figure 3.28: Infection of HeLa cells with *P. aeruginosa* strain 1007 (MOI 10) containing GST-MAM7 beads for 1 hour and Immunostaining with hoechst (DNA) and phalloidin (actin). Left to right: DIC image, phalloidin-stained image, hoechst-stained image, and overlaid phalloidin & hoechst-stained images. 60 x magnification.

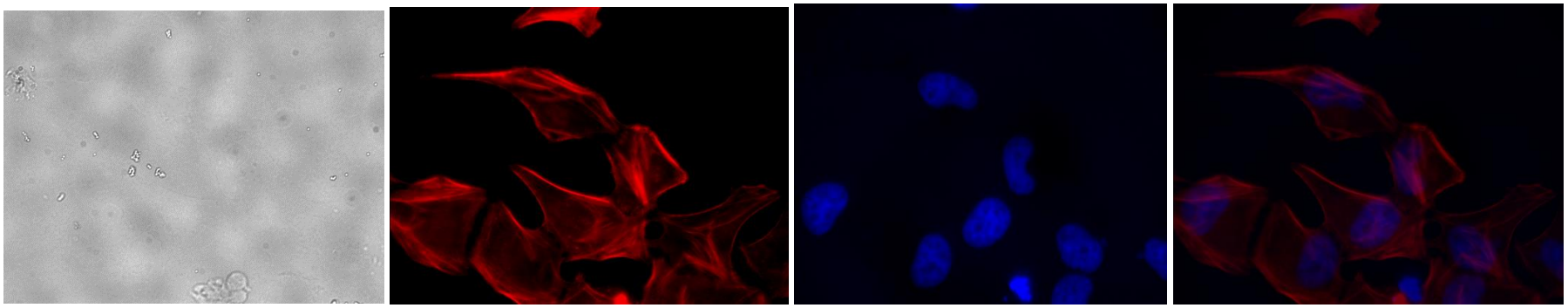

Figure 3.29: Infection of HeLa cells with *P. aeruginosa* strain 1007 (MOI 10) containing GST-MAM7 beads for 5 hours and Immunostaining with hoechst (DNA) and phalloidin (actin). Left to right: DIC image, phalloidin-stained image, hoechst-stained image, and overlaid phalloidin & hoechst-stained images. 60 x magnification.

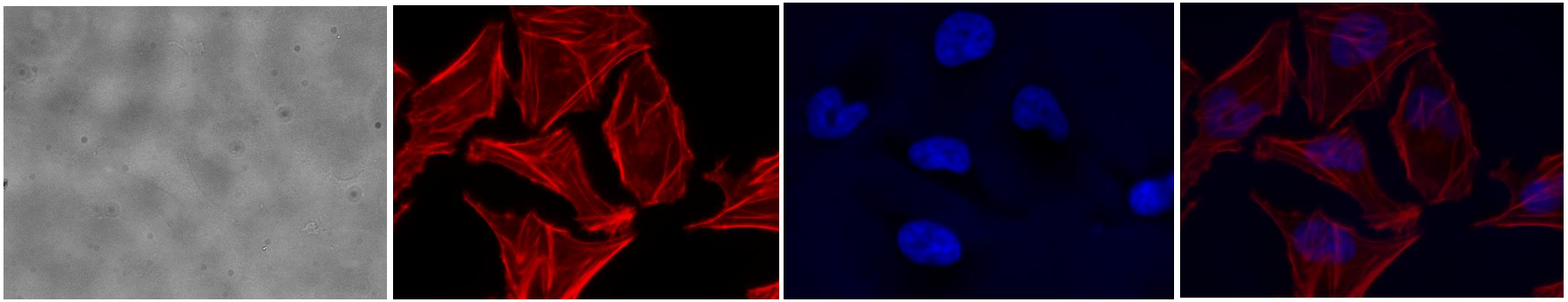

Figure 3.30: Infection of HeLa cells with *P. aeruginosa* strain 1008 (MOI 10) containing GST beads for 1 hour and Immunostaining with hoechst (DNA) and phalloidin (actin). Left to right: DIC image, phalloidin-stained image, hoechst-stained image, and overlaid phalloidin & hoechst-stained images. 60 x magnification.

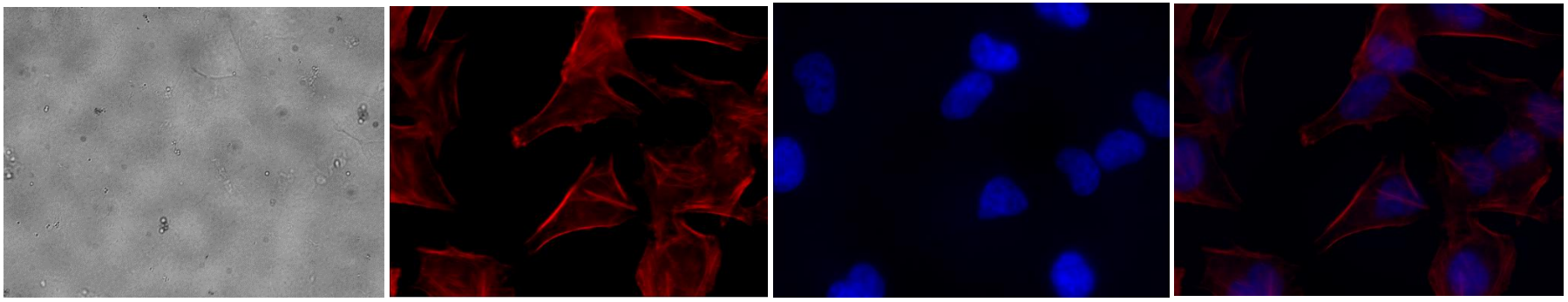

Figure 3.31: Infection of HeLa cells with *P. aeruginosa* strain 1008 (MOI 10) containing GST beads for 5 hours and Immunostaining with hoechst (DNA) and phalloidin (actin). Left to right: DIC image, phalloidin-stained image, hoechst-stained image, and overlaid phalloidin & hoechst-stained images. 60 x magnification.

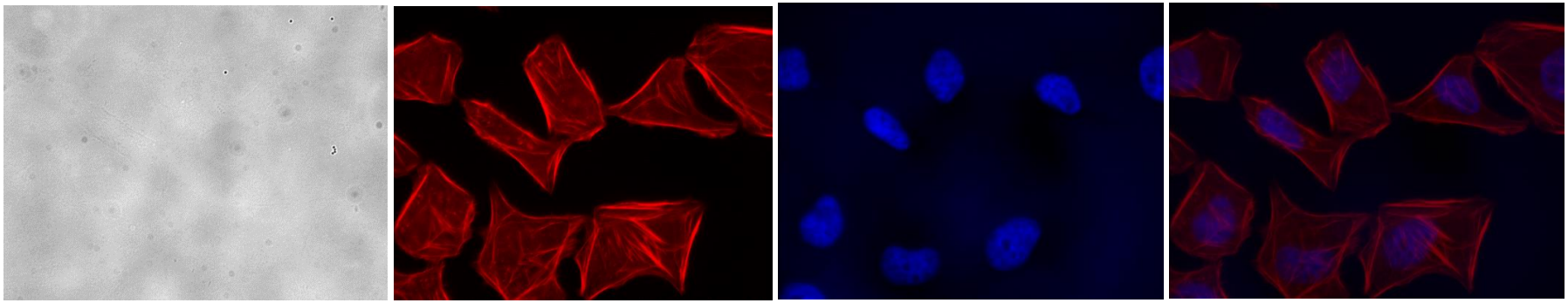

Figure 3.32: Infection of HeLa cells with *P. aeruginosa* strain 1008 (MOI 10) containing GST-MAM7 beads for 1 hour and Immunostaining with hoechst (DNA) and phalloidin (actin). Left to right: DIC image, phalloidin-stained image, hoechst-stained image, and overlaid phalloidin & hoechst-stained images. 60 x magnification.

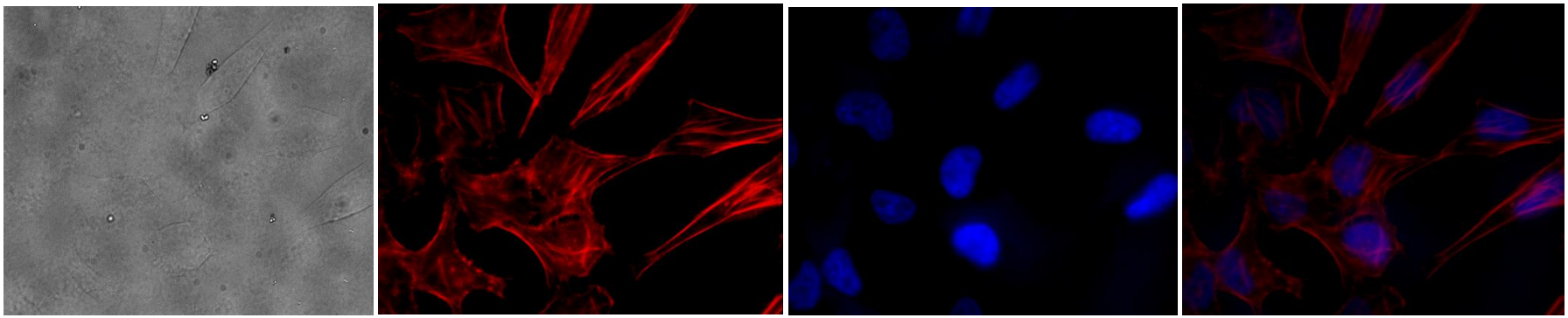

Figure 3.33: Infection of HeLa cells with *P. aeruginosa* strain 1009 (MOI 10) containing GST beads for 1 hour and Immunostaining with hoechst (DNA) and phalloidin (actin). Left to right: DIC image, phalloidin-stained image, hoechst-stained image, and overlaid phalloidin & hoechst-stained images. 60 x magnification.

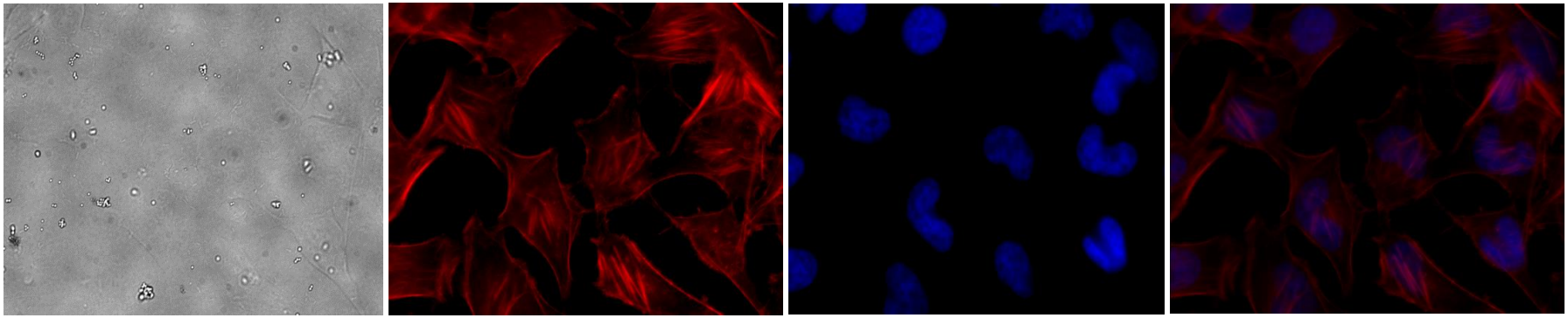

Figure 3.34: Infection of HeLa cells with *P. aeruginosa* strain 1009 (MOI 10) containing GST beads for 5 hours and Immunostaining with hoechst (DNA) and phalloidin (actin). Left to right: DIC image, phalloidin-stained image, hoechst-stained image, and overlaid phalloidin & hoechst-stained images. 60 x magnification.

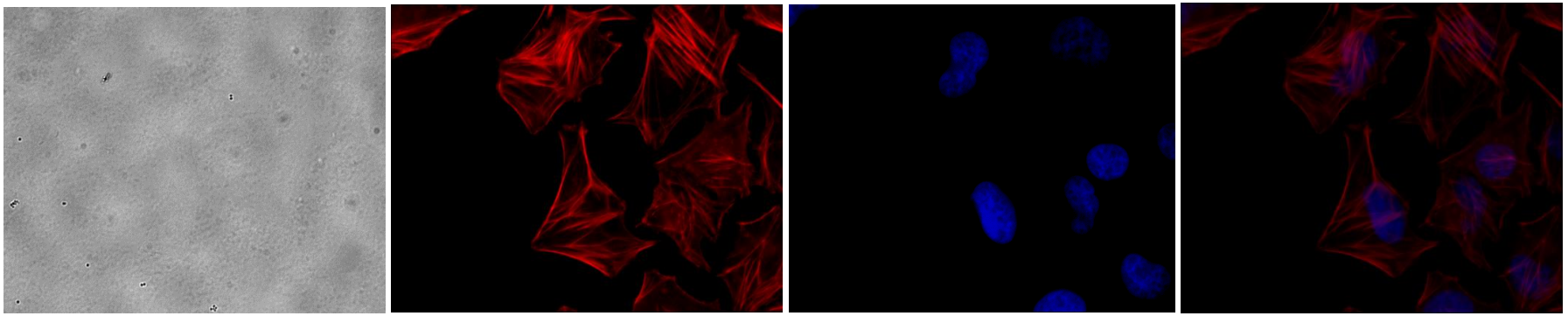

Figure 3.35: Infection of HeLa cells with *P. aeruginosa* strain 1009 (MOI 10) containing GST-MAM7 beads for 1 hour and Immunostaining with hoechst (DNA) and phalloidin (actin). Left to right: DIC image, phalloidin-stained image, hoechst-stained image, and overlaid phalloidin & hoechst-stained images. 60 x magnification.

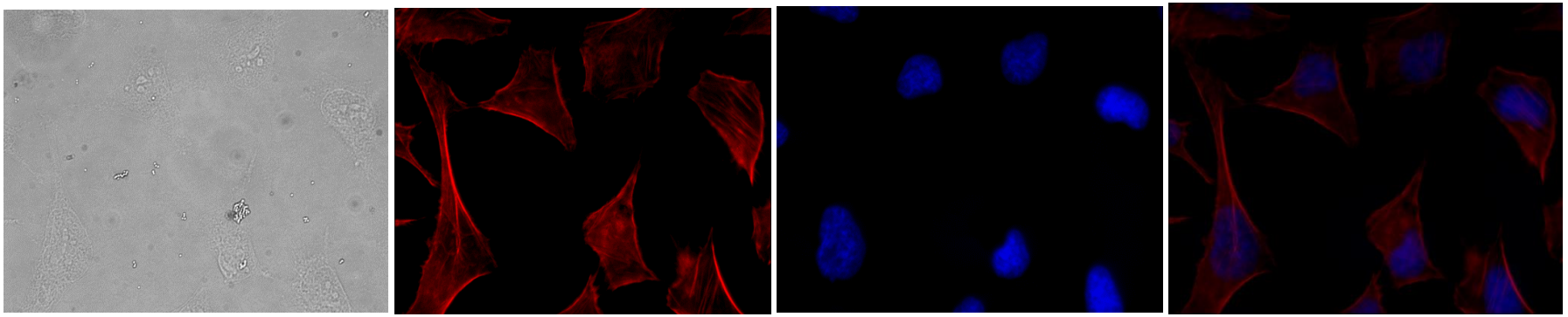

Figure 3.36: Infection of HeLa cells with *P. aeruginosa* strain 1009 (MOI 10) containing GST-MAM7 beads for 5 hours and Immunostaining with hoechst (DNA) and phalloidin (actin). Left to right: DIC image, phalloidin-stained image, hoechst-stained image, and overlaid phalloidin & hoechst-stained images. 60 x magnification.

4.0 Discussion

4.1 Research hypothesis and experimental aims

The aim of this project was to generate experimental data in support of *in silico* modelling for anti-virulence therapy (Ternent, unpublished), by exploring the attachment of six clinical *P. aeruginosa* isolates to HeLa cells - a cell type which is likely to be encountered prior to infection. The isolates were obtained from the Queen Elizabeth hospital in Birmingham following an outbreak in the Burns Unit; isolates 992 and 1004 were taken from the water supply, and isolates 985, 1007, 1008 and 1009 were isolated from a patient at various times during a two week antibiotic treatment.

Prior to this study, there was no significant difference between the growth rates of all six *P. aeruginosa* isolates and MIC data suggested that all six isolates were resistant to imipenem (>8 µg/mL) and sensitive to meropenem, with the exception of isolate 1004, which was resistant to meropenem (>8 µg/mL) and interestingly showed high macrophage attachment compared to the other strains (unpublished data).

During this study, attachment of each *P. aeruginosa* strain to HeLa cell monolayers was explored in the presence and absence of 4-methylumbelliferyl α-D-mannopyranoside and GST-MAM7 beads, which present two distinct approaches to reduce bacterial attachment to host cells. Anti-adhesion therapy presents a novel approach for the treatment of bacterial infections, which is thought to generate little to no selective pressure for the development of resistance; however as clinical therapies are currently unavailable, *in silico* modelling is a useful tool for analysing their efficacy.

4.2 The effect of 4 methylumbelliferyl α-D-mannopyranoside on the attachment of *P. aeruginosa* to HeLa cells

Functional characterisation of the *P. aeruginosa* genome has identified an array of genes which are central to virulence and pathogenicity (Stover, Pham et al. 2000), including those required for attachment to host cells. Bacterial attachment to host cells is considered a prerequisite for infection because adhesion allows the delivery of extracellular toxins and effector proteins to the host cytosol that enable the establishment and spread of infection. Attachment is mediated by a complex network of proteins, including adhesins, which act as cell recognition molecules to secure bacteria onto host cells (Sharon and Lis 1989). This is particularly important for bacteria that must overcome shear forces to remain in the human body, including those that invade the urinary and respiratory tracts. Inhibiting the expression of specific adhesins has been shown to attenuate bacterial virulence and therefore provides a promising strategy for the development of anti-virulence treatment.

The initial aim of this study was to explore baseline *P. aeruginosa* attachment to HeLa cells over the course of a 5 hour infection and incubation period, with enumeration of attached bacteria in CFUs/mL at 0, 0.5, 1, 1.5, 2, 3, 4 and 5 hours. After establishing the baseline dynamics of *P. aeruginosa* attachment, 4-methylumbelliferyl α-D-mannopyranoside was explored as an anti-attachment compound to target and bind *P. aeruginosa* FimH. The FimH protein is a D-mannose sensitive adhesin, located at the tip of Type 1 fimbriae in many bacteria, and therefore presents a universal target for a number of bacteria. FimH anchors the bacterial cell to the host cell through binding to cell surface mannose residues

specifically recognised by the protein. The specificity of the binding enables the formation of tight carbohydrate-protein complexes (Sharon and Lis 1989).

Through the addition of 100 µM of 4-methylumbelliferyl α-D-mannopyranoside to bacterial stocks of MOI 10 and MOI 1 prior to infection of HeLa cells, it was hypothesised that the compound would antagonise *P. aeruginosa* FimH and therefore reduce attachment to the epithelial cells. At MOI 10 for all bacterial strains under study, the presence of 4-methylumbelliferyl α-D-mannopyranoside resulted in a decrease in attachment at all time-points studied, however few data points were statistically significant as calculated by the student T test. At MOI 1, the observed trend was similar, however less data points were statistically significant. Taken together, it is unclear if 4-methylumbelliferyl α-D-mannopyranoside was effective in reducing the attachment of *P. aeruginosa* to HeLa cells and the data obtained in this study suggests that more repeats are necessary to generate statistically sound data. Previous studies of adhesin gene expression revealed that specific adhesins are expressed at different phases of infection; therefore, bacteria secrete multiple adhesins to facilitate efficient attachment and it is possible that FimH is not essential for attachment in the *P. aeruginosa* strains tested between 0 and 5 hours post infection *in vitro*. It would be interesting to inactivate FimH in the strains to further explore this possibility. Furthermore, it has been suggested that although FimH binds to mannose receptors on host cells with high specificity, it is likely that FimH binds to other ligands, depending on the environment, such as *E. coli* attachment to the urinary tract, and in biofilms. This suggests that bacteria are adaptable depending on environmental stressors, which could include the potential inhibition of attachment to

host cells. Alternatively, at a concentration of 100 μM, 4-methylumbelliferyl α-D-mannopyranoside may not be effective in reducing attachment of *P. aeruginosa* to HeLa cells, which highlights the importance of tailoring potential anti-virulence therapies for specific bacterial infections. It would be interesting to compare the efficacy of 4-methylumbelliferyl α-D-mannopyranoside in reducing the attachment of other pathogenic bacterial species to HeLa cells, because FimH could be a potentially universal bacterial target for therapy. Previous studies using a similar anti-attachment compound indicated that a high inhibitor concentration was required to inhibit haemoagglutination of horse red blood cells by *E. coli* (Nagahori, Lee et al. 2002), and it is likely that anti-adhesion compounds are more effective if the ligands or receptors are in excess of the bacterial cells to maximise competitive replacement at the site of infection. At unfavourable ratios, the anti-adhesive is unable to discriminate between bacteria that have already bound to host cells, therefore any unbound molecules would be cleared during the removal stage of the infection and attachment assay. Clinically, this suggests that use of anti-attachment therapy alone may only be beneficial as a prophylactic treatment as opposed to an on-going infection, where bacteria are already attached to host cells.

4.3 The effect of GST-MAM7 beads on the attachment of *P. aeruginosa* to HeLa cells

The second approach tested to reduce *P. aeruginosa* attachment to HeLa cells in this study was to mimic *P. aeruginosa* MAM7. GST-MAM7 beads have been effective in reducing adhesion to host cells in a number of bacteria by competitive replacement and binding to phosphatidic acid and fibronectin host cell receptors (Krachler, Ham et

al. 2012). In this study, the efficacy of GST-MAM7 beads was compared to a control of GST-only beads. The data generated indicates that between 0 and 1.5 hours post-infection with each *P. aeruginosa* strain, there were modest differences in attachment in the presence of GST-MAM7 beads. However between 1.5 hours and 2 hours post-infection with each bacterial strain tested, attachment decreased, suggesting that *P. aeruginosa* was somehow caused to detach from the HeLa cells at the later time points. Despite the observed decrease, few data points were statistically significant as calculated by the student T test, owing to the variability between the data points used to calculate the mean log value. This highlights a limitation in the assay as the number of colony forming units counted for each time point was not always consistent, and would therefore benefit from further repeats to generate statistically sound data and confirm the observations in this study. Although bacterial viability was not confirmed for the detached bacteria, previous studies involving GST-MAM7 beads have not described any cytotoxicity from the beads - further confirmed by the inclusion of GST-only beads in the study, which do not follow this trend of decreased attachment between 0 and 5 hours.

Immunostaining and fluorescent microscopy was carried out in order to explore HeLa cell morphology during *P. aeruginosa* attachment at 1 and 5 hours, in the presence of GST-MAM7 beads, compared with GST-only beads. In all strains under study, the presence of GST-only beads led to an acceleration in actin stress-fibre formation in HeLa cells at 5 hours, compared to 1 hour post-infection. DIC images showed that the proportion of bacterial cells attached to HeLa cells at 5 hours increased in the presence of GST-only beads, suggesting that the GST-MAM7 beads reduced

bacterial attachment to the cells at 5 hours. Where GST-MAM7 beads were used during infection, no significant changes in HeLa cell morphology were seen that would suggest cell death; no significant changes in hoechst DNA-binding was observed in the presence of GST-MAM7 and GST beads, furthermore, observed changes in HeLa cell morphology in the presence of GST-MAM7 and GST beads were subtle. Taken together, the present study was unable to identify the cause of *P. aeruginosa* detachment between 1.5 and 2 hours-post infection in the presence of GST-MAM7 beads. Similarly to FimH, it is possible that *P. aeruginosa* MAM7 was not required for initial bacterial attachment at 0-1.5 hours. It would be interesting to study the gene expression profile of MAM7 during different time-points of the assay to explore this hypothesis further. A longer incubation time (5 hours +) may provide optimal visualisation of the effect of GST-MAM7 beads on the HeLa phenotype during infection, compared with GST beads. Additionally, it would be interesting to count the number of GST-MAM7 beads bound to each HeLa cell during this assay using fluorescently labelled beads, to better explore the efficacy of the beads in reducing bacterial attachment to HeLa cells.

4.4 Conclusions of the study

The data generated during this study has contributed to the development of *in silico* modelling for anti-virulence therapy. Bacteria that are resistant to antibiotics, particularly frontline treatments, are an increasing threat to healthcare, particularly in nosocomial environments where patients are generally immunocompromised and exposed to a variety of opportunistic bacteria capable of causing secondary infections. Since their discovery, the pipeline of new antibiotics is becoming

increasingly thin, therefore it has been suggested that the focus of new treatments for bacterial infections should shift from discovering new antibiotics, to the discovery of therapeutics with novel targets. One of these strategies aims to promote clearance via the host immune system through inhibition of bacterial virulence. Examples include preventing the delivery of virulence toxins to the host cytosol, targeting the regulation of virulence genes to reduce their expression, and preventing bacterial attachment to host cells.

Mathematical modelling can be used to explore the efficacy and viability of anti-virulence therapies *in silico* (Ternent, unpublished). Theoretical data suggests that anti-virulence therapy is likely to be of clinical benefit when administered in combination with suitable antibiotics that aim to clear the susceptible population of cells. *In silico* modelling can be used to identify optimal treatment regimes; however every infection, bacterial strain and patient are different, therefore strategies and treatment doses must be tailored to the specific conditions of the host. As many of the parameters described in the model are estimated values, they are not accurate. Consequently, further experimental data must be generated in order to fully establish more accurate parameters for the model, to enable pathogen-specificity, patient-specificity and infection site-specificity. This will enable the model to establish when treatment would be effective in an individual, and at what concentrations the treatment would be effective.

4.5 Limitations of the study

During infection and attachment assays, the mean concentration of each bacterial strain inoculated at time = 0 (input control) was consistently lower than the bacteria

recovered at 5 hours, which suggests that for the duration of this assay, *P. aeruginosa* was proliferating. As a result, the assay was unable to determine how proliferation affected attachment from 0 to 5 hours. It is possible that the increase in attachment observed throughout the study was due to the proliferation of bacteria that were already attached at an earlier time point. In order to explore this further, a preliminary assay was carried out in which each *P. aeruginosa* strain was inoculated onto a HeLa cell monolayer and incubated for 30 minutes at 37°C, 5% CO_2. Following incubation, bacterial suspensions were removed and each well filled with 1 mL of pre-warmed colourless DMEM, before carrying out the infection assay as previously described. This assay was conducted in order to determine the rate of proliferation of *P. aeruginosa* attached at 30 minutes post-infection. Unfortunately, due to the time constraints of the project and the requirement of further assay optimisation, the data is incomplete and therefore not included in this project.

Alternatively, to measure the percentage of attached bacteria at each time point during the assay, it would be useful to enumerate detached bacteria at each time point, and use the values to calculate the percentage of attached bacteria at each time point. However, this may be inaccurate because non-attached bacteria would need to be removed from the 24-well MTT after each PBS wash, which may dilute the bacteria too much to be plated accurately. Centrifugation to pellet the bacteria and resuspending in a reduced volume may also distort the results, due to additional manipulation steps, where cells may be lost.

During Immunostaining and fluorescence microscopy during this study, it was important to consider the effect of photobleaching on each slide, resulting in a reduction in the time a sample can be observed. Photobleaching was minimised as

much as possible, by storing slides in a dark box when not in use and minimising illumination during fluorescence analysis. Additionally, poor image resolution limited the visualisation of images and Epifluorescence may be favourable for future studies.

4.6 Proposed further work

The current study aimed to explore the dynamics of *P. aeruginosa* attachment to HeLa cells as 2D monolayers, which may not be an accurate representation of how the strains behave when encountered with the cells within a host organism. Specifically, the data generated during the infection and attachment assays may vary considerably if the cells were in a multicellular environment and under sheer forces that more closely mimic the environment *P. aeruginosa* is likely to encounter in the host organism.

For example, FimH mannose affinity increases during conditions of increased mechanical force, which may enhance the ability of bacteria to anchor onto host cells to avoid clearance (Yakovenko, Sharma et al. 2008). It would be interesting to complement the data obtained during this study with infection and attachment of 3D cell cultures that more closely mimic an infection site.

Expression of bacterial adhesins are induced as a result of different environmental factors; therefore it would be interesting to explore how bacterial attachment is affected by altering a number of environmental variables including temperature and pH. Although the study temperature used during the duration of this project was 37°C, which is the typical body temperature of the host organism, further insights into the dynamics of bacterial attachment could be gained from repeat assays at a range of

temperatures. Similarly, bacteria must be able to withstand acidic pH in the stomach, so it would be interesting to explore how pH correlates with the attachment of *P. aeruginosa* to host cells.

If there was more time during this study, further exploration of the interactions between GST-MAM7 beads and bacterial attachment could have been achieved by fluorescently-labelling the 6 *P. aeruginosa* strains and carrying out live-cell imaging over the 5 hour infection period. The technique would have been useful to study binding of 4-methylumbelliferyl α-D-mannopyranoside to the bacteria, in addition to how the GST-MAM7 beads reduced attachment of the strains between 1.5 and 2 hours post-infection. Alternatively, fluorescent reporter genes tagged to FimH and MAM7 in the *P. aeruginosa* strains may be useful in studying whether gene expression increased at particular time-point during infection and therefore when treatment with the respective attachment inhibitor may be most optimal. However, such further work may not reveal more about the changes to HeLa cell morphology over the infection period. It would be possible to explore the cytotoxic effect of the *P. aeruginosa* strains during the infection period using a lactate dehydrogenase (LDH) release assay because infection would cause the HeLa cells to lyse and release LDH into the culture medium, which can then be used as a measure of invasion. Krachler et al (2012) reported that the cytotoxicity of *P. aeruginosa* in the presence of GST-MAM7 reduced from 76% to 4% (Krachler, Ham et al. 2012), so may provide additional data for this study. Alternatively, Trypan blue staining may be useful to determine the relative live and dead HeLa cells during the infection period.

In this study, 4-methylumbelliferyl α-D-mannopyranoside showed modest promise in reducing the adhesion of *P. aeruginosa* to HeLa cells, however it would be interesting to explore the efficacy of multiple attachment inhibitors with different targets, for example 4-methylumbelliferyl α-D-mannopyranoside and GST-MAM7 beads, and how these affect *P. aeruginosa* attachment during the same infection assay.

5.0 References

Alonso, A., E. Campanario, et al. (1999). "Emergence of multidrug-resistant mutants is increased under antibiotic selective pressure in Pseudomonas aeruginosa." Microbiology-Sgm 145: 2857-2862.

Alvarez-Ortega, C. and C. S. Harwood (2007). "Responses of Pseudomonas aeruginosa to low oxygen indicate that growth in the cystic fibrosis lung is by aerobic respiration (vol 65, pg 153, 2007)." Molecular Microbiology 65(2): 582-582.

Arason, V. A., K. G. Kristinsson, et al. (1996). "Do antimicrobials increase the carriage rate of penicillin resistant pneumococci in children? Cross sectional prevalence study." British Medical Journal 313(7054): 387-391.

Arruda, S., G. Bomfim, et al. (1993). "Cloning of an Mycobacterium-Tuberculosis DNA Fragment Associated with Entry and Survival inside Cells." Science 261(5127): 1454-1457.

Ayliffe, G. A. J., J. R. Babb, et al. (1974). "Pseudomonas-Aeruginosa in Hospital Sinks." Lancet 2(7880): 578-581.

Bidhendi, S.M, M. Sattari, et al. (2007). "Blocking adherance of uropathogenic Esherichia colu isolate to HEP-2 cells and bladder of mice in the presence of antibody against p-fimbriae." Biologicals 35(2): 99-105

Breathnach, A.S., M.D. Cubbon, et al. (2012). "Multidrug-resistant Pseudomonas aeruginosa outbreaks in two hospitals: association with contaminated hospital waste-water systems." Journal or Hospital Infection 82(1):19-24.

Brint, J.M., Ohman, D.E. (1995). “Synthesis of multiple exoproducts in Pseudomonas aeruginosa is under the control of RhIR-RhII, another set of regulators in strain PAO1 with homology to the autoinducer-responsive LuxR-Lux1 family.” J. Bacteriol 177: 7155-7163.

Blackwood, L. L., R. M. Stone, et al. (1983). "Evaluation of Pseudomonas-Aeruginosa Exotoxin-a and Elastase as Virulence Factors in Acute Lung Infection." Infection and Immunity 39(1): 198-201.

Bodey, G. P., R. Bolivar, et al. (1983). "Infections Caused by Pseudomonas-Aeruginosa." Reviews of Infectious Diseases 5(2): 279-313.

Boekema, B. K. H. L., J. P. M. Van Putten, et al. (2004). "Host cell contact-induced transcription of the type IV fimbria gene cluster of Actinobacillus pleuropneumoniae." Infection and Immunity 72(2): 691-700.

Bouckaert, J., J. Berglund, et al. (2005). "Receptor binding studies disclose a novel class of high-affinity inhibitors of the Escherichia coli FimH adhesin." Molecular Microbiology 55(2): 441-455.

Carson, L. A., M. S. Favero, et al. (1973). "Morphological, Biochemical, and Growth Characteristics of Pseudomonas-Cepacia from Distilled Water." Applied Microbiology 25(3): 476-483.

Chapon-Herve, V., Akrim, M., et al. (1997). “Regulation of the xcp secretion pathway by multiple quorum-sensing modulons in Pseudomonas aeruginosa.” Mol. Microbiol 24: 1169-1178.

Chitale, S., S. Ehrt, et al. (2001). "Recombinant Mycobacterium tuberculosis protein associated with mammalian cell entry." Cellular Microbiology 3(4): 247-254.

Chopra, I. and M. Roberts (2001). "Tetracycline antibiotics: Mode of action, applications, molecular biology, and epidemiology of bacterial resistance." Microbiology and Molecular Biology Reviews 65(2): 232-+.

Choudhury, D., A. Thompson, et al. (1999). "X-ray structure of the FimC-FimH chaperone-adhesin complex from uropathogenic Escherichia coli." Science 285(5430): 1061-1066.

Costerton, J. W., P. S. Stewart, et al. (1999). "Bacterial biofilms: A common cause of persistant infections. "Science 284(5418): 1318-1322.

Crespo, M. D., C. Puorger, et al. (2012). "Quality control of disulfide bond formation in pilus subunits by the chaperone FimC." Nature Chemical Biology 8(8): 707-713.

Davies, D. G., M. R. Parsek, et al. (1998). "The involvement of cell-to-cell signals in the development of a bacterial biofilm." Science 280(5361): 295-298.

Densen, P. and G. L. Mandell (1978). "Gonococcal Interactions with Polymorphonuclear Neutrophils - Importance of Phagosome for Bactericidal Activity." Journal of Clinical Investigation 62(6): 1161-1171.

Doi, O., M. Ogura, et al. (1968). "Inactivation of Kanamycin Neomycin and Streptomycin by Enzymes Obtained in Cells of Pseudomonas Aeruginosa." Applied Microbiology 16(9): 1276-&.

Donlan, R. M. (2001). "Biofilms and device-associated infections." Emerging Infectious Diseases 7(2): 277-281.

Edwards, J. R., P. J Turner, et al. (1989). "In vitro antibacterial activity of SM-7338, a carbapenem antibiotic with stability to dehydropeptidase I. Antimicrob Agents Chemother 33(2): 215-222.

Feldman, M., R. Bryan, et al. (1998). "Role of flagella in pathogenesis of Pseudomonas aeruginosa pulmonary infection." Infection and Immunity 66(1): 43-51.

Firon, N., S. Ashkenazi, et al. (1987). "Aromatic Alpha-Glycosides of Mannose Are Powerful Inhibitors of the Adherence of Type-1 Fimbriated Escherichia-Coli to Yeast and Intestinal Epithelial-Cells." Infection and Immunity 55(2): 472-476.

Fitos, I., K. Heremans, et al. (1979). "Binding Study of 4-Methylumbelliferyl Alpha-D-Mannopyranoside to Dimeric Concanavalin-a under High-Pressure." Reaction Kinetics and Catalysis Letters 12(4): 393-397.

Frost, L. S., R. Leplae, et al. (2005). "Mobile genetic elements: The agents of open source evolution." Nature Reviews Microbiology 3(9): 722-732.

Galan, J. E. and A. Collmer (1999). "Type III secretion machines: Bacterial devices for protein delivery into host cells." Science 284(5418): 1322-1328.

Gambello, M.J., Kaye, S. et al. (1993). “LasR of Pseudomonas aeruginosa is a transcriptional activator of the alkaline protease gene (apr) and an enhancer of exotoxin A expression.” Infect. Immun. 61(4): 1180-1184.

Gessard, C. 1882a. Sur les colorations bleue et verte des linges a pansements. C.R. Acad. Sci. 94:536-538. 1882b. De la pyocyanine et de son microbe. These Fac. Med. Paris, No 248, 1-66.

Govan, J. R. W. and J. W. Nelson (1992). "Microbiology of Lung Infection in Cystic-Fibrosis." British Medical Bulletin 48(4): 912-930.

Green, S. K., M. N. Schroth, et al. (1974). "Agricultural Plants and Soil as a Reservoir for Pseudomonas-Aeruginosa." Applied Microbiology 28(6): 987-991.

Hahn, H. P. (1997). "The type-4 pilus is the major virulence-associated adhesin of Pseudomonas aeruginosa - A review." Gene 192(1): 99-108.

Han, Z. F., J. S. Pinkner, et al. (2010). "Structure-Based Drug Design and Optimization of Mannoside Bacterial FimH Antagonists." Journal of Medicinal Chemistry 53(12): 4779-4792.

Hancock, R. E. W. (1998). "Resistance mechanisms in Pseudomonas aeruginosa and other nonfermentative gram-negative bacteria." Clinical Infectious Diseases 27: S93-S99.

Harris, A., C. Torres-Viera, et al. (1999). "Epidemiology and clinical outcomes of patients with multiresistant Pseudomonas aeruginosa." Clinical infectious diseases : an official publication of the Infectious Diseases Society of America 28(5): 1128-1133.

Hassett, D.J., Ma, J.F., et al. (1999). "Quorum sensing in Pseudomonas aeruginosa controls expression of catalase and superoxide dismutase genes and mediates biofilm susceptibility to hydrogen peroxide." Mol. Microbiol. 34(5): 1082-1093.

Hayes, C. S., S. K. Aoki, et al. (2010). "Bacterial Contact-Dependent Delivery Systems." Annual Review of Genetics, Vol 44 44: 71-90.

Kesado, T., Hashizume, T, et al. (1980). "Antibacterial activities of a New Stabilised Thienamycin, N-Formimidoyl Thienamycin, in comparison with other antibiotics." Antimicrobial Agents and Chemotherapy 912-917.

Kipnis, E., T. Sawa, et al. (2006). "Targeting mechanisms of Pseudomonas aeruginosa pathogenesis." Medecine Et Maladies Infectieuses 36(2): 78-91.

Kirkeby, S., M. Wimmerova, et al. (2007). "The mink as an animal model for Pseudomonas aeruginosa adhesion: binding of the bacterial lectins (PA-IL and PA-IIL) to neoglycoproteins and to sections of pancreas and lung tissues from healthy mink." Microbes and Infection 9(5): 566-573.

Kohler, T., M. MicheaHamzehpour, et al. (1997). "Characterization of MexE-MexF-OprN, a positively regulated multidrug efflux system of Pseudomonas aeruginosa." Molecular Microbiology 23(2): 345-354.

Kohler, T., M. MicheaHamzehpour, et al. (1997). "Differential selection of multidrug efflux systems by quinolones in Pseudomonas aeruginosa." Antimicrobial Agents and Chemotherapy 41(11): 2540-2543.

Kotter, S., U. Krallmann-Wenzel, et al. (1998). "Multivalent ligands for the mannose-specific lectin on type 1 fimbriae of Escherichia coli: syntheses and testing of trivalent alpha-D-mannoside clusters." Journal of the Chemical Society-Perkin Transactions 1(14): 2193-2200.

Krachler, A. M., H. Ham, et al. (2011). "Outer membrane adhesion factor multivalent adhesion molecule 7 initiates host cell binding during infection by Gram-negative pathogens." Proceedings of the National Academy of Sciences of the United States of America 108(28): 11614-11619.

Krachler, A. M., H. Ham, et al. (2012). "Turnabout is fair play Use of the bacterial Multivalent Adhesion Molecule 7 as an antimicrobial agent." Virulence 3(1): 68-71.

Krachler, A. M. and K. Orth (2013). "Targeting the bacteria-host interface: Strategies in anti-adhesion therapy." Virulence 4(4): 284-294.

Kumar, A., M. Bose, et al. (2003). "Analysis of expression profile of mammalian cell entry (mce) operons of Mycobacterium tuberculosis." Infection and Immunity 71(10): 6083-6087.

Kummerer, K. (2004). "Resistance in the environment." Journal of Antimicrobial Chemotherapy 54(2): 311-320.

Langermann, S., R. Mollby, et al. (2000). "Vaccination with FimH adhesin protects cynomolgus monkeys from colonization and infection by uropathogenic Escherichia coli." Journal of Infectious Diseases 181(2): 774-778.

Langermann, S., S. Palaszynski, et al. (1997). "Prevention of mucosal Escherichia coli infection by FimH-adhesin-based systemic vaccination." Science 276(5312): 607-611.

Lau, G. W., H. M. Ran, et al. (2004). "Pseudomonas aeruginosa pyocyanin is critical for lung infection in mice." Infection and Immunity 72(7): 4275-4278.

Lebreton, F., E. Riboulet-Bisson, et al. (2009). "ace, Which Encodes an Adhesin in Enterococcus faecalis, Is Regulated by Ers and Is Involved in Virulence." Infection and Immunity 77(7): 2832-2839.

Leffler, H. and C. Svanborgeden (1981). "Glycolipid Receptors for Uropathogenic Escherichia-Coli on Human-Erythrocytes and Uroepithelial Cells." Infection and Immunity 34(3): 920-929.

Mendelson, M. H., A. Gurtman, et al. (1994). "Pseudomonas-Aeruginosa Bacteremia in Patients with Aids." Clinical Infectious Diseases 18(6): 886-895.

Montie, T. C., D. Doylehuntzinger, et al. (1982). "Loss of Virulence Associated with Absence of Flagellum in an Isogenic Mutant of Pseudomonas-Aeruginosa in the Burned-Mouse Model." Infection and Immunity 38(3): 1296-1298.

Nagahori, N., R. T. Lee, et al. (2002). "Inhibition of adhesion of type 1 fimbriated Escherichia coli to highly mannosylated ligands." Chembiochem 3(9): 836-844.

Nakano, M., T. Deguchi, et al. (1997). "Mutations in the gyrA and parC genes in fluoroquinolone-resistant clinical isolates of Pseudomonas aeruginosa." Antimicrobial Agents and Chemotherapy 41(10): 2289-2291.

Noble, W. C. and J. A. Savin (1966). "Steroid Cream Contaminated with Pseudomonas Aeruginosa." Lancet 1(7433): 347-&.

Ochsner, U.A., Reiser, J. (1995). “Autoinducer-mediated regulation of rhamnolipid biosurfactant synthesis in Pseudomonas aeruginosa.” Proc. Natl. Acad. Sci. U.S.A. 92:5624-6428.

Ohman, D. E., J. C. Sadoff, et al. (1980). "Toxin a-Deficient Mutants of Pseudomonas-Aeruginosa Pa103 - Isolation and Characterization." Infection and Immunity 28(3): 899-908.

Pessi, G. and Haas, D. (2000). “Transcriptional control of the Hydrogen Cyanide Biosynthetic genes in hcnABC by the anaerobic regulator ANR and the Quorum-sensing regulators LasR amd RhlR in Pseudomonas aeruginosa.” J. Bacteriol 182(24): 6940-6949.

Piddock, L. J. V. (2006). "Clinically relevant chromosomally encoded multidrug resistance efflux pumps in bacteria." Clinical Microbiology Reviews 19(2): 382-+.

Pollack, M., N. S. Taylor, et al. (1977). "Exotoxin Production by Clinical Isolates of Pseudomonas-Aeruginosa." Infection and Immunity 15(3): 776-780.

Poole, K. (2001). "Multidrug efflux pumps and antimicrobial resistance in Pseudomonas aeruginosa and related organisms." Journal of Molecular Microbiology and Biotechnology 3(2): 255-263.

Poole, K. (2004). "Efflux-mediated multiresistance in Gram-negative bacteria." Clinical Microbiology and Infection 10(1): 12-26.

Ran, H. M., D. J. Hassett, et al. (2003). "Human targets of Pseudomonas aeruginosa pyocyanin." Proceedings of the National Academy of Sciences of the United States of America 100(24): 14315-14320.

Rodriguez-Martinez, J. M., L. Poirel, et al. (2009). "Extended-Spectrum Cephalosporinases in Pseudomonas aeruginosa." Antimicrobial Agents and Chemotherapy 53(5): 1766-1771.

Rodriguez, V.B., B.A. Kidd. (2013). "Allosteric coupling in the bacterial adhesive protein FimH." The Journal of Biological Chemistry (288): 24128-24139

Sauer, K., Camper, A. K, et al. (2002). "Pseudomonas aeruginosa displays multiple phenotypes during development as a biofilm." J. Bacteriol 184(4): 1140-1154.

Sauer, F.G., H. Remaut, et al. (2004). "Fiber assemby by the chaperone-usher pathway." Molecular Cell Research 1694(1-3): 259-267.

Schroeter, J. 1872. Ueber einige durch Bacterien gebildete Pigmente. Beitr. Biol. Pflanz, 1:109-126.

Sharon, N. and H. Lis (1989). "Lectins as Cell Recognition Molecules." Science 246(4927): 227-234.

Sperling, O., A. Fuchs, et al. (2006). "Evaluation of the carbohydrate recognition domain of the bacterial adhesin FimH: design, synthesis and binding properties of mannoside ligands." Organic & Biomolecular Chemistry 4(21): 3913-3922.

Stover, C. K., X. Q. Pham, et al. (2000). "Complete genome sequence of Pseudomonas aeruginosa PAO1, an opportunistic pathogen." Nature 406(6799): 959-964.

Swartz, M. N. (1994). "Hospital-acquired infections: diseases with increasingly limited therapies." Proceedings of the National Academy of Sciences of the United States of America 91(7): 2420-2427.

Tchesnokova, V., P. Aprikian, et al. (2011). "Type 1 Fimbrial Adhesin FimH Elicits an Immune Response That Enhances Cell Adhesion of Escherichia coli." Infect. Immun 79(10): 3895-3904.

Ternent, L., Dyson, R. J., Krachler, AM., Jabbari, S. (2014). "Bacterial fitness shapes the population dynamics of antibiotic-resistant and -susceptible bacteria in a model of combined antibiotic and anti-virulence treatment" Unpublished.

Toder, D.S., Ferrell, S.J., et al. (1994). “lasA and lasB genes of Pseudomonas aeruginosa: analysis of transcription and gene product activity.” Infect. Immun. 62(4): 1320-1327.

Tomasz, A. (1979). "Mechanism of the Irreversible Anti-Microbial Effects of Penicillins - How the Beta-Lactam Antibiotics Kill and Lyse Bacteria." Annual Review of Microbiology 33: 113-137.

Van Delden, C. and B. H. Iglewski (1998). "Cell-to-cell signaling and Pseudomonas aeruginosa infections." Emerging Infectious Diseases 4(4): 551-560.

Yakovenko, O., S. Sharma, et al. (2008). "FimH forms catch bonds that are enhanced by mechanical force due to allosteric regulation." Journal of Biological Chemistry 283(17): 11596-11605.

Whiteley, M., Lee, K.M, et al. (1999). “Identification of genes controlled by quorum sensing in *Pseudomonas aeruginosa*.” Proc. Natl. Acad. Sci. U.S.A. 96(24): 13904-13909.

Williams, P., Bainton, N.J., et al. (1992). “Small molecule-mediated density-dependent control of gene expression in prokaryotes: Bioluminescence and the biosynthesis of carbapenem antibiotics.” FEMS Microbiology Letters (100): 161-168.

Williams, P., Winzer, K., Chan, et al. (2007). “Look who’s talking:communication and quorum sensing in the bacterial world.” Pholos Trans R Soc Lond B Biol Sci 362(1483): 1119-34.

Winzer, K., Falconer, N.C., et al. (2000). “The Pseudomonas aeruginosa lectins PA-IL and PA-IIL are controlled by quorum sensing and by RpoS.” J. Bacteriol 182: 6401-6411.

World Health Organisation. 2014. Antimicrobial resistance: global report on surveillance 2014.